

Fighting Noise with Noise: Causal Inference with Many Candidate Instruments

Xinyi Zhang, Linbo Wang, Stanislav Volgushev and Dehan Kong
University of Toronto, Department of Statistical Sciences

Abstract

Instrumental variable methods provide useful tools for inferring causal effects in the presence of unmeasured confounding. To apply these methods with large-scale data sets, a major challenge is to find valid instruments from a possibly large candidate set. In practice, most of the candidate instruments are often not relevant for studying a particular exposure of interest. Moreover, not all relevant candidate instruments are valid as they may directly influence the outcome of interest. In this article, we propose a data-driven method for causal inference with many candidate instruments that addresses these two challenges simultaneously. A key component of our proposal is a novel resampling method, which constructs pseudo variables to remove irrelevant candidate instruments having spurious correlations with the exposure. Synthetic data analyses show that the proposed method performs favourably compared to existing methods. We apply our method to a Mendelian randomization study estimating the effect of obesity on health-related quality of life.

Keywords: A/B tests; Mendelian randomization; Selection bias; Spurious Correlation

1 Introduction

The instrumental variable (IV) model is a workhorse in causal inference using observational data. It is especially useful when standard adjustment methods are biased due to unmeasured confounding. The key idea is to find an exogenous variable to extract random variation in the exposure and use this random variation to estimate the causal effect. This exogenous variable is known as the instrumental variable or instrument if it is related to the exposure, but does not affect the outcome except through the exposure.

In the past, selection of appropriate exogenous variables that can serve as valid instruments was typically driven by expert knowledge (e.g. Angrist & Krueger, 1991). In recent years, applied researchers have increasingly sought to employ large-scale observational data sets to identify causal relationships. As the size and complexity of data sets grow, it becomes increasingly difficult to build a knowledge-based instrumental variable model for modern data applications. A prominent example in genetic epidemiology is Mendelian randomization (MR), which uses genetic variants, such as single-nucleotide polymorphisms (SNPs), as instruments to assess the causal relationship between a risk factor and an outcome (e.g. Burgess et al., 2015). The candidate instrument set includes millions of SNPs in the human genome. This challenge also arises in the literature using multi-condition experiments as instruments (e.g. Eckles et al., 2016; Goldman

& Rao, 2016; Peysakhovich & Eckles, 2018). For example, in tech companies, it is common to have routine product experimentation such as A/B tests. These large collections of randomized experiments provide natural candidates for finding instrumental variables.

Modern large-scale complex systems call for data-driven methods that find valid instruments from a high-dimensional candidate set. Two main challenges arise from such a pursuit. First, often most of the candidate instruments are not relevant for studying a particular exposure of interest. To deal with this problem, a common approach is to employ a screening procedure (e.g. Fan & Lv, 2008) to select variables in the candidate set that are associated with the exposure. For example, in genetics, it is common to use genome-wide association studies (GWAS) or variants thereof to identify genetic variants that are relevant to a risk factor. Recent studies have suggested choosing a less conservative selection threshold than the traditional 5×10^{-8} for MR applications (e.g. Zhao et al., 2020), in order to include more SNPs that are associated with the risk factors and hence improve the efficiency of the resulting causal effect estimate; see also Barber & Candes (2019) for a similar recommendation in a related context. This is especially important for datasets with small to moderate sample sizes, for which standard GWAS has limited power so that only very few or even no genetic variants may be selected; see our data application in Section 6 for an example. However, a less conservative selection threshold will result in more false positives, i.e. SNPs having spurious correlations with the risk factor of interest. Using these SNPs as instruments will undermine the validity of downstream MR procedures. A similar problem also arises in multi-condition experiments as most of the experiments have very small effects on the exposure (Peysakhovich & Eckles, 2018).

Moreover, some of the candidate instruments found to be associated with the exposure might not be valid as they may directly influence the outcome of interest. For example, in MR studies, this problem arises due to pleiotropy, a phenomenon that one genetic variant influences multiple traits and possibly through independent pathways. In response to this concern, recently there has been a surging interest in methods that make valid causal inference in the presence of invalid instruments. Kolesar et al. (2015) and Bowden et al. (2015) provided inferential methods for treatment effects in the presence of invalid instruments. Their methods assume that the direct effects of these invalid instruments are uncorrelated with the associations between the instruments and the exposure. Cheng & Liao (2015) studied the selection of valid instruments by assuming that one knows a collection of valid IVs a priori. Another popular assumption, known as the “majority rule” (Bowden et al., 2016; Kang et al., 2016; Windmeijer et al., 2019; Hartford et al., 2021), assumes that at least 50% of the candidate instruments are valid. Relaxing the majority rule, Guo et al. (2018) and Windmeijer et al. (2021) assume that the largest group of Wald ratios with equal values corresponds to valid instruments, referred to as the “plurality rule.” They also developed two-stage thresholding procedures to identify valid IVs and consistently estimate causal effects. In the MR context, Morrison et al. (2020) proposed a method based on genome-wide summary statistics that accounts for both uncorrelated and correlated pleiotropic effects, while Zhao et al. (2020) proposed a consistent causal effect estimator by adjusting the profile likelihood of the summary data under a two-sample MR design where the exposure and the outcome are observed from two independent samples.

The developments in the present paper are motivated by the somewhat surprising finding that a naive combination of existing methods for solving the two challenges discussed earlier leads to biased causal inference. More precisely, we observe that estimates from this naive combination are close to the ordinary least squares (OLS) estimate that does not account for any unmeasured confounding.

Our contributions in the paper are two-fold. We first provide a theoretical characterization of the observation described above. In particular, we show that estimates from exogenous variables having spurious correlations with the exposure are concentrated in a region that can be separated from the true causal effect. Remarkably in our theoretical analysis, we explicitly take into account the randomness in the first marginal screening step, while most of the existing literature treats this as pre-processing and does not account for its randomness.

We then introduce a novel strategy that addresses this challenge. A key component of our proposal is a resampling method that constructs pseudo variables to identify and remove spurious variables. The idea of pseudo variables has been investigated before in other contexts, most notably in forward selection (Wu et al., 2007). It is also similar in spirit to knockoffs (Barber & Candès, 2015) although our construction of pseudo variables is much simpler.

To facilitate inference, we also consider a variation of our proposal using sample splitting, in which one portion of the data is used to detect spurious variables, and the remaining data are used to identify the valid instruments and estimate the causal effects.

The rest of this article is organized as follows. In Section 2, we provide background information of IV analysis and our models. We illustrate the challenges of identifying valid instruments from a large candidate set using a simulated example and provide theoretical justifications for our findings in Section 3. Section 4 details the proposed procedures. In Section 5, we evaluate the performance of our procedures via simulations. In Section 6, we apply the proposed methods to the Wisconsin Longitudinal Study data and examine the causal effect of obesity on Health-Related Quality of Life (HRQL). We conclude with discussions in Section 7.

2 Background

The instrumental variable (IV) approach is a popular method for inferring causality from observational studies. It introduces exogenous variables called instruments to control for unmeasured confounding U . Conditioning on observed covariates, a variable Z is called an IV for estimating the causal effect of an exposure D on an outcome Y if it satisfies the three core conditions (e.g. Didelez & Sheehan, 2007; Wang & Tchetgen Tchetgen, 2018) below:

- I1 **Relevance:** Z is associated with the exposure;
- I2 **Exclusion restriction:** Z has no direct effect on the outcome;
- I3 **Independence:** Z is independent of unmeasured variables that affect the exposure and the outcome.

Figure 1 gives a causal graph representation of the IV model.

Suppose we have n independent samples $(Y_i, D_i, \mathbf{Z}_i, \mathbf{X}_i)$ from the distribution of $(Y, D, \mathbf{Z}, \mathbf{X})$, where Y is a continuous outcome of interest, D is a continuous exposure, $\mathbf{Z} = (Z_1, \dots, Z_p)^\top \in \mathbb{R}^p$ denotes candidate instrumental variables, and $\mathbf{X} = (X_1, \dots, X_q)^\top \in \mathbb{R}^q$ represents baseline covariates. We assume

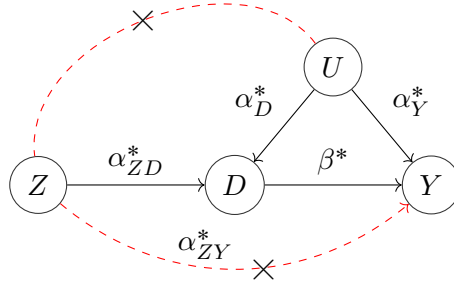


Figure 1: Graphical illustration of an IV model: Z denotes a valid instrument, D, Y represent the exposure and outcome, respectively and U is the unobserved confounding. Parameters on the arrows represent effects on the linear scale. Red dashed lines with \times indicate absence of arrows.

that D and Y are generated from the following linear structural equation models:

$$D = \mathbf{Z}^T \boldsymbol{\gamma}^* + \mathbf{X}^T \boldsymbol{\psi}^* + \mathbf{U}^T \boldsymbol{\alpha}_D^* + \epsilon_D; \quad (2.1)$$

$$Y = \mathbf{Z}^T \boldsymbol{\pi}^* + \beta^* D + \mathbf{X}^T \boldsymbol{\phi}^* + \mathbf{U}^T \boldsymbol{\alpha}_Y^* + \epsilon_Y. \quad (2.2)$$

The parameter β^* measures the causal effect of the exposure D on the outcome Y , which is the quantity of primary interest. Parameter $\boldsymbol{\gamma}^* \in \mathbb{R}^p$ characterizes the partial correlations between the instruments and the exposure. Parameter $\boldsymbol{\pi}^* \in \mathbb{R}^p$ measures the degree of violation of the exclusion restriction assumption I2. Similarly, parameters $\boldsymbol{\psi}^*, \boldsymbol{\phi}^* \in \mathbb{R}^q$ refer to the effects of observed covariates on the exposure and the outcome respectively. Parameters $\boldsymbol{\alpha}_D^* \in \mathbb{R}^g$ and $\boldsymbol{\alpha}_Y^* \in \mathbb{R}^g$ represent the direct effects of the multivariate unobserved confounders $\mathbf{U} \in \mathbb{R}^g$ on D and Y , respectively. The dimension g is fixed. Unmeasured confounding \mathbf{U} and random errors ϵ_D, ϵ_Y are independently distributed with mean zero and covariance matrix/variance $\Sigma_U, \sigma_D^2, \sigma_Y^2$, respectively. We further assume that Z_j is independent of ϵ_D, ϵ_Y and \mathbf{U} for $j = 1, \dots, p$. This assumption is generally considered plausible in MR studies after controlling for population stratification (Smith, 2007; Zhao et al., 2020) and holds by design in multi-condition experiments. An instrument Z_j is called relevant if $\gamma_j^* \neq 0$, and is called irrelevant otherwise. For relevant instruments, if $\pi_j^* = 0$, then Z_j is a valid instrument; otherwise, it is called an invalid instrument.

For the rest of the paper, we suppress dependence on covariates \mathbf{X} for simplicity. With this, models (2.1) and (2.2) take the reduced forms

$$D = \mathbf{Z}^T \boldsymbol{\gamma}^* + \mathbf{U}^T \boldsymbol{\alpha}_D^* + \epsilon_D, \quad (2.3)$$

$$Y = \mathbf{Z}^T \boldsymbol{\Gamma}^* + \mathbf{U}^T (\beta^* \boldsymbol{\alpha}_D^* + \boldsymbol{\alpha}_Y^*) + e, \quad (2.4)$$

where $\boldsymbol{\Gamma}^* = \boldsymbol{\pi}^* + \beta^* \boldsymbol{\gamma}^*$ and $e = \beta^* \epsilon_D + \epsilon_Y$. Let $\mathbb{Z} \in \mathbb{R}^{n \times p}$, $\mathbf{D} \in \mathbb{R}^n$ and $\mathbf{Y} \in \mathbb{R}^n$ denote the collection of observations for (Z, D, Y) from n independent units, respectively. Here \mathbb{Z} is also called the design matrix. Without loss of generality, assume that $\mathbb{Z}, \mathbf{D}, \mathbf{Y}$ are all centered.

Given a valid instrument Z_j , the causal effect β^* may be identified as the Wald ratio (Lawlor et al., 2008).

Alternatively, given a set of valid instruments \mathbf{Z}_{valid} , a popular procedure to estimate the causal effect under linear models is the two-stage least squares (2SLS) estimator given by $\hat{\beta}_{2SLS} = (\mathbf{D}^T \mathbf{P} \mathbf{D})^{-1} (\mathbf{D}^T \mathbf{P} \mathbf{Y})$, where $\mathbf{P} = \mathbf{Z}_{valid} (\mathbf{Z}_{valid}^T \mathbf{Z}_{valid})^{-1} \mathbf{Z}_{valid}^T$ is a projection matrix and \mathbf{Z}_{valid} is the design matrix corresponding to the valid instruments.

In practice, prior knowledge of instrument validity is often not available. Nevertheless, the causal effect can still be identified and estimated from data under the majority rule that more than 50% of the candidate IVs are valid. In this case, among the Wald ratios constructed using individual candidate IVs, more than 50% are equal to the true causal effect β^* . As a result, β^* can be identified as the median of these Wald ratios (e.g. Han, 2008; Bowden et al., 2016). The majority rule may be relaxed to the so-called plurality rule, which assumes that the largest group of invalid instruments with the same Wald ratio is smaller than the group of valid instruments, whose Wald ratio equals the true causal effect. In this case, the mode of the Wald ratios constructed using individual candidate IVs corresponds to the true causal effect (e.g. Guo et al., 2018; Windmeijer et al., 2021).

3 Challenges for Causal Inference with Many Candidate Instruments

3.1 A naive combination of existing approaches with screening

In this section, we consider the causal effect estimation problem under models (2.1) and (2.2), where the number of candidate instruments far exceeds the sample size. For example, in the genetics application detailed in Section 6, there are 3,683,868 candidate instruments measured on a data set of 3023 subjects. The ultra-high dimensional nature of the candidate instrument set makes standard regularization methods like the lasso computationally challenging. In this case, it is common to apply a marginal screening procedure to quickly screen out variables that are unlikely to be relevant to the exposure (e.g. Fan & Lv, 2008). For example, one may select the top s candidate instruments by ranking the absolute marginal estimates $|\sum_{i=1}^n D_i Z_{ij}| / (\sum_{i=1}^n Z_{ij}^2)$ for $1 \leq j \leq p$. We then let $\hat{\mathcal{S}}_1 \subset \{1, \dots, p\}$ be the index set of the top s candidate instruments, and $\mathbf{Z}_{\hat{\mathcal{S}}_1}$ be the corresponding candidate instruments. We denote the design matrix of $\mathbf{Z}_{\hat{\mathcal{S}}_1}$ as $\mathbb{Z}_{\hat{\mathcal{S}}_1} \in \mathbb{R}^{n \times s}$.

The marginal screening step may include candidate instruments that are marginally correlated but conditionally uncorrelated with the exposure. To further estimate the set of relevant instruments defined in a joint model, we first evaluate joint relevance strength for candidates $\mathbf{Z}_{\hat{\mathcal{S}}_1}$ selected from marginal screening and subsequently perform a hard thresholding step (Donoho & Johnstone, 1994). If $\hat{\mathcal{S}}_1$ includes all the relevant instruments, then models (2.1) and (2.2) still hold with $\mathbf{Z} \in \mathbb{R}^p$ replaced by $\mathbf{Z}_{\hat{\mathcal{S}}_1} \in \mathbb{R}^s$, and parameters γ^* and π^* replaced by $\gamma_{\hat{\mathcal{S}}_1}^*, \pi_{\hat{\mathcal{S}}_1}^* \in \mathbb{R}^s$, respectively. The parameter $\mathbf{\Gamma}_{\hat{\mathcal{S}}_1}^*$ in the reduced model is defined similarly to $\mathbf{\Gamma}^*$ as $\mathbf{\Gamma}_{\hat{\mathcal{S}}_1}^* = \pi_{\hat{\mathcal{S}}_1}^* + \beta^* \gamma_{\hat{\mathcal{S}}_1}^*$. To estimate the coefficients $\gamma_{\hat{\mathcal{S}}_1}^*$ and $\mathbf{\Gamma}_{\hat{\mathcal{S}}_1}^*$ in potentially high dimensional settings, we proceed using the de-biased lasso estimator in van de Geer et al. (2014), which is defined as follows,

$$\begin{aligned} \hat{\mathbf{\Gamma}}_{\hat{\mathcal{S}}_1} &= \tilde{\mathbf{\Gamma}}_{\hat{\mathcal{S}}_1} + \frac{1}{n} \mathbf{M} \mathbb{Z}_{\hat{\mathcal{S}}_1}^T (\mathbf{Y} - \mathbb{Z}_{\hat{\mathcal{S}}_1} \tilde{\mathbf{\Gamma}}_{\hat{\mathcal{S}}_1}), \\ \hat{\gamma}_{\hat{\mathcal{S}}_1} &= \tilde{\gamma}_{\hat{\mathcal{S}}_1} + \frac{1}{n} \mathbf{M} \mathbb{Z}_{\hat{\mathcal{S}}_1}^T (\mathbf{D} - \mathbb{Z}_{\hat{\mathcal{S}}_1} \tilde{\gamma}_{\hat{\mathcal{S}}_1}), \end{aligned} \quad (3.1)$$

with the lasso estimator $\tilde{\Gamma}_{\hat{\mathcal{S}}_1} = \operatorname{argmin}_{\Gamma \in \mathbb{R}^{s \times s}} \{\|\mathbf{Y} - \mathbb{Z}_{\hat{\mathcal{S}}_1} \Gamma\|_2^2/n + 2\lambda_\Gamma \|\Gamma\|_1\}$, and the lasso estimator $\tilde{\gamma}_{\hat{\mathcal{S}}_1}$ is obtained similarly. Here the matrix $\mathbf{M} \in \mathbb{R}^{s \times s}$ is an estimate of the precision matrix $\Sigma_{\hat{\mathcal{S}}_1}^{-1}$; see Appendix G for more details on the construction of \mathbf{M} . Following Donoho & Johnstone (1994), the hard thresholding step proceeds by comparing $|\hat{\gamma}_{\hat{\mathcal{S}}_1, l}|$ with a threshold $\delta_n \times \operatorname{SE}(\hat{\gamma}_{\hat{\mathcal{S}}_1, l})$, where $\delta_n = \sqrt{\omega \log(\max\{n, s\})}$ and the standard error of the de-biased lasso estimate $\hat{\gamma}_{\hat{\mathcal{S}}_1, l}$ for $1 \leq l \leq s$ is

$$\operatorname{SE}(\hat{\gamma}_{\hat{\mathcal{S}}_1, l}) = \sqrt{[\mathbf{M} \hat{\Sigma}_{\hat{\mathcal{S}}_1} \mathbf{M}^\top / n]_{ll} \|\mathbf{D} - \mathbb{Z}_{\hat{\mathcal{S}}_1} \tilde{\gamma}_{\hat{\mathcal{S}}_1}\|^2 / n} \quad (3.2)$$

with $[\]_{ll}$ representing the l th diagonal element of the matrix. Here ω in the threshold is a tuning parameter that controls the number of candidates estimated as relevant to the exposure. We use $\hat{\mathcal{S}}_2$ to denote the set of candidate instruments that pass this joint thresholding step, that is, $\hat{\mathcal{S}}_2 = \{l : 1 \leq l \leq s, |\hat{\gamma}_{\hat{\mathcal{S}}_1, l}| \geq \delta_n \times \operatorname{SE}(\hat{\gamma}_{\hat{\mathcal{S}}_1, l})\}$.

Now suppose that the plurality rule holds for $\hat{\mathcal{S}}_2$, i.e. the number of invalid instruments with the same Wald ratio $\Gamma_{\hat{\mathcal{S}}_1, l}^* / \gamma_{\hat{\mathcal{S}}_1, l}^*$ for $l \in \hat{\mathcal{S}}_2$ is smaller than the number of valid instruments in $\hat{\mathcal{S}}_2$. To estimate valid instruments under this plurality rule, one may apply the voting framework by Guo et al. (2018). Specifically, their voting procedure uses pairwise comparisons to test whether two candidates have the same Wald ratios by testing $H_0^{(j, l)} : \Gamma_{\hat{\mathcal{S}}_1, j}^* - \gamma_{\hat{\mathcal{S}}_1, j}^* (\Gamma_{\hat{\mathcal{S}}_1, l}^* / \gamma_{\hat{\mathcal{S}}_1, l}^*) = 0$. For each voter $l \in \hat{\mathcal{S}}_2$, the collection $\{j \in \hat{\mathcal{S}}_2 : H_0^{(j, l)} \text{ not rejected}\}$ would be candidates that l is in favor of. Once the polls close, by counting the number of votes for each candidate, the candidates that win the most votes are estimated as valid instruments. See Guo et al. (2018) for more detailed discussions.

We summarize the aforementioned procedure in Algorithm 1, which simply combines marginal screening and existing work that identifies valid instruments under the plurality rule.

3.2 A numerical example

In this section we analyze the naive approach from the previous section in a simulated example. We generate 1000 data sets of size $n = 500$ with $p = 50,000$ candidate instruments. The true causal effect β^* is set to be 2. Candidate instruments Z_1, Z_2 are invalid, Z_3, \dots, Z_9 are valid, and $Z_{10}, \dots, Z_{50,000}$ are irrelevant. The valid instruments are distributed according to $\mathbf{Z}_{3:9} \sim N(\mathbf{0}, \Sigma_v)$ with $[\Sigma_v]_{jk} = 0.25^{|j-k|}$. The other candidate instruments $Z_j, j = 1, 2, 10, \dots, 50,000$, observed covariates X_1, X_2 , random error ϵ_Y , and a univariate unobserved confounding U are generated from independent standard normal distributions. The treatment D and the outcome Y follow models (2.1) and (2.2), where $(\alpha_D^*, \alpha_Y^*) = (4, -3)$, the relevance strength $\gamma_{1:9}^* = 3$ and the degree of violation to the exclusion restriction assumption is characterized by $\pi_{1:2}^* = (-3.5, 3.5)^\top$; the effects of the observed covariates on the exposure and the outcome are given by $\psi^* = (1.5, 2)^\top$ and $\phi^* = (1.2, 1.5)^\top$, respectively. For simplicity, we let $\epsilon_D = 0$.

To reduce the dimension of candidate instruments and exclude variables that are unlikely to be informative to the exposure, following Step 1 of Algorithm 1, we first marginally regress the exposure on each candidate instrument and keep the top 500 with the largest marginal associations in absolute value. We then apply Steps 2 – 4 of Algorithm 1 to this remaining set for identifying valid IVs and estimating the causal effect. Empirical results suggest that most of the valid instruments identified by Algorithm 1 (Naive) are in fact irrelevant. On average across 1000 Monte Carlo runs, the ‘‘Naive’’ algorithm identifies 15.27 variables

Algorithm 1 Naive algorithm: causal effect estimation with many candidate instruments

INPUT: Design matrix $\mathbb{Z} \in \mathbb{R}^{n \times p}$, observed exposure $\mathbf{D} \in \mathbb{R}^n$, observed outcome $\mathbf{Y} \in \mathbb{R}^n$.

1. Marginal screening (Fan & Lv, 2008):

For $j = 1, \dots, p$, compute $\hat{\rho}_j = |\sum_{i=1}^n Z_{ij} D_i| / \sum_{i=1}^n Z_{ij}^2$.

Select the s variables with the largest $\hat{\rho}_j$ and denote them as $\hat{\mathcal{S}}_1$.

2. Joint thresholding (Donoho & Johnstone, 1994; van de Geer et al., 2014):

Fit a linear model for $\mathbf{D} \sim \mathbb{Z}_{\hat{\mathcal{S}}_1}$: let $\hat{\gamma}_{\hat{\mathcal{S}}_1}$ be the debiased lasso estimate defined in (3.1); here $\mathbb{Z}_{\hat{\mathcal{S}}_1}$ is formed by columns of \mathbb{Z} indexed by $\hat{\mathcal{S}}_1$. Also obtain their standard error estimate $\text{SE}(\hat{\gamma}_{\hat{\mathcal{S}}_1, l})$ in (3.2).

Fit a linear model for $\mathbf{Y} \sim \mathbb{Z}_{\hat{\mathcal{S}}_1}$ and obtain the debiased lasso estimate $\hat{\Gamma}_{\hat{\mathcal{S}}_1}$ in a similar fashion.

Estimate the relevant variables $\hat{\mathcal{S}}_2 = \{1 \leq l \leq s : |\hat{\gamma}_{\hat{\mathcal{S}}_1, l}| \geq \delta_n \times \text{SE}(\hat{\gamma}_{\hat{\mathcal{S}}_1, l})\}$, where $\delta_n = \sqrt{\omega \log(\max\{n, s\})}$ and ω is a tuning parameter.

3. Voting (Guo et al., 2018):

For $j, l \in \hat{\mathcal{S}}_2$, test $H_0^{(j, l)} : \Gamma_{\hat{\mathcal{S}}_1, j}^* - \gamma_{\hat{\mathcal{S}}_1, j}^* \left(\frac{\Gamma_{\hat{\mathcal{S}}_1, l}^*}{\gamma_{\hat{\mathcal{S}}_1, l}^*} \right) = 0$.

For $l \in \hat{\mathcal{S}}_2$, find candidates that l votes for: $\hat{\mathcal{V}}_l = \{j \in \hat{\mathcal{S}}_2 : H_0^{(j, l)} \text{ not rejected}\}$.

Count votes for $j \in \hat{\mathcal{S}}_2$: $\text{vc}_j = \sum_{l \in \hat{\mathcal{S}}_2} \mathbb{1}(j \in \hat{\mathcal{V}}_l)$.

Find valid IVs: $\hat{\mathcal{S}}_4 = \{\text{argmax}_{j \in \hat{\mathcal{S}}_2} \text{vc}_j\}$.

4. Causal effect estimation: Take $\hat{\mathcal{S}}_4, \mathbf{D}, \mathbf{Y}$ as input into 2SLS to estimate causal effect and construct a confidence interval.
-

as valid IVs, among which 15.25 are in fact irrelevant. The resulting causal effect estimate is 1.78 on average and the empirical coverage probability is 1%, compared to a nominal level of 95%.

To provide insights into this problem, we study the causal effect estimates from Z_j^l s with $j \in \hat{\mathcal{S}}_2$. In Figure 2(a), we plot the histograms of causal effect estimates aggregated over the 1000 Monte Carlo runs. We use different colors to distinguish the estimates produced by the valid, invalid IVs and irrelevant variables. One can see that the plurality rule is violated empirically even after joint thresholding: the largest number of causal effect estimates with similar values corresponds to irrelevant variables. The latter variables shall be referred to as “spurious instruments.” The plurality rule is violated here because there are much more irrelevant candidate instruments to begin with, and the sample size is small relative to the number of candidate instruments. Somewhat surprisingly, all spurious instruments lead to similar causal effect estimates. Moreover, these effect estimates lie in a region that is separated from those estimates regarding the valid IVs. As a result, Algorithm 1 that assumes the plurality rule misidentifies the spurious instruments as valid IVs, as shown in Figure 2(b). A theoretical explanation of those findings is given in the following subsection.

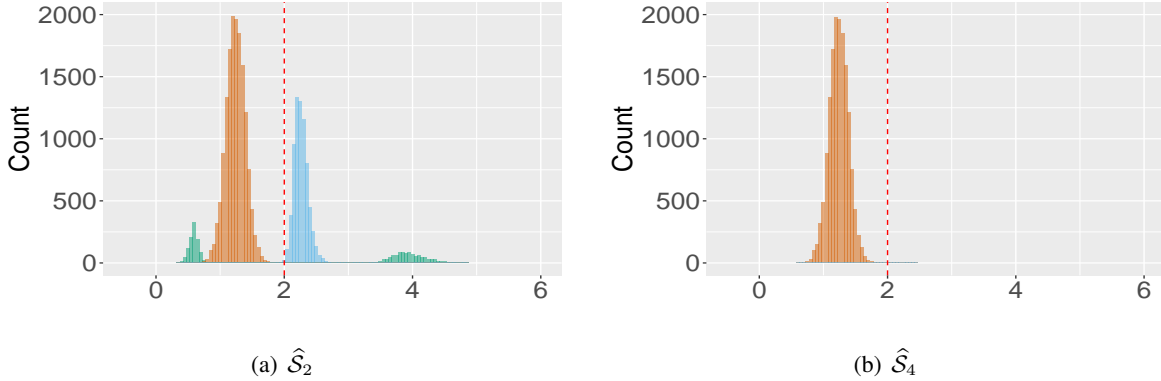


Figure 2: Histograms of causal effect estimates aggregated over the 1000 Monte Carlo runs: (a) plots the estimates by candidate instruments that pass the joint thresholding step ($\hat{\mathcal{S}}_2$) of Algorithm 1, and (b) plots the estimates by candidate instruments identified as valid instruments ($\hat{\mathcal{S}}_4$) by Algorithm 1. The blue pile represents causal effect estimates by valid IVs; the green piles represent those by invalid IVs; the orange pile represents those by irrelevant variables. The red dashed line is the true causal effect $\beta^* = 2$.

3.3 Results for causal estimates from variables passing joint thresholding

In this section, we theoretically characterize the behaviour of causal effect estimates from spurious, valid, and invalid instruments that pass joint thresholding. Before introducing our concentration bounds, we define the sets of relevant and irrelevant variables in $\hat{\mathcal{S}}_1$, the set of variables selected by marginal screening

$$\check{\mathcal{R}} = \{l : 1 \leq l \leq s, \gamma_{\hat{\mathcal{S}}_1, l}^* \neq 0\}, \quad \check{\mathcal{I}} = \{l : 1 \leq l \leq s, \gamma_{\hat{\mathcal{S}}_1, l}^* = 0\}.$$

The assumptions imposed to establish the theoretical results are presented in the following:

- A1. Unmeasured confounders U_i 's are *i.i.d.* $N(\mathbf{0}, \Sigma_U)$ where $\Sigma_U \in \mathbb{R}^{g \times g}$ and g is fixed. Random

errors ϵ_{iD} 's are *i.i.d.* $N(0, \sigma_D^2)$ and ϵ_{iY} 's are *iid* $N(0, \sigma_Y^2)$. Further $\epsilon_{iD}, \epsilon_{iY}$ and U_i are mutually independent for $i = 1, \dots, n$ and are all independent of Z_{ij} for $1 \leq i \leq n$ and $1 \leq j \leq p$.

A2. Let $\Sigma \in \mathbb{R}^{p \times p}$ be the covariance matrix of $\mathbf{Z} \in \mathbb{R}^p$. There exist constants $C_L, C_R, B > 0$ such that for all p , $\lambda_{\min}(\Sigma) \geq C_L > 0$, $\lambda_{\max}(\Sigma) \leq C_R < \infty$, and $\max_{1 \leq j \leq p} \Sigma_{jj} \leq B$. Further assume \mathbf{Z}_i are *i.i.d* sub-gaussian with variance proxy σ^2 and zero mean, i.e., for any $\lambda \in \mathbb{R}$ and unit vector $\mathbf{u} \in \mathcal{S}^{p-1}$, $E \left\{ e^{\lambda \mathbf{u}^T (\Sigma^{-1/2} \mathbf{Z}_1)} \right\} \leq e^{\frac{\sigma^2 \lambda^2}{2}}$. Denote by $\kappa = \|\Sigma^{-1/2} \mathbf{Z}_1\|_{\psi_2}$ the sub-Gaussian norm of $\Sigma^{-1/2} \mathbf{Z}_i$ for $i = 1, \dots, n$, where κ is a finite positive constant.

A3. Variables irrelevant the exposure are also irrelevant to the outcome, i.e. $\{k : \gamma_k^* = 0\} \subseteq \{k : \pi_k^* = 0\}$.

A4. The number of variables relevant to the exposure D , denoted by s_1^* , is fixed. The number of invalid instruments that violate the exclusion restriction assumption (I2) is also fixed and denoted by s_2^* .

A5. There exist positive $c_0, C_0, \check{c}_0, \check{C}_0$ such that $c_0 \leq |\gamma_k^*| \leq C_0$ for all relevant variables k and for all invalid instrument k , the degree of violation satisfies $\check{c}_0 \leq |\pi_k^*| \leq \check{C}_0$. There exists $c > 0$ such that $\min_{k: \gamma_k^* \neq 0} |\text{cov}(D/\gamma_k^*, Z_k)| \geq c$.

A6. Let $\eta_{\max} = \max(1, B \sup_{\mathcal{S}: |\mathcal{S}|=s} \max_{1 \leq j \leq s} \|[\Sigma_{\mathcal{S}}^{-1}]_{-j,j}\|_1)$, where $\Sigma_{\mathcal{S}}^{-1}$ denotes the inverse of $\Sigma_{\mathcal{S}}$ formed by rows and columns of Σ indexed by \mathcal{S} and $[\]_{-j,j}$ represents the j th column without the j th component of the matrix. Assume $\eta_{\max} = o((n/\log p)^{1/8})$.

A7. Let $\lambda_\gamma = C_\gamma \sqrt{(\log p)/n}$ with $C_\gamma \geq 5.7 \sqrt{B(\boldsymbol{\alpha}_D^{*\top} \Sigma_U \boldsymbol{\alpha}_D^* + \sigma_D^2)}$ and $\lambda_\Gamma = C_\Gamma \sqrt{(\log p)/n}$ with $C_\Gamma \geq 5.7 \sqrt{B\{(\beta^* \boldsymbol{\alpha}_D^* + \boldsymbol{\alpha}_Y^*)^\top \Sigma_U (\beta^* \boldsymbol{\alpha}_D^* + \boldsymbol{\alpha}_Y^*) + \beta^{*2} \sigma_D^2 + \sigma_Y^2\}}$, where $\lambda_\gamma, \lambda_\Gamma$ are tuning parameters in the lasso problems defined after (3.1). Moreover, the tuning parameters in the nodewise lasso problems (G.1) satisfy $\lambda_j \equiv 4a_2 \eta_{\max} \sqrt{(\log p)/n}, j = 1, \dots, s$ and a constant $a_2 > 4\sqrt{3}eB\kappa^2$.

Assumptions A1 and A2 are distribution assumptions for candidate instruments, unmeasured confounding and random errors in the models (2.1) and (2.2). In A3 we for simplicity assume that candidates that are irrelevant to the exposure are also irrelevant to the outcome. This can be relaxed at the cost of additional technicalities in the arguments. Similarly, assumption A4 is made for simplicity and can be relaxed at the cost of more technical arguments. The relevance strength for valid and invalid instruments is provided in A5; A5 also rules out candidates that are marginally uncorrelated but jointly correlated with the exposure. We can allow the relevance strength to decay at rates $c_0 \gtrsim \eta_{\max} \sqrt{(\log p)/n}$ at the cost of introducing additional technicalities in the proofs. Assumption A6 gives conditions on maximal row-wise ℓ_1 norm for precision matrix $\Sigma_{\hat{\mathcal{S}}_1}^{-1}$ uniformly over all $\hat{\mathcal{S}}_1$ of cardinality s . Restrictions on this quantity are also considered in [van de Geer et al. \(2014\)](#). Conditions for lasso tuning parameters are collected in A7.

3.3.1 Concentration of estimates from spurious instruments

We now consider concentration of Wald ratios from spurious instruments that pass joint thresholding.

Theorem 3.1 (Concentration results for spurious instruments). Suppose assumptions A1–A7 hold. Further assume $\log p = O(n^{\tau_1})$ for $0 < \tau_1 < 1$, $n^{\tau_2} = O(s)$ for $0 < \tau_2 < 1$ and $(\log p)^{3/4} = o(n^{1/4}\sqrt{\log s})$. Let

$$\tilde{C} := \frac{8 \left\{ \text{var}(\boldsymbol{\alpha}_Y^{*\top} \mathbf{U}) - \frac{\text{cov}^2(\boldsymbol{\alpha}_Y^{*\top} \mathbf{U}, \boldsymbol{\alpha}_D^{*\top} \mathbf{U})}{\text{var}(\boldsymbol{\alpha}_D^{*\top} \mathbf{U} + \epsilon_D)} + \sigma_Y^2 \right\}^{1/2}}{\sqrt{\text{var}(\boldsymbol{\alpha}_D^{*\top} \mathbf{U} + \epsilon_D)}}$$

There exists a constant $C_1 > 0$ independent of ω such that for n, p sufficiently large

$$P \left(\cup_{l \in \tilde{\mathcal{I}} \cap \hat{\mathcal{S}}_2} \left\{ \left| \frac{\hat{\Gamma}_{\hat{\mathcal{S}}_1, l}}{\hat{\gamma}_{\hat{\mathcal{S}}_1, l}} - \beta^* - C_* \right| > \tilde{C} / \sqrt{\omega} \right\} \right) \leq 2s^{-3} + e^{-C_1 \log(n \wedge p)}.$$

Theorem 3.1 formally verifies the empirical observation that estimates from spurious instruments concentrate in a region around $\beta^* + C_*$. The width of this region shrinks for higher threshold parameters ω and can be made small if ω is chosen sufficiently large.

The centering $\beta^* + C_*$ coincides with the ordinary least squares estimate, and also appears in the weak IV literature (Nelson & Startz, 1990b; Bound et al., 1995; Stock et al., 2002) which suggest that as the instrumental strength approaches zero, the causal effect estimate approaches $\beta^* + C_*$. These results, however, assume that the number of weak instruments is fixed or increases at a slower rate than the sample size. Moreover, they place additional constraints on the convergence rate of the relevance strength of weak IVs. In contrast, we allow the number of irrelevant candidate instruments before screening to grow at an exponential rate and explicitly take into account randomness from both – first stage screening and hard thresholding based on the debiased lasso. This makes our theoretical analysis substantially more involved.

3.3.2 Concentration of estimates by relevant instruments

Next, consider the behaviour of causal effect estimates from relevant instruments that pass joint thresholding.

Theorem 3.2 (Concentration results for relevant (valid and invalid) instruments). Suppose assumptions A1, A2 and A4–A7 hold. Further assume $\log p = O(n^{\tau_1})$ for $0 < \tau_1 < 1$ and $n^{\tau_2} = O(s)$ for $0 < \tau_2 < 1$. Then the set $\hat{\mathcal{S}}_2$ includes all relevant variables with probability going to one. Moreover, there exist constants $C_1, C_2 > 0$ such that the following holds when n, p are sufficiently large

$$P \left(\max_{l \in \tilde{\mathcal{R}} \cap \hat{\mathcal{S}}_2} \left| \frac{\hat{\Gamma}_{\hat{\mathcal{S}}_1, l}}{\hat{\gamma}_{\hat{\mathcal{S}}_1, l}} - \left(\beta^* + \frac{\pi_{\hat{\mathcal{S}}_1, l}^*}{\gamma_{\hat{\mathcal{S}}_1, l}^*} \right) \right| > C_2 \sqrt{\frac{\log p}{n}} \frac{\eta_{max}}{C_L} \right) \leq e^{-C_1 \log(n \wedge p)}.$$

Theorem 3.2 confirms that estimates from valid IV's concentrate around the true causal effect and causal effect estimates from invalid IVs which violate the exclusion restriction assumption (I2) concentrate around $\beta^* + \pi_{\hat{\mathcal{S}}_1, l}^* / \gamma_{\hat{\mathcal{S}}_1, l}^*$, even after marginal screening and joint thresholding via debiased lasso estimates.

Combining the findings in Theorem 3.1 and Theorem 3.2 shows that the estimates from valid instruments can be separated from those from spurious instruments with probability going to one for ω satisfying

$$\frac{1}{\sqrt{\omega}} < \frac{|\text{cov}(\boldsymbol{\alpha}_D^{*\top} \mathbf{U}, \boldsymbol{\alpha}_Y^{*\top} \mathbf{U})|}{\tilde{C} \text{var}(\boldsymbol{\alpha}_D^{*\top} \mathbf{U} + \epsilon_D)} \quad (3.3)$$

Indeed, from Theorem 3.2 we see that causal estimates from all valid instruments will concentrate around the true effect β^* . In contrast, estimates from spurious instruments concentrate within the interval $[\beta^* + C_* - \tilde{C}/\sqrt{\omega}, \beta^* + C_* + \tilde{C}/\sqrt{\omega}]$ as shown in Theorem 3.1. This interval does not contain β^* provided that $\tilde{C}/\sqrt{\omega} < |C_*|$, which can always be achieved by choosing ω sufficiently large.

Results in this section formalize the intuition for why a naive application of the procedure to identify valid instruments under plurality after applying marginal screening can fail – all estimates from spurious instruments concentrate around the same value, leading to a violation of the empirical plurality rule. Our results also suggest a way out: since valid and invalid instruments still concentrate around the same values as without marginal screening, and since all estimates from spurious instruments are similar and separated from valid instruments, all that we need is to identify estimates from spurious instruments. This motivates the methodology in the next section.

4 Fighting Noise with Noise

As established in the previous sections, a major challenge for causal inference with many candidate instruments is the presence of spurious instruments and distinguishing the valid instruments from the spurious ones. To solve this problem, the key idea in our developments is to add independent noises, known as pseudo variables, to the initial candidate instrument set. These pseudo variables mimic the behaviour of the irrelevant variables in the original set, as both of them are independent of the exposure D .

Specifically, since the vast majority of candidate instruments in most applications are irrelevant, we propose to generate p pseudo variables Z_{p+1}, \dots, Z_{2p} by randomly permuting the rows of the design matrix $\mathbb{Z} \in \mathbb{R}^{n \times p}$. The resulting matrix $\tilde{\mathbb{Z}} \in \mathbb{R}^{n \times p}$ is independent of D and has the same correlation structure as the original candidate instruments \mathbb{Z} . The expanded candidate instrument matrix $\tilde{\mathbb{Z}} \in \mathbb{R}^{n \times 2p}$ is defined as the concatenation of \mathbb{Z} and $\tilde{\mathbb{Z}}$; see step 0 of Algorithm 2.

Steps 1–2 of Algorithm 2 are direct applications of Steps 1–2 of Algorithm 1 with inputs \mathbf{D} , \mathbf{Y} and $\tilde{\mathbb{Z}}$. To be more specific, we use marginal screening and joint thresholding to estimate relevant variables to the exposure within the expanded set of $2p$ candidates. With slight abuse of notation, we use $\check{\mathcal{S}}_1 \subset \{1, \dots, 2p\}$ to denote the index set of the s candidate instruments selected from marginal screening. Let $\hat{\Gamma}_{\check{\mathcal{S}}_1}$ and $\hat{\gamma}_{\check{\mathcal{S}}_1}$ denote the debiased lasso estimators based on the candidate instruments in $\check{\mathcal{S}}_1$. The resulting estimated set of relevant instruments is $\check{\mathcal{S}}_2 = \{1 \leq l \leq s : |\hat{\gamma}_{\check{\mathcal{S}}_1, l}| \geq \delta_n \times \text{SE}(\hat{\gamma}_{\check{\mathcal{S}}_1, l})\}$, where $\delta_n = \sqrt{\omega \log(\max\{n, s\})}$ and the standard error $\text{SE}(\hat{\gamma}_{\check{\mathcal{S}}_1, l})$ is obtained similarly to (3.2).

Remark 4.1. The tuning parameter ω plays an important role in our procedure. As we demonstrated theoretically, larger values for ω lead to better concentration of effect estimates from spurious instruments passing joint thresholding. At the same time, large values of ω mean that the joint thresholding step filters out more variables. In finite samples this can lead to discarding some valid instruments, leading to efficiency loss in downstream analyses.

In Step 3 of Algorithm 2, we identify the spurious instruments and remove them from the candidate set, together with all the pseudo variables. Specifically, we calculate the ratio estimate $\hat{\beta}^{(l)} = \hat{\Gamma}_{\check{\mathcal{S}}_1, l} / \hat{\gamma}_{\check{\mathcal{S}}_1, l}$ for each $l \in \check{\mathcal{S}}_2$. We then remove all the pseudo variables from $\check{\mathcal{S}}_2$, together with all the candidate instruments whose corresponding causal effect estimate $\hat{\beta}^{(l)}$ falls into the range of causal effect estimates corresponding to the pseudo variables. The resulting set of candidate instruments is denoted as $\check{\mathcal{S}}_3$.

In Step 4 of Algorithm 2, we develop a mode-finding procedure to distinguish the valid instruments from the invalid and remaining spurious instruments. Similar to the literature on invalid IVs, we assume the plurality rule holds in $\check{\mathcal{S}}_3$, i.e. the largest group of invalid or remaining spurious instruments with the same Wald ratio is smaller than the group of valid instruments. Recall that the population mode of $\{\beta^{(j)} : j \in \check{\mathcal{S}}_3\}$ is the value that appears most frequently, i.e.

$$\text{mode}\{\beta^{(l)} : l \in \check{\mathcal{S}}_3\} = \underset{\beta^{(l)} : l \in \check{\mathcal{S}}_3}{\text{argmax}} |\{j \in \check{\mathcal{S}}_3 : \beta^{(j)} = \beta^{(l)}\}|, \quad (4.1)$$

where $|\cdot|$ denotes cardinality of a set and we define $\beta^{(j)} = \beta^* + C_*$ for indices j corresponding to irrelevant instruments. Under the population plurality rule the set \mathcal{V} of valid instruments in $\check{\mathcal{S}}_3$ is given by $\mathcal{V} = \{j \in \check{\mathcal{S}}_3 : \beta^{(j)} = \text{mode}\{\beta^{(l)} : l \in \check{\mathcal{S}}_3\}\}$.

To account for statistical uncertainty due to estimating $\beta^{(l)}$ in (4.1), we say two estimates $\hat{\beta}^{(j)}$ and $\hat{\beta}^{(l)}$ are close if $|\hat{b}^{(j,l)}|/\text{SE}(\hat{b}^{(j,l)})$ is below a certain threshold; here $\hat{b}^{(j,l)} = \hat{\beta}^{(l)} - \hat{\beta}^{(j)}$ is the distance between the estimates $\hat{\beta}^{(j)}$ and $\hat{\beta}^{(l)}$, and $\text{SE}(\hat{b}^{(j,l)})$ is given in (H.1) of the appendix. Following [Donoho & Johnstone \(1994\)](#), we recommend $\sqrt{\omega^2 \log(\max\{n, s\})}$ as the threshold. Here we use ω^2 to account for the number of pairwise comparisons. The estimated set $\check{\mathcal{S}}_4$ of valid instruments consists of all candidate instruments whose corresponding causal effect estimates is close to the maximal number of other causal effect estimates as formalized in Step 4 of Algorithm 2.

Once we have identified the set of valid IVs, it is straightforward to estimate the causal effect using two-stage least squares. This is summarized in Step 5 of Algorithm 2.

Remark 4.2. The voting algorithm implemented in Section 3.2, originally developed by [Guo et al. \(2018\)](#), uses a different approach than our Step 4 in Algorithm 2. It treats each of the candidate instrument $Z_l, l \in \check{\mathcal{S}}_3$ as an expert, and each expert casts votes for other $Z_j, j \in \check{\mathcal{S}}_3$. Importantly, this voting algorithm is not symmetric in that expert l casting vote for j does not imply expert j casting vote for l . In fact, under their algorithm, an effect estimate with a larger variance is likely to receive more votes. This is undesirable as the effect estimates with larger variances likely come from weak or spurious IVs. The procedure we propose solves this problem under our setting.

Algorithm 2 plays a key role in removing most irrelevant variables, but can introduce selection bias into causal effect estimate. A classical approach to deal with selection bias is sample splitting. Below, we discuss how sample splitting can be implemented in the present context. Divide data into two halves: H_1 of size n_1 and H_2 of size n_2 . The first subsample is used to identify and remove the irrelevant variables, corresponding to Steps 0–3 of Algorithm 2. On the second subsample, we apply an additional joint thresholding step to further estimate relevant variables to the exposure. Then we use the proposed mode finding algorithm in Step 4 of Algorithm 2 to identify the valid instruments and estimate the causal effect. These steps are summarized in Algorithm 1, with details discussed in Section A, both in the supplementary materials.

Although sample splitting can deal with selection bias in theory, it results in smaller samples used for identifying valid instruments and in the final estimation step. This can lead to reduced efficiency and imprecise inference in smaller samples, which may outweigh the benefits of removing selection bias. We observe this effect in some of our simulations reported in Section 5.

Algorithm 2 Fighting noise with noise

INPUT: Design matrix $\mathbb{Z} \in \mathbb{R}^{n \times p}$, observed exposure $\mathbf{D} \in \mathbb{R}^n$, observed outcome $\mathbf{Y} \in \mathbb{R}^n$.

0. Pseudo variables generation:

Generate p pseudo variables Z_{p+1}, \dots, Z_{2p} by randomly permuting the rows of \mathbb{Z} ;

Denote the resulting design matrix as $\bar{\mathbb{Z}}$, and the concatenation of \mathbb{Z} and $\bar{\mathbb{Z}}$ as $\tilde{\mathbb{Z}}$.

1+2 Marginal screening and joint thresholding:

Apply Steps 1 and 2 of Algorithm 1 with $\mathbb{Z} \in \mathbb{R}^{n \times p}$ replaced by $\tilde{\mathbb{Z}} \in \mathbb{R}^{n \times 2p}$. The resulting set of variables that pass marginal and joint thresholding is denoted by $\check{\mathcal{S}}_2$. Denote pseudos in $\check{\mathcal{S}}_2$ by $\hat{\mathcal{P}}$.

3. Irrelevant variables removal:

For each $l \in \check{\mathcal{S}}_2$, calculate a causal effect estimate $\hat{\beta}^{(l)} = \hat{\Gamma}_{\check{\mathcal{S}}_1, l} / \hat{\gamma}_{\check{\mathcal{S}}_1, l}$;

Remove variables similar to pseudo variables in their causal effect estimate $\hat{\beta}^{(l)}$ from $\check{\mathcal{S}}_2$:

$$\check{\mathcal{S}}_3 = \check{\mathcal{S}}_2 \setminus \left\{ l \in \check{\mathcal{S}}_2 : \min_{j \in \hat{\mathcal{P}}} \hat{\beta}^{(j)} \leq \hat{\beta}^{(l)} \leq \max_{j \in \hat{\mathcal{P}}} \hat{\beta}^{(j)} \right\}.$$

4. Mode finding:

For $j, l \in \check{\mathcal{S}}_3$, compute $\hat{b}^{(j,l)} = \hat{\beta}^{(l)} - \hat{\beta}^{(j)}$ and $\text{SE}(\hat{b}^{(j,l)})$;

For $j \in \check{\mathcal{S}}_3$, find the number of candidates leading to a similar causal effect estimate with Z_j :

$$V_j = \left| \left\{ l \in \check{\mathcal{S}}_3 : |\hat{b}^{(j,l)}| / \text{SE}(\hat{b}^{(j,l)}) \leq \sqrt{\omega^2 \log(\max\{n, s\})} \right\} \right|;$$

Find valid IVs using the plurality rule:

$$\check{\mathcal{S}}_4 = \left\{ j : V_j = \max_{l \in \check{\mathcal{S}}_3} V_l \right\}.$$

5. Causal effect estimation: Take $\hat{\mathcal{S}}_4, \mathbf{D}, \mathbf{Y}$ as input into 2SLS to estimate causal effect and construct confidence interval.

5 Simulation Studies

In this section, we run numerical experiments to evaluate the performance of the proposed methods. The simulation setting here is the same as in the motivating example in Section 3.2, except that here we consider various values of the random error variance in the exposure $\sigma_D^2 = 0, 2, 4$. We include the following methods for comparison:

- “Proposed (full)” represents our proposed method in Algorithm 2. The lasso penalization parameter $\lambda_\gamma, \lambda_\Gamma$ are chosen equal to $\sqrt{(\log p)/n}$, which is approximately 0.15. For the node-wise lasso, we follow van de Geer et al. (2014) and choose the same tuning parameter λ_j using 10-fold cross-validation among all node-wise regressions. We take $\omega = 2.01$ (Donoho & Johnstone, 1994; Donoho, 1995).
- “Proposed (split)” refers to the sample splitting method outlined at the end of Section 4 and detailed in Algorithm 1 of the supplementary materials. We choose $n_1 = 300$ and $n_2 = 200$. The tuning parameters are chosen similarly to the “Proposed (full)”. To be more specific, on the first sample, we use $\sqrt{(\log s)/n_1}$ in the joint threshold to estimate relevant variables, while on the second sample, we use $\sqrt{(\log q)/n_2}$ in joint thresholding, where q denotes the number of remaining candidates after removing spurious IVs.
- “Naive” is the naive Algorithm 1. The tuning parameters $\lambda_\gamma, \lambda_\Gamma$ are chosen in the same way as “Proposed (full)”.
- “Oracle” is the 2SLS estimator based on valid instruments only, which provides a benchmark for comparison.

Motivated by the data application in Section 6, for the implementation of the methods “Proposed (full)”, “Proposed (split)” and “Naive”, we take $s = 500$ in the marginal screening step. We measure the performance through 1000 Monte Carlo simulations. Simulation results regarding estimated bias, root-mean-square error (RMSE) and empirical coverage are summarized in Table 1.

The simulation results suggest that the proposed procedure using full data outperforms competing methods in terms of bias, efficiency and validity of inference. Similar to our findings in Section 3.2, estimates by “Naive” are biased. Although sample splitting gives acceptable empirical coverage when σ_D^2 is small, the bias and RMSE are much larger compared to the ones obtained by the proposed method using full data. When the variance of the random error in the exposure ϵ_D increases, the performance of “Proposed (full)” remains similar, which indicates that our approach using full data works even when the variance of unobserved confounding is relatively small compared to that of the random error ϵ_D . For the sample splitting method, one can see the RMSE increases and the coverage probability decreases further below the nominal level when ϵ_D increases.

To better understand the performance of various methods as summarized in Table 1, we report the average number of valid, invalid and spurious instruments in \check{S}_2, \check{S}_3 and \check{S}_4 respectively in Table 2. The results show that “Naive” misidentifies spurious instruments as valid and misses many or almost all the valid instruments. The sample splitting procedure can find most valid instruments when the variance σ_D^2 is small. However, the estimated set of valid instruments will include some invalid ones since we only use part

Table 1: Performance summary for various methods and σ_D^2 across 1000 Monte Carlo runs with $n = 500$ and $p = 50,000$. We make the numbers bold for the method with the best performance except for the oracle estimate. Standard errors are presented in the bracket if applicable. For simplicity, we write $SE = 0.00$ if $SE < 0.005$

| | Method | Bias $\times 10$ (SE $\times 10$) | RMSE $\times 10$ | Coverage (Nominal = 95%) |
|------------------|------------------|------------------------------------|------------------|--------------------------|
| $\sigma_D^2 = 0$ | Proposed (full) | -0.10(0.02) | 0.66 | 0.92 |
| | Proposed (split) | -0.26(0.07) | 2.16 | 0.90 |
| | Naive | -2.23(0.02) | 2.28 | 0.01 |
| | Oracle | -0.02(0.01) | 0.28 | 0.94 |
| $\sigma_D^2 = 2$ | Proposed (full) | -0.08(0.02) | 0.56 | 0.92 |
| | Proposed (split) | -0.18(0.08) | 2.38 | 0.87 |
| | Naive | -1.82(0.02) | 1.94 | 0.06 |
| | Oracle | -0.02(0.01) | 0.27 | 0.94 |
| $\sigma_D^2 = 4$ | Proposed (full) | -0.16(0.04) | 1.24 | 0.90 |
| | Proposed (split) | -0.09(0.09) | 2.86 | 0.82 |
| | Naive | -1.09(0.02) | 1.28 | 0.21 |
| | Oracle | -0.02(0.01) | 0.27 | 0.94 |

Table 2: Average number of invalid, valid IVs and irrelevant variables in \check{S}_2 (the candidate set after joint thresholding), \check{S}_3 (the candidate set after removing spurious instruments) and \check{S}_4 (the estimated set of valid IVs), respectively. Note that “Naive” is applied without including pseudo variables. The results are based on $n = 500$, $p = 50,000$ and 1000 Monte Carlo runs. “-” stands for “inapplicable”

| | Method | \check{S}_2 | | | \check{S}_3 | | | \check{S}_4 | | |
|------------------|------------------|---------------|-------|------------|---------------|-------|------------|---------------|-------|------------|
| | | Invalid | Valid | Irrelevant | Invalid | Valid | Irrelevant | Invalid | Valid | Irrelevant |
| $\sigma_D^2 = 0$ | Proposed (full) | 2.00 | 7.00 | 30.53 | 1.99 | 6.99 | 1.87 | 0.00 | 6.69 | 0.51 |
| | Proposed (split) | 1.93 | 7.00 | 48.12 | 1.84 | 6.74 | 2.08 | 0.19 | 6.73 | 0.07 |
| | Naive | 2.00 | 7.00 | 15.26 | - | - | - | 0.00 | 0.02 | 15.25 |
| $\sigma_D^2 = 2$ | Proposed (full) | 2.00 | 7.00 | 35.19 | 1.97 | 6.99 | 1.95 | 0.01 | 6.88 | 1.04 |
| | Proposed (split) | 1.92 | 7.00 | 53.37 | 1.80 | 6.46 | 2.01 | 0.24 | 6.42 | 0.05 |
| | Naive | 2.00 | 7.00 | 17.67 | - | - | - | 0.00 | 0.60 | 17.66 |
| $\sigma_D^2 = 4$ | Proposed (full) | 2.00 | 7.00 | 39.55 | 1.98 | 6.61 | 2.00 | 0.04 | 6.50 | 1.16 |
| | Proposed (split) | 1.92 | 7.00 | 58.00 | 1.81 | 5.29 | 2.01 | 0.33 | 5.19 | 0.12 |
| | Naive | 2.00 | 7.00 | 20.45 | - | - | - | 0.00 | 2.93 | 20.45 |

of the data and the estimates have larger variation than those obtained using the full sample. Consequently, the resulting causal effect estimate has moderate bias and the empirical coverage deviates from the nominal level. In comparison, using our proposed method on the full sample can locate spurious instruments with the help of pseudo variables and correctly identify most valid instruments even if σ_D^2 is large.

To provide further insights, we plot the distribution of $\hat{\beta}^{(j)}$ collected from all Monte Carlo runs for valid, invalid and spurious instruments in $\check{\mathcal{S}}_2$, $\check{\mathcal{S}}_3$ and $\check{\mathcal{S}}_4$ respectively in (a)-(c) of Figure 3, obtained from “Proposed (full)” under $\sigma_D^2 = 0$. We can see that causal effect estimates from spurious instruments and valid instruments are separable. Most spurious instruments lie in the region formed by causal effect estimates from pseudo variables, and thus are removed by following the proposed procedure. Thereafter the collection of valid instruments satisfies the plurality rule empirically, so the mode-finding step is able to identify the valid instruments.

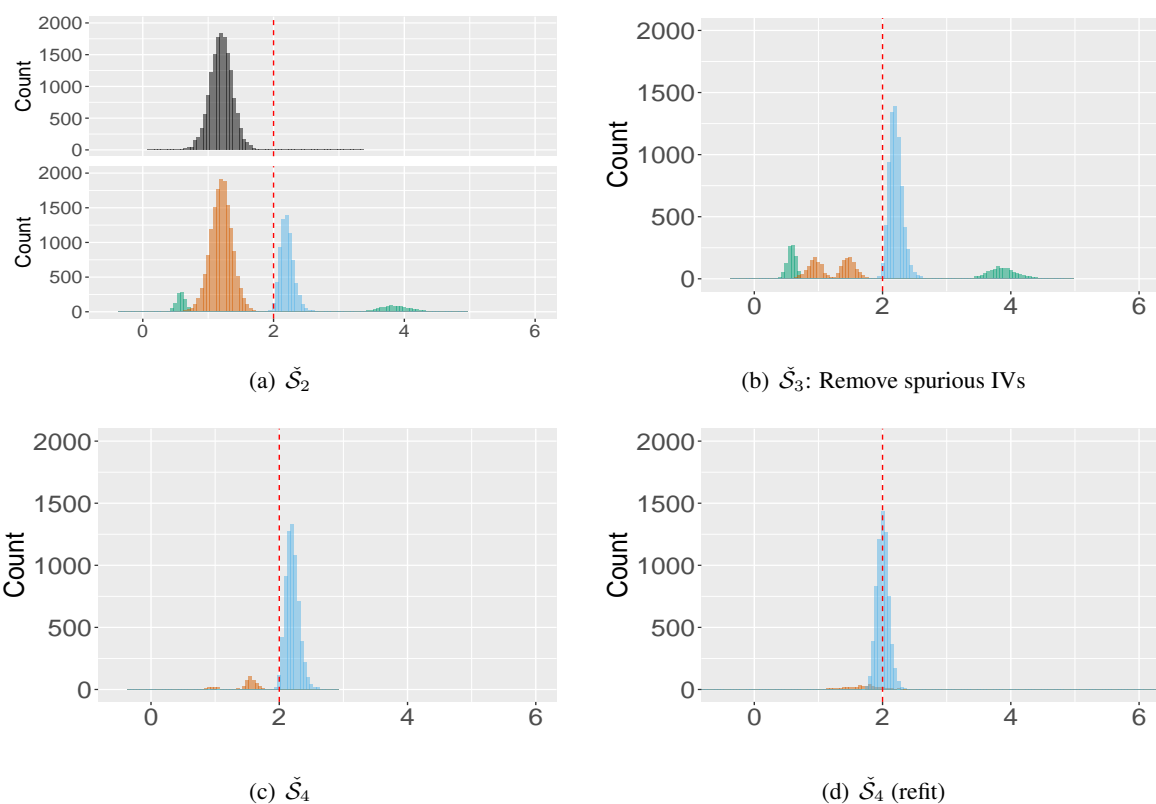


Figure 3: Plots (a)-(d) correspond to the simulation in Section 5: Plots (a) to (c) are histograms of causal effect estimates from valid, invalid and spurious instruments in $\check{\mathcal{S}}_2$, $\check{\mathcal{S}}_3$ and $\check{\mathcal{S}}_4$ respectively obtained from Algorithm 2 across 1000 Monte Carlo runs. The blue pile represents causal effect estimates by valid IVs; the green piles represent those by invalid IVs; the orange pile represents those by irrelevant variables in the initial candidate set; the black pile represents those by pseudo variables. The red dashed line is the true causal effect $\beta^* = 2$. The results are based on $(n, p, \sigma_D^2) = (500, 50, 000, 0)$. Plot (d) gives the distribution of effect estimates from refitted model.

To further evaluate the performance of the proposed method, we consider a variety of additional settings

in Section F of the supplementary materials. In particular, under the same data generating setting here, we evaluate our method when there are much more noise variables to start with. Additionally, we consider scenarios where irrelevant variables are correlated with valid instruments, some irrelevant variables are correlated with each other, and simulations under multivariate unmeasured confounders. We also carry out numerical experiments, in which the “independence” IV assumption (I3) is violated. Furthermore, since irrelevant variable can be seen as an extreme case of the weak instrument, we compare with competing methods (Donald & Newey, 2001; Carrasco, 2012; Carrasco & Tchuente, 2015) in the econometric literature that deal with many IVs where some are possibly weak.

6 Real Data Application

We apply the proposed procedure to evaluate the effect of obesity on Health-Related Quality of Life (HRQL). Obesity increases the risks of many health problems, such as heart disease, diabetes, high blood pressure, and certain cancers. Mechanical stress resulting from obesity can also impair mental well-being (Myers & Rosen, 1999; Katz et al., 2000). Health-related quality of life (HRQL) is emerging as an important outcome in obesity studies, which refers to the overall effects of medical conditions on physical and mental functioning and well-being as subjectively evaluated and reported by the patient (Fontaine et al., 1996). The development of standardized measures of HRQL helps us better understand the impact of a given illness on physical and mental health, and further influences public health policies.

To examine the causal relationship between obesity and HRQL, we use data from the Wisconsin Longitudinal Study (WLS). The WLS genetic data is sponsored by the National Institute on Aging (grant numbers R01AG009775, R01AG033285, and R01AG041868) and was conducted by the University of Wisconsin. More information can be found at <https://www.ssc.wisc.edu/wlsresearch/>. Study participants were graduates from Wisconsin high schools in 1957 and their siblings (Herd et al., 2014). Our analysis focuses on unrelated graduates reinterviewed in 2011. We take BMI as the exposure, a measure commonly used to define obesity. It ranges from 12 to 64 in the data set. The healthy range for BMI is between 18.5 and 24.9. As shown in Figure 6 in the supplementary materials, for underweight and normal individuals, HRQL is positively correlated with BMI, while for overweight or obese ones, HRQL is negatively correlated with BMI. Motivated by this observation, We shall restrict our analysis to participants whose BMI is above 25. There are 3023 subjects in total, 51% of which are females. In our analysis, the average BMI is 30.6 with standard deviation 4.93. To measure HRQL, we use the Health Utility Index Mark 3 (HUI-3) which takes values between -0.22 and 1. HUI-3 measured on the subjects in our analysis has mean 0.786 and standard deviation 0.227. We adjust for observed covariates including age, gender and year of education. Among participants considered in our analysis, the average age is 71.2 years old with standard deviation 0.9; the average education length is 13.8 years with standard deviation 2.38. We also adjust for the top six principal components to account for population stratification (Patterson et al., 2006; Sanderson et al., 2021), which are obtained by performing principal components analysis (PCA) on unrelated study participants.

We begin with a crude analysis that ignores the unmeasured confounding. Simply regressing the HUI-3 on BMI gives the OLS estimate -0.011 with 95% CI $[-0.013, -0.009]$. However, unmeasured factors such as smoking status and the use of alcohol may confound the relationship between BMI and HUI-3. In

response to this potential problem, we use the MR method to investigate the causal relationship between these two. After quality control (QC) filtering of SNPs, we get a candidate set of 3,683,868 genetic variants in our MR analysis. Details of the QC steps are discussed in Section B.2 of the supplementary materials. Following Algorithm 2, we generate pseudo variables by randomly permuting the SNP design matrix by rows, resulting in a candidate set of 7,367,736 variants in total.

We first apply a marginal screening step to quickly reduce the dimension of initial candidate instruments via ranking the marginal correlation in absolute value between each candidate instrument and the exposure. A common choice is to keep $\lfloor n/\log(n) \rfloor$ candidates (Fan & Lv, 2008), which is approximately 460 in our analysis. We round it to the nearest multiple of 100. Specifically, in the marginal screening step, by ranking the absolute marginal strength of association with BMI, we keep the top 500 candidate instruments, denoted by $\check{\mathcal{S}}_1(\text{Proposed})$. There were 268 true variants and 232 pseudo ones included in this set. To further identify genetic variants related to BMI, we fit a joint model for the 500 candidate instruments.

We visualize in Figure 4(a) the result from our proposed method. Specifically, a total of 75 SNPs ($\check{\mathcal{S}}_2(\text{Proposed})$) pass the joint thresholding, corresponding to all the points shown in Figure 4(a). The 34 points on the left of the orange dashed line correspond to true genetic variants, while the 37 red dots on the right correspond to pseudo variants. In $\check{\mathcal{S}}_2(\text{Proposed})$, causal effect estimates from 71 SNPs fall into the region formed by pseudo variants, which is represented by the band between the two black dashed lines. These SNPs are estimated as spurious and are removed from the candidate set. The remaining 4 points outside the region are genetic variants that are estimated to be relevant to BMI ($\check{\mathcal{S}}_3(\text{Proposed})$). An application of the proposed mode-finding procedure on $\check{\mathcal{S}}_3(\text{Proposed})$ gives us 3 valid instruments ($\check{\mathcal{S}}_4(\text{Proposed})$), corresponding to the blue squares in Figure 4(a): “rs144468788” on chromosome 2 and in the MIR4432 host gene (MIR4432HG); “rs113116137” and “rs2546230” on chromosome 8, and “rs113116137” is in the CUB And Sushi Multiple Domains 1 (CSMD1) gene. The purple point at the bottom represents the estimated invalid instrument. Finally, we fit two-stage least squares using the three identified valid IVs and obtain the causal effect estimate $\hat{\beta} = -0.039$ with 95% confidence interval $[-0.052, -0.025]$. This suggests that in the overweight or obese population, one unit increase in BMI will result in 0.039 unit decrease of HUI-3. In other words, one standard deviation increase in BMI leads to roughly one standard deviation decrease in health-related quality of life.

To explore that the standard GWAS threshold might be too stringent to retain genetic variants associated with the trait of interest in our data application, we apply the genome-wide significance p -value threshold of 5×10^{-8} to the true genetic variants to identify significant associations with BMI. This gives us only one SNP “rs148605555” on chromosome 9. Although the SNP is estimated as relevant to BMI using our procedure, that is, the SNP is in the set $\check{\mathcal{S}}_2(\text{Proposed})$, the associated effect estimate given by -0.008 lies in the middle of the estimated range by pseudos and thus the SNP is identified as spurious in the proposed method. In addition, the effect estimate of the SNP that passes the GWAS threshold is close to the OLS estimate, an indication that this might be a spurious one.

For comparison, we also apply Algorithm 1, denoted by “Naive”, to this data set. The results are visualized in Figure 4(b). Specifically, we apply marginal screening to the true genetic variants only and keep the top 500 ($\hat{\mathcal{S}}_1(\text{Naive})$) by ranking absolute marginal strength concerning the exposure. The joint thresholding step keeps 44 variants ($\hat{\mathcal{S}}_2(\text{Naive})$), and 29 of them are estimated as valid IVs ($\hat{\mathcal{S}}_4(\text{Naive})$). Comparing the candidate instruments retained after the joint thresholding, we note that $\check{\mathcal{S}}_2(\text{Proposed})$ and

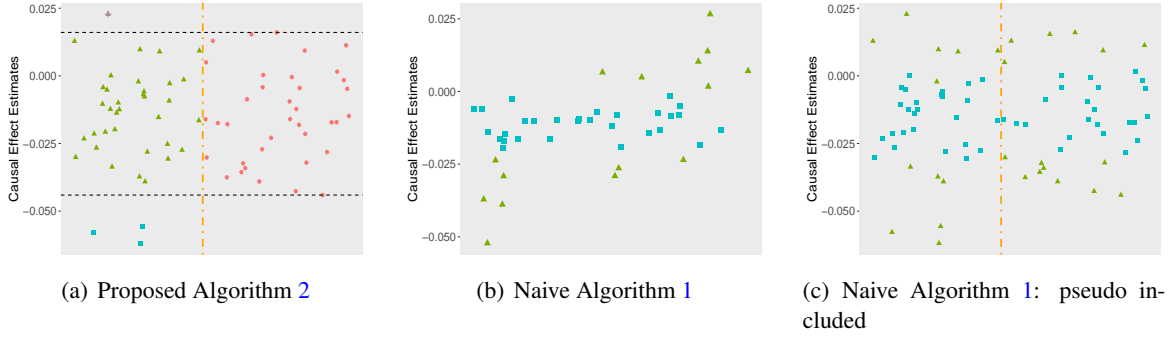


Figure 4: Causal effect estimates from estimated relevant SNPs versus SNP index. (a): Causal effect estimates associated with genetic variants in $\check{\mathcal{S}}_2(\text{Proposed})$. The orange dot-dashed line separates pseudo and real genetic variants. Red dots represent pseudo SNPs and all the others are true genetic variants. The two black dashed lines represent the estimated range. The three blue squares represent valid instruments identified through our procedure, and the gray diamond represents the invalid instrument we identified. (b): Causal effect estimates from relevant SNPs estimated by Algorithm 1 (“Naive”) which is applied to true variants only. The blue squares represent valid IVs identified by “Naive” and green triangles represent estimated invalid IVs. (c) Results from Algorithm 1 with pseudos included. The orange dot-dashed line separates pseudo and real genetic variants. Green triangles refer to SNPs identified as invalid. The blue squares are SNPs identified as valid instruments.

$\hat{\mathcal{S}}_2(\text{Naive})$ have 15 variants in common, and only one common variant “rs144468788”, corresponding to the point at the bottom left corner in Figure 4(b), is also estimated as relevant by “Proposed”, i.e. $\{\text{rs144468788}\} \subset \check{\mathcal{S}}_3(\text{Proposed})$. The “rs144468788” is estimated as invalid by “Naive”, but valid by “Proposed”, i.e., $\hat{\mathcal{S}}_4(\text{Naive}) \cap \check{\mathcal{S}}_4(\text{Proposed}) = \emptyset$. Interestingly, the resulting causal effect estimate by “Naive”, that is -0.010 (95% CI $[-0.015, -0.005]$), is roughly the same as the OLS estimate, equivalently saying that one standard deviation increase in BMI leads to approximately 0.2 standard deviation decrease in health-related quality of life.

To further understand the behaviour of the naive Algorithm 1 with this data set, we apply this method to the candidate set $\check{\mathcal{S}}_1(\text{Proposed})$ obtained after marginal screening in our procedure. In doing this, we pretend that the analyst does not know which variables in $\check{\mathcal{S}}_1(\text{Proposed})$ are pseudo variables. Analysis results in Figure 4(c) show that as expected, “Naive” misidentifies many pseudo variables as valid instruments. The resulting causal effect estimate, -0.012 (95% CI $[-0.016, -0.008]$), which is close to the OLS estimate. That is to say, one standard deviation increase in BMI roughly leads to 0.2 standard deviation decrease in health-related quality of life.

In our data application, we did not implement the sample splitting Algorithm 1 for two main reasons: for one thing, the sample splitting method suffers from power loss, which is also demonstrated in our numerical experiments. And for another, the SNP matrix is encoded as 0,1,2, which represents possible genotypes. Splitting the data might dramatically change the genotype distribution since possibly some genotypes appear more often in one portion of the data but not the other (Barber & Candes, 2019).

We close this section by performing additional numerical studies to explore the uncertainty of the aforementioned results, due to the randomness induced by generating pseudo variants. We run the procedure 50

times by repeatedly permuting the true SNP design matrix to generate pseudos. The median of causal effect estimates is -0.037 . For comparison, we also repeat Algorithm 1 to the same candidate set used in our procedure 50 times. The median of the resulting effect estimates is -0.010 .

7 Discussion

To make causal inference with many candidate instruments, it is common to first reduce the dimension of candidate instruments with screening procedures. If the number of candidate instruments is large, and/or the sample size is small to moderate, there may be more spurious instruments than valid instruments in the estimated set of variables relevant to the exposure. In this paper, we show that this can lead to biased causal inference. In particular, the resulting causal effect estimate may be close to the OLS estimate that does not account for any unmeasured confounding. We also develop a novel strategy that constructs pseudo variables to find the spurious instruments.

We note that spurious instruments may not be a practical problem if the number of candidate instruments is moderate, or if the sample size is very large. For example, this may not be a major concern in large-scale GWAS with hundreds of thousands of samples.

Our work is related to a strand of research in econometrics on consistent estimation in instrumental variables regression with many (possibly weak) instruments (e.g. [Chao & Swanson, 2005](#); [Hansen et al., 2008](#); [Carrasco & Tchuente, 2015](#)). The setup they consider only involves valid instruments, while our method deals with the potential irrelevant and invalid instruments in the candidate instruments set. Our method may also be extended to deal with weak instruments. On a high level, a weak instrument behaves like a valid, invalid or spurious instrument depending on the rate of convergence of the instrumental strength. Under the simple setting as displayed in Figure 5, where the instrument Z is weakly correlated with the exposure D and is independent of the unobserved confounding U , [Nelson & Startz \(1990b\)](#) has shown that the Wald estimate satisfies the expansion below

$$\hat{\beta} - \beta^* = \frac{\widehat{\text{cov}}(Z, U)}{\frac{1}{\alpha^*} \widehat{\text{cov}}(Z, U) + \gamma^*}. \quad (7.1)$$

Here $\widehat{\text{cov}}$ denotes the sample covariance. The limit of the right-hand side of (7.1) depends on the rate at which the relevance parameter γ^* converges to 0. Specifically, if the covariance term $\widehat{\text{cov}}(Z, U)$ converges in probability to zero at $n^{-1/2}$ rate, then the bias of IV estimate concentrates at α^* when $\gamma^* = 0$ or $\gamma^* \rightarrow 0$ faster than $n^{-1/2}$. If $\gamma^* \rightarrow 0$ slower than $n^{-1/2}$, then the bias is asymptotically zero and Z behaves like a valid instrument. When $\gamma^* \rightarrow 0$ at the $n^{-1/2}$ rate, or mathematically, $\gamma^* = cn^{-1/2}$ for some constant $c > 0$, Z behaves like an invalid instrument with the degree of violation determined by c . Extending this result for effect estimation after screening and thresholding is an interesting topic for future research.

Our framework is also applicable under the two-sample design where the exposure and the outcome are collected from two independent samples, say Λ_1 and Λ_2 of sizes n_1 and n_2 respectively. Here effect estimates from spurious instruments are still separable from valid instruments. But different from the one-sample design, now effect estimates from selected irrelevant variables are centered around zero since these variables exhibit spurious correlation with the exposure only on Λ_1 but not with the outcome on Λ_2 . For better illustration, we consider a simple setting where $D = \alpha_D^* U$ and $Y = \beta^* D + \alpha_Y^* U$ and assume n_1, n_2

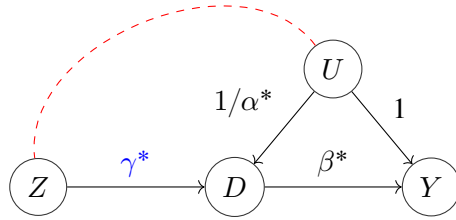


Figure 5: Graphical illustration of an instrumental variable model: Z denotes a weak instrument, D, Y represent the exposure and outcome, respectively and U is the unobserved confounding. Parameters on the arrows represent effects on the linear scale. The red dashed line refers to sample correlation.

are of the same order. Suppose only one variable Z_{j_0} survives the marginal screening, which implies that the spurious correlation between Z_{j_0} and D_{Λ_1} is the maximal correlation between D_{Λ_1} and candidate Z_j for all $1 \leq j \leq p$. One can show that the effect of Z_{j_0} on the exposure is of order $\sqrt{(\log p)/n_1}$, while the effect of Z_{j_0} on the outcome converges to zero faster at rate $1/\sqrt{n_2}$. We leave this extension for future work.

In addition, our current framework only considers invalid instruments that have a direct effect on the outcome. Empirical evidence (see Section F.6 of the supplementary materials for more details) demonstrates that our method is robust to the violation of independence assumption (I3), it would be of interest to extend our theory and validate the proposed work in more general contexts. It is also worth exploring whether our findings can be adapted to models with multiple treatments.

References

- Wisconsin Longitudinal Study. Produced and distributed by the University of Wisconsin with funding from the National Institute on Aging (grant numbers R01AG009775, R01AG033285, and R01AG041868), Madison, WI.
- ANGRIST, J. D. & KEUEGER, A. B. (1991). Does compulsory school attendance affect schooling and earnings? *The Quarterly Journal of Economics* **106**, 979–1014.
- BARBER, R. F. & CANDLES, E. J. (2015). Controlling the false discovery rate via knockoffs. *Ann. Statist.* **43**, 2055–2085.
- BARBER, R. F. & CANDLES, E. J. (2019). A knockoff filter for high-dimensional selective inference. *Ann. Statist.* **47**, 2504–2537.
- BOUND, J., JAEGER, D. A. & BAKER, R. M. (1995). Problems with instrumental variables estimation when the correlation between the instruments and the endogeneous explanatory variable is weak. *J Am Statist Assoc.* **90**, 443–450.
- BOWDEN, J., SMITH, G. D. & BURGESS, S. (2015). Mendelian randomization with invalid instruments: effect estimation and bias detection through Egger regression. *Int. J. Epidemiol.* **44**, 512–525.

- BOWDEN, J., SMITH, G. D., HAYCOCK, P. C. & BURGESS, S. (2016). Consistent estimation in Mendelian randomization with some invalid instruments using a weighted median estimator. *Genet. Epidemiol.* **40**, 304–314.
- BROWNING, S. (2008). Missing data imputation and haplotype phase inference for genome-wide association studies. *Hum Genet.* **124**, 439–450.
- BÜHLMANN, P. & VAN DE GEER, S. (2011). *Statistics for High-Dimensional Data*. Springer Series in Statistics. Springer.
- BURGESS, S., TIMPSON, N. J., EBRAHIM, S. & SMITH, G. D. (2015). Mendelian randomization: where are we now and where are we going? *Int J Epidemiol.* **44**, 379–388.
- CARRASCO, M. (2012). A regularization approach to the many instruments problem. *J. Econom.* **170**, 383–398.
- CARRASCO, M. & TCHUENTE, G. (2015). Regularized LIML for many instruments. *J. Econom.* **186**, 427–442.
- CHAO, J. C. & SWANSON, N. R. (2005). Consistent estimation with a large number of weak instruments. *Econometrica* **73**, 1673–1692.
- CHENG, X. & LIAO, Z. (2015). Select the valid and relevant moments: An information-based LASSO for GMM with many moments. *J. Econom.* **186**, 443–464.
- DE BAKKER, P. I., FERREIRA, M. A., JIA, X., NEALE, B. M., RAYCHAUDHURI, S. & VOIGHT, B. F. (2008). Practical aspects of imputation-driven meta-analysis of genome-wide association studies. *Hum Mol Genet.* **17**, R122–R128.
- DIDELEZ, V. & SHEEHAN, N. (2007). Mendelian randomization as an instrumental variable approach to causal inference. *Stat Methods Med Res.* **16**, 309–330.
- DONALD, S. G. & NEWEY, W. K. (2001). Choosing the number of instruments. *Econometrica.* **69**, 1161–1191.
- DONOHO, D. (1995). De-noising by soft-thresholding. *IEEE Trans. Inform. Theory* **41**, 613–627.
- DONOHO, D. L. & JOHNSTONE, I. M. (1994). Ideal spatial adaptation by wavelet shrinkage. *Biometrika.* **81**, 425–455.
- ECKLES, D., KIZILCEC, R. F. & BAKSHY, E. (2016). Estimating peer effects in networks with peer encouragement designs. *Proceedings of the National Academy of Sciences* **113**, 7316–7322.
- FAN, J. & LV, J. (2008). Sure independence screening for ultrahighdimensional feature space. *J. R. Statist. Soc. B.* **70**, 849–911.
- FONTAINE, K. R., CHESKIN, L. J. & BAROFSKY, I. (1996). Health-related quality of life in obese persons seeking treatment. *J Fam Pract.* **43**, 265–270.

- GOLDMAN, M. & RAO, J. (2016). Experiments as instruments: Heterogeneous position effects in sponsored search auctions. *EAI Endorsed Trans. Serious Games* **3**, e2.
- GUO, Z., KANG, H., CAI, T. T. & SMALL, D. S. (2018). Confidence intervals for causal effects with invalid instruments by using two-stage hard thresholding with voting. *J. R. Statist. Soc. B.* **80**, 793–815.
- HAN, C. (2008). Detecting invalid instruments using l_1 -GMM. *Econ. Lett.* **101**, 285–287.
- HANSEN, C., HAUSMAN, J. & NEWEY, W. (2008). Estimation with many instrumental variables. *J. Bus. Econ. Statist.* **26**, 398–422.
- HARTFORD, J. S., VEITCH, V., SRIDHAR, D. & LEYTON-BROWN, K. (2021). Valid causal inference with (some) invalid instruments. *ICML*. **139**, 4096–4106.
- HERD, P., CARR, D. & ROAN, C. (2014). Cohort Profile: Wisconsin Longitudinal Study (WLS). *Int. J. Epidemiol.* **43**, 34–41.
- HOWIE, B., MARCHINI, J. & STEPHENS, M. (2011). Genotype imputation with thousands of genomes. *G3 (Bethesda)*. **1**, 457–470.
- HOWIE, B. N., DONNELLY, P. & MARCHINI, J. (2009). A flexible and accurate genotype imputation method for the next generation of genome-wide association studies. *PLoS Genet* **5**, e1000529.
- JAVANMARD, A. & MONTANARI, A. (2014). Confidence intervals and hypothesis testing for high-dimensional regression. *J. Mach. Learn. Res.* **15**, 2869–2909.
- KANG, H., ZHANG, A., CAI, T. T. & SMALL, D. S. (2016). Instrumental variables estimation with some invalid instruments and its application to Mendelian randomization. *J. Am. Statist. Ass.* **111**, 132–144.
- KATZ, D. A., MCHORNEY, C. A. & ATKINSON, R. L. (2000). Impact of obesity on health-related quality of life in patients with chronic illness. *J Gen Intern Med.* **15**, 789–796.
- KOLESAR, M., CHETTY, R., FRIEDMAN, J., GLAESER, E. & IMBENS, G. W. (2015). Identification and inference with many invalid instruments. *J. Bus. Econ. Statist.* **33**, 474–484.
- LAURIE, C. C., DOHENY, K. F., MIREL, D. B. et al. (2010). Quality control and quality assurance in genotypic data for genome-wide association studies. *Genet Epidemiol.* **34**, 591–602.
- LAWLOR, D. A., HARBORD, R. M., STERNE, J. A. C., TIMPSON, N. & SMITH, G. D. (2008). Mendelian randomization: Using genes as instruments for making causal inferences in epidemiology. *Statist. Med.* **27**, 1133–1163.
- LI, Y., WILLER, C., SANNA, S. & ABECASIS, G. (2009). Genotype imputation. *Annu Rev Genomics Hum Genet.* **10**, 387–406.
- LI, Y., WILLER, C. J., DING, J., SCHEET, P. & ABECASIS, G. R. (2010). MaCH: Using sequence and genotype data to estimate haplotypes and unobserved genotypes. *Genet Epidemiol.* **34**, 816–834.

- MARCHINI, J., HOWIE, B., MYERS, S., MCVEAN, G. & DONNELLY, P. (2007). A new multipoint method for genome-wide association studies by imputation of genotypes. *Nat. Genet.* **39**, 906–913.
- MORRISON, J., KNOBLAUCH, N., MARCUS, J. H. et al. (2020). Mendelian randomization accounting for correlated and uncorrelated pleiotropic effects using genome-wide summary statistics. *Nat. Genet.* **52**, 740–747.
- MYERS, A. & ROSEN, J. C. (1999). Obesity stigmatization and coping: relation to mental health symptoms, body image, and self-esteem. *Int J Obes Relat Metab Disord.* **23**, 221–230.
- NELSON, C. R. & STARTZ, R. (1990a). The distribution of the instrumental variables estimator and its t-ratio when the instrument is a poor one. *J. Bus.* **63**, S125–S140.
- NELSON, C. R. & STARTZ, R. (1990b). Some further results on the exact small sample properties of the instrumental variable estimator. *Econometrica.* **58**, 967–976.
- PATTERSON, N., PRICE, A. L. & REICH, D. (2006). Population structure and eigenanalysis. *PLoS Genet.* **2**, e190.
- PEYSAKHOVICH, A. & ECKLES, D. (2018). Learning causal effects from many randomized experiments using regularized instrumental variables. In *Proceedings of the 2018 World Wide Web Conference*.
- SANDERSON, E., RICHARDSON, T. G., HEMANI, G. & SMITH, G. D. (2021). The use of negative control outcomes in Mendelian randomization to detect potential population stratification. *Int J Epidemiol.* **50**, 1350–1361.
- SCHEET, P. & STEPHENS, M. (2006). A fast and flexible statistical model for large-scale population genotype data: Applications to inferring missing genotypes and haplotypic phase. *Am. J. Hum. Genet.* **78**, 629–644.
- SMITH, G. D. (2007). Capitalizing on Mendelian randomization to assess the effects of treatments. *J R Soc Med.* **100**, 432–435.
- STOCK, J. H., WRIGHT, J. H. & YOGO, M. (2002). A survey of weak instruments and weak identification in generalized method of moments. *J. Bus. Econ. Statist.* **20**, 518–529.
- STOCK, J. H. & YOGO, M. (2005). *Testing for Weak Instruments in Linear IV Regression*, chap. 5. Cambridge University Press, pp. 80–108.
- VAN DE GEER, S., BÜHLMANN, P., RITOV, Y. & DEZEURE, R. (2014). On asymptotically optimal confidence regions and tests for high-dimensional models. *Ann. Statist.* **42**, 1166–1202.
- VERSHYNIN, R. (2012). *Introduction to the non-asymptotic analysis of random matrices*, chap. 5. Cambridge Univ. Press.
- VERSHYNIN, R. (2018). *High-Dimensional Probability: An Introduction with Applications in Data Science* *High-Dimensional Probability: An Introduction with Applications in Data Science*.

- WAINWRIGHT, M. J. (2019). *High-Dimensional Statistics: A Non-Asymptotic Viewpoint*. Cambridge University Press.
- WANG, L. & TCHETGEN TCHETGEN, E. (2018). Bounded, efficient and multiply robust estimation of average treatment effects using instrumental variables. *J. R. Statist. Soc. B.* **80**, 531–550.
- WINDMEIJER, F., FARBMACHER, H., DAVIES, N. & SMITH, G. D. (2019). On the use of the lasso for instrumental variables estimation with some invalid instruments. *J. Am. Statist. Ass.* **114**, 1339–1350.
- WINDMEIJER, F. A., LIANG, X., HARTWIG, F. P. & BOWDEN, J. (2021). The confidence interval method for selecting valid instrumental variables. *J. R. Statist. Soc. B.* **83**, 752–776.
- WU, Y., BOOS, D. D. & STEFANSKI, L. A. (2007). Controlling variable selection by the addition of pseudovariables. *J. Am. Statist. Ass.* **102**, 235–243.
- ZHAO, Q., WANG, J., HEMANI, G., BOWDEN, J. & SMALL, D. S. (2020). Statistical inference in two-sample summary-data Mendelian randomization using robust adjusted profile score. *Ann. Statist.* **48**, 1742–1769.

Supplementary Materials

The supplementary file is organized as follows. We introduce the sample splitting algorithm in Section A. More details on our real data application are provided in Section B. We introduce the notations used throughout the paper in Section C. Technical details are collected in Section D. We discuss in Section E the derivation of standard error for bias estimate. Additional simulations to demonstrate the robustness of the proposed method are presented in Section F.

A Alternative Algorithm by Sample Splitting

To deal with selection bias and perform statistical inference on the causal effect estimate, we consider the sample splitting version of the proposed method. Specifically, we split the sample into two halves: H_1 and H_2 . The sizes of H_1 and H_2 are denoted by n_1 and n_2 respectively, which satisfy $n_1 + n_2 = n$ and $n_1 = cn_2$ for some constant $c > 0$. In our numerical experiments, we take $c = 1.5$. Let $\mathbf{Z}^{(1)} \in \mathbb{R}^{n_1 \times p}$, $\mathbf{D}^{(1)} \in \mathbb{R}^{n_1}$ and $\mathbf{Y}^{(1)} \in \mathbb{R}^{n_1}$ denote the collection of data on H_1 , and correspondingly $\mathbf{Z}^{(2)} \in \mathbb{R}^{n_2 \times p}$, $\mathbf{D}^{(2)} \in \mathbb{R}^{n_2}$ and $\mathbf{Y}^{(2)} \in \mathbb{R}^{n_2}$ represent the data on H_2 . We use H_1 to find spurious instruments. We generate p pseudo variables on H_1 by randomly permuting the rows of $\mathbf{Z}^{(1)}$. Let $\bar{\mathbf{Z}}^{(1)}$ be the design matrix associated with pseudo variables. Combine the p -dimensional pseudo variables with the initial p -dimensional candidate instruments, and we use $\tilde{\mathbf{Z}}^{(1)} \in \mathbb{R}^{n_1 \times 2p}$ to denote the resulting design matrix defined on H_1 . Identification of valid IVs and estimation of causal effect together with inference are performed on H_2 . The procedure with sample splitting is summarized in Algorithm 1. We discuss this alternative method in details in Sections A.1 and A.2.

A.1 Estimation of valid instruments

We first apply marginal screening to the subsample H_1 to reduce the dimension of $\tilde{\mathbf{Z}}^{(1)} \in \mathbb{R}^{2p}$, which is concatenation of the initial p -dimensional candidate instruments and pseudo variables. Let $\check{\mathcal{S}}_1 \in \{1, \dots, 2p\}$ be the index set of candidates selected by marginal screening and assume that $\check{\mathcal{S}}_1$ include all the relevant instruments. We use $\tilde{\mathbf{Z}}_{\check{\mathcal{S}}_1}^{(1)}$ to represent the design matrix formed by columns of $\tilde{\mathbf{Z}}^{(1)}$ indexed by $\check{\mathcal{S}}_1$. Then we fit the reduced form models (2.3) and (2.4) on the first subsample H_1 with design matrix $\tilde{\mathbf{Z}}_{\check{\mathcal{S}}_1}^{(1)}$, and obtain de-biased lasso estimators $\hat{\gamma}_{\check{\mathcal{S}}_1}^{(1)}$ and $\hat{\Gamma}_{\check{\mathcal{S}}_1}^{(1)}$. We also calculate the standard error $\text{SE}(\hat{\gamma}_{\check{\mathcal{S}}_1, l}^{(1)})$ for $1 \leq l \leq s$. We refer to (3.1) and (3.2) in the main paper for more details on the de-biased lasso estimators and their estimated standard errors. To further estimate the set of relevant instruments that are conditionally associated with the exposure, we implement the joint thresholding and let $\check{\mathcal{S}}_2 = \{l : 1 \leq l \leq s, |\hat{\gamma}_{\check{\mathcal{S}}_1, l}^{(1)}| \geq \delta_n \times \text{SE}(\hat{\gamma}_{\check{\mathcal{S}}_1, l}^{(1)})\}$ denote the set of candidates passing the joint thresholding, where $\delta_n = \sqrt{\omega \log(\max\{n_1, s\})}$. Next, locate spurious instruments by estimating the range of causal effect estimates from pseudo variables in $\check{\mathcal{S}}_2$ and remove spurious IVs from the candidate set together with pseudo variables. The remaining set is represented by $\check{\mathcal{S}}_3$ with cardinality q and let $\mathbf{Z}_{\check{\mathcal{S}}_3} \in \mathbb{R}^q$ denote the associated candidate instruments. Further assume the plurality rule holds in $\check{\mathcal{S}}_3$, i.e. the largest group of invalid or remaining spurious instruments with the same Wald ratio is smaller than the group of valid instruments. The procedure implemented on H_1 is outlined as

Steps 00–3 in Algorithm 1.

Henceforth, we focus on the second subsample H_2 . We have shown in Lemma D.1 that relevant variables can pass joint thresholding with high probability. By assuming that $\check{\mathcal{S}}_3$ includes all relevant variables, the models (2.1) and (2.2) hold with \mathbf{Z} replaced by $\mathbf{Z}_{\check{\mathcal{S}}_3}$, and parameters γ^*, π^* substituted by $\gamma_{\check{\mathcal{S}}_3}^*, \pi_{\check{\mathcal{S}}_3}^* \in \mathbb{R}^q$. Similarly, the reduced form parameter $\mathbf{\Gamma}^*$ would become $\mathbf{\Gamma}_{\check{\mathcal{S}}_3}^* = \pi_{\check{\mathcal{S}}_3}^* + \beta^* \gamma_{\check{\mathcal{S}}_3}^*$. We use $\mathbf{Z}_{\check{\mathcal{S}}_3}^{(2)} \in \mathbb{R}^{n_2 \times q}$ to denote the design matrix associated with $\check{\mathcal{S}}_3$ on H_2 . As q is much smaller than n_2 , we apply OLS to $\mathbf{D}^{(2)}, \mathbf{Z}_{\check{\mathcal{S}}_3}^{(2)}$ and $\mathbf{Y}^{(2)}, \mathbf{Z}_{\check{\mathcal{S}}_3}^{(2)}$ respectively in order to obtain estimates $\hat{\gamma}_{\check{\mathcal{S}}_3}^{(2)}, \hat{\mathbf{\Gamma}}_{\check{\mathcal{S}}_3}^{(2)} \in \mathbb{R}^q$, and calculate the standard error of $\hat{\gamma}_{\check{\mathcal{S}}_3, l}^{(2)}$ for $1 \leq l \leq q$,

$$\text{SE}(\hat{\gamma}_{\check{\mathcal{S}}_3, l}^{(2)}) = \sqrt{\frac{\left[\left(\mathbf{Z}_{\check{\mathcal{S}}_3}^{(2)\top} \mathbf{Z}_{\check{\mathcal{S}}_3}^{(2)} \right)^{-1} \right]_{ll} \left\| \mathbf{D}^{(2)} - \mathbf{Z}_{\check{\mathcal{S}}_3}^{(2)} \hat{\gamma}_{\check{\mathcal{S}}_3}^{(2)} \right\|^2}{n_2}}.$$

Then we apply another joint thresholding by comparing $|\hat{\gamma}_{\check{\mathcal{S}}_3, l}^{(2)}|$ with $\delta_n \times \text{SE}(\hat{\gamma}_{\check{\mathcal{S}}_3, l}^{(2)})$, presented as Step 4 in Algorithm 1. Here $\delta_n = \sqrt{\omega \log n_2}$. Let $\tilde{\mathcal{S}}_3 \subset \{1, \dots, q\}$ be the index set of candidates passing this joint thresholding on the second portion of data.

In Step 5 of Algorithm 1, we estimate valid IVs via mode finding. For $j \in \tilde{\mathcal{S}}_3$, calculate causal estimate $\hat{\beta}^{(2, j)} = \hat{\mathbf{\Gamma}}_{\check{\mathcal{S}}_3, j}^{(2)} / \hat{\gamma}_{\check{\mathcal{S}}_3, j}^{(2)}$. Take $\hat{\beta}^{(2, j)}$ as the underlying truth and compute the bias for estimate $\hat{\beta}^{(2, l)}$ for $l \in \tilde{\mathcal{S}}_3$, denoted by $\hat{b}^{(2, j, l)} = \hat{\beta}^{(2, l)} - \hat{\beta}^{(2, j)}$, and the standard error $\text{SE}(\hat{b}^{(2, j, l)})$. We discuss details of $\text{SE}(\hat{b}^{(2, j, l)})$ in Section E. We say two estimates $\hat{\beta}^{(2, l)}$ and $\hat{\beta}^{(2, j)}$ are close if $|\hat{b}^{(2, j, l)}| \leq \text{SE}(\hat{b}^{(2, j, l)}) \sqrt{\omega^2 \log n_2}$. Here we use ω^2 instead ω since we are conducting pairwise tests. Note that $\hat{b}^{(2, j, l)}$ remains the same if we swap j, l , which implies that if $|\hat{b}^{(2, j, l)}|$ pass the threshold, then the candidate j would be also in favor of l by symmetry. The mode is then estimated to be the effect estimate $\hat{\beta}^{(2, l)}$ that is close to the other estimates most frequently. Candidate instruments in $\tilde{\mathcal{S}}_3$ whose corresponding causal effect estimates are close to the mode are identified as valid IVs, denoted by $\check{\mathcal{S}}_4$.

A.2 Estimation of causal effect and statistical inference

We borrow the idea from Guo et al. (2018) for the construction of causal effect estimate and its associated confidence interval. On the second subsample H_2 , we estimate the causal effect as follows

$$\hat{\beta}_{\text{split}} = \frac{\left\{ \hat{\gamma}_{\check{\mathcal{S}}_3, \check{\mathcal{S}}_4}^{(2)} \right\}^\top \widehat{\mathbf{W}} \hat{\mathbf{\Gamma}}_{\check{\mathcal{S}}_3, \check{\mathcal{S}}_4}^{(2)}}{\left\{ \hat{\gamma}_{\check{\mathcal{S}}_3, \check{\mathcal{S}}_4}^{(2)} \right\}^\top \widehat{\mathbf{W}} \hat{\gamma}_{\check{\mathcal{S}}_3, \check{\mathcal{S}}_4}^{(2)}}, \quad (\text{A.1})$$

where $\hat{\gamma}_{\check{\mathcal{S}}_3, \check{\mathcal{S}}_4}^{(2)}$ is a subvector of $\hat{\gamma}_{\check{\mathcal{S}}_3}^{(2)}$ indexed by $\check{\mathcal{S}}_4$ and similarly for $\hat{\mathbf{\Gamma}}_{\check{\mathcal{S}}_3, \check{\mathcal{S}}_4}^{(2)}$. The weighting matrix

$$\widehat{\mathbf{W}} = \left[\widehat{\mathbf{\Sigma}}_{\check{\mathcal{S}}_3}^{(2)} \right]_{\check{\mathcal{S}}_4, \check{\mathcal{S}}_4} - \left[\widehat{\mathbf{\Sigma}}_{\check{\mathcal{S}}_3}^{(2)} \right]_{\check{\mathcal{S}}_4, \check{\mathcal{S}}_4} \left\{ \left[\widehat{\mathbf{\Sigma}}_{\check{\mathcal{S}}_3}^{(2)} \right]_{\check{\mathcal{S}}_4^c, \check{\mathcal{S}}_4^c} \right\}^{-1} \left[\widehat{\mathbf{\Sigma}}_{\check{\mathcal{S}}_3}^{(2)} \right]_{\check{\mathcal{S}}_4^c, \check{\mathcal{S}}_4} \quad (\text{A.2})$$

with $\widehat{\mathbf{\Sigma}}_{\check{\mathcal{S}}_3}^{(2)}$ representing the sample covariance matrix of candidate instruments corresponding to $\check{\mathcal{S}}_3$ on the second subsample H_2 , i.e., $\widehat{\mathbf{\Sigma}}_{\check{\mathcal{S}}_3}^{(2)} = \left\{ \mathbf{Z}_{\check{\mathcal{S}}_3}^{(2)} \right\}^\top \mathbf{Z}_{\check{\mathcal{S}}_3}^{(2)} / n_2$, and $\left[\widehat{\mathbf{\Sigma}}_{\check{\mathcal{S}}_3}^{(2)} \right]_{\mathcal{I}_1, \mathcal{I}_2}$ is formed by rows and columns of $\widehat{\mathbf{\Sigma}}_{\check{\mathcal{S}}_3}^{(2)}$

indexed by \mathcal{I}_1 and \mathcal{I}_2 respectively.

The asymptotic variance of $\hat{\beta}_{\text{split}}$ is given by $(\boldsymbol{\alpha}_Y^{*\text{T}} \Sigma_u \boldsymbol{\alpha}_Y^* + \sigma_Y^2)/v_{\text{split}}$ with

$$v_{\text{split}} = \boldsymbol{\gamma}_{\check{\mathcal{S}}_3, \mathcal{T}_*}^{*\text{T}} \left([\boldsymbol{\Sigma}_{\check{\mathcal{S}}_3}]_{\mathcal{T}_*, \mathcal{T}_*} - [\boldsymbol{\Sigma}_{\check{\mathcal{S}}_3}]_{\mathcal{T}_*, \mathcal{T}_*^c} \left\{ [\boldsymbol{\Sigma}_{\check{\mathcal{S}}_3}]_{\mathcal{T}_*^c, \mathcal{T}_*^c} \right\}^{-1} [\boldsymbol{\Sigma}_{\check{\mathcal{S}}_3}]_{\mathcal{T}_*^c, \mathcal{T}_*} \right) \boldsymbol{\gamma}_{\check{\mathcal{S}}_3, \mathcal{T}_*}^*, \quad (\text{A.3})$$

where $\mathcal{T}_* = \{l : \gamma_{\check{\mathcal{S}}_3, l}^* \neq 0, \text{ for } 1 \leq l \leq q\} \subset \{1, \dots, q\}$ is the index set of relevant instruments defined on $\check{\mathcal{S}}_3$, and v_{split} is estimated by

$$\hat{v}_{\text{split}} = \widehat{\text{var}}(\hat{\beta}_{\text{split}}) = \frac{\hat{\Theta}_{11} + \hat{\beta}_{\text{split}}^2 \hat{\Theta}_{22} - 2\hat{\beta}_{\text{split}} \hat{\Theta}_{12}}{\{\hat{\boldsymbol{\gamma}}_{\check{\mathcal{S}}_3, \check{\mathcal{S}}_4}^{(2)}\}^{\text{T}} \widehat{\mathbf{W}} \hat{\boldsymbol{\gamma}}_{\check{\mathcal{S}}_3, \check{\mathcal{S}}_4}^{(2)}}, \quad (\text{A.4})$$

where

$$\begin{aligned} \hat{\Theta}_{11} &= \frac{1}{n_2} \left\| \mathbf{Y}^{(2)} - \mathbb{Z}_{\check{\mathcal{S}}_3}^{(2)} \hat{\boldsymbol{\Gamma}}_{\check{\mathcal{S}}_3}^{(2)} \right\|_2^2, \\ \hat{\Theta}_{22} &= \frac{1}{n_2} \left\| \mathbf{D}^{(2)} - \mathbb{Z}_{\check{\mathcal{S}}_3}^{(2)} \hat{\boldsymbol{\gamma}}_{\check{\mathcal{S}}_3}^{(2)} \right\|_2^2, \\ \hat{\Theta}_{12} &= \frac{1}{n_2} \left(\mathbf{Y}^{(2)} - \mathbb{Z}_{\check{\mathcal{S}}_3}^{(2)} \hat{\boldsymbol{\Gamma}}_{\check{\mathcal{S}}_3}^{(2)} \right)^{\text{T}} \left(\mathbf{D}^{(2)} - \mathbb{Z}_{\check{\mathcal{S}}_3}^{(2)} \hat{\boldsymbol{\gamma}}_{\check{\mathcal{S}}_3}^{(2)} \right). \end{aligned} \quad (\text{A.5})$$

We then can further obtain the $100(1 - \alpha)\%$ confidence interval for β :

$$\left[\hat{\beta}_{\text{split}} - z_{1-\alpha/2} \sqrt{\hat{v}_{\text{split}}/n_2}, \hat{\beta}_{\text{split}} + z_{1-\alpha/2} \sqrt{\hat{v}_{\text{split}}/n_2} \right], \quad (\text{A.6})$$

where $z_{1-\alpha/2}$ is the $(1 - \alpha/2)$ -quantile of the standard normal distribution. See Steps 6 and 7 of Algorithm 1 for an outline of estimation of causal effect and construction of confidence interval.

B More Details on Data Application

B.1 Relationship between BMI and HUI-3

We display the observed relationship between BMI and Health Utility Index Mark 3 (HUI-3) in Figure 6. We can learn from Figure 6-(a) that HUI-3 has a positive association with BMI when BMI is lower than 25, and is negatively associated with BMI when BMI is higher than 25. This is consistent with the fact that both underweight and overweight are linked with a range of adverse health conditions. Meanwhile, the healthy weight range is between 18.5 and 24.9. We provide additional plot in Figure 6-(b) to emphasize that as BMI increases over 25, the risk for lower quality of life increases, which is our focus in the data application.

B.2 WLS Data Pre-processing

For genomic data, we use imputed genetic variants extracted from whole-genome sequencing on 22 chromosomes, in which unobserved genotypes in the study sample are estimated from the haplotype or genotype reference panel (Browning, 2008; Li et al., 2009). This allows us to examine the evidence for association

Algorithm 1 Fighting noise with noise – sample splitting

INPUT: Design matrix $\mathbb{Z} \in \mathbb{R}^{n \times p}$, observed exposure $\mathbf{D} \in \mathbb{R}^n$, observed outcome $\mathbf{Y} \in \mathbb{R}^n$.

00. Divide data into two halves:

H_1 of size n_1 and H_2 of size n_2 ;

Denote the associated data as $\mathbb{Z}^{(1)} \in \mathbb{R}^{n_1 \times p}$, $\mathbf{D}^{(1)} \in \mathbb{R}^{n_1}$, $\mathbf{Y}^{(1)} \in \mathbb{R}^{n_1}$, and $\mathbb{Z}^{(2)} \in \mathbb{R}^{n_2 \times p}$, $\mathbf{D}^{(2)} \in \mathbb{R}^{n_2}$, $\mathbf{Y}^{(2)} \in \mathbb{R}^{n_2}$.

0. Pseudo variables generation on H_1 :

Generate p pseudo variables $Z_{p+1}^{(1)}, \dots, Z_{2p}^{(1)}$ by randomly permuting the rows of $\mathbb{Z}^{(1)}$;

Denote the resulting design matrix as $\bar{\mathbb{Z}}^{(1)}$, and the concatenation of $\mathbb{Z}^{(1)}$ and $\bar{\mathbb{Z}}^{(1)}$ as $\tilde{\mathbb{Z}}^{(1)}$.

1. Marginal screening on H_1 :

For $j = 1, \dots, 2p$, compute $\hat{\rho}_j = |\sum_{i=1}^{n_1} \tilde{Z}_{ij}^{(1)} D_i^{(1)}| / \sum_{i=1}^{n_1} (\tilde{Z}_{ij}^{(1)})^2$;

Select the s variables with the largest $\hat{\rho}_j$ and denote them as \check{S}_1 .

2. Joint thresholding on H_1 :

Fit a linear model for $\mathbf{D}^{(1)} \sim \tilde{\mathbb{Z}}_{\check{S}_1}^{(1)}$: let $\hat{\gamma}_{\check{S}_1}^{(1)}$ be the debiased lasso estimate constructed similarly to (3.1) in the main paper; here $\tilde{\mathbb{Z}}_{\check{S}_1}^{(1)}$ is formed by columns of $\tilde{\mathbb{Z}}^{(1)}$ indexed by \check{S}_1 . Also obtain their standard error estimate $\text{SE}(\hat{\gamma}_{\check{S}_1, l}^{(1)})$.

Fit a linear model for $\mathbf{Y}^{(1)} \sim \tilde{\mathbb{Z}}_{\check{S}_1}^{(1)}$ and obtain the estimate $\hat{\Gamma}_{\check{S}_1}^{(1)}$ in a similar fashion.

Estimate the relevant variables $\check{S}_2 = \{l \in [s] : |\hat{\gamma}_{\check{S}_1, l}^{(1)}| \geq \delta_n \times \text{SE}(\hat{\gamma}_{\check{S}_1, l}^{(1)})\}$, where $\delta_n = \sqrt{\omega \log(\max\{n_1, s\})}$, where ω is a tuning parameter. Denote pseudos in \check{S}_2 by $\hat{\mathcal{P}}$.

3. Irrelevant variables removal:

For $l \in \check{S}_2$, calculate causal effect estimate $\hat{\beta}^{(1, l)} = \hat{\Gamma}_{\check{S}_1, l}^{(1)} / \hat{\gamma}_{\check{S}_1, l}^{(1)}$;

Remove variables similar to pseudo variables in their causal effect estimate $\hat{\beta}^{(1, l)}$ from \check{S}_2 :

$$\check{S}_3 = \check{S}_2 \setminus \left\{ l \in \check{S}_2 : \min_{j \in \hat{\mathcal{P}}} \hat{\beta}^{(1, j)} \leq \hat{\beta}^{(1, l)} \leq \max_{j \in \hat{\mathcal{P}}} \hat{\beta}^{(1, j)} \right\}.$$

Denote the cardinality of \check{S}_3 as q .

Algorithm S1 (continue)

4. Joint thresholding on H_2 :

Let $\mathbb{Z}_{\tilde{\mathcal{S}}_3}^{(2)} \in \mathbb{R}^{n_2 \times q}$ denote the associated design matrix of $\tilde{\mathcal{S}}_3$ on H_2 . Fit a linear model for $\mathbf{D}^{(2)} \sim \mathbb{Z}_{\tilde{\mathcal{S}}_3}^{(2)}$: obtain the OLS estimator $\hat{\gamma}_{\tilde{\mathcal{S}}_3}^{(2)}$ and standard error estimate $\text{SE}(\hat{\gamma}_{\tilde{\mathcal{S}}_3, l}^{(2)})$ for $1 \leq l \leq q$;

Fit a linear model for $\mathbf{Y}^{(2)} \sim \mathbb{Z}_{\tilde{\mathcal{S}}_3}^{(2)}$ and obtain the estimate $\hat{\Gamma}_{\tilde{\mathcal{S}}_3}^{(2)}$ in a similar fashion;

Further approximate the set of relevant instruments as $\tilde{\mathcal{S}}_3 = \{l \in [q] : |\hat{\gamma}_{\tilde{\mathcal{S}}_3, l}^{(2)}| \geq \delta_n \times \text{SE}(\hat{\gamma}_{\tilde{\mathcal{S}}_3, l}^{(2)})\}$, where $\delta_n = \sqrt{\omega \log n_2}$.

5. Mode-finding on H_2 :

For $l \in \tilde{\mathcal{S}}_3$, calculate causal effect estimate $\hat{\beta}^{(2,l)} = \hat{\Gamma}_{\tilde{\mathcal{S}}_3, l}^{(2)} / \hat{\gamma}_{\tilde{\mathcal{S}}_3, l}^{(2)}$;

For $j, l \in \tilde{\mathcal{S}}_3$, compute $\hat{b}^{(2,j,l)} = \hat{\beta}^{(2,l)} - \hat{\beta}^{(2,j)}$ and $\text{SE}(\hat{b}^{(2,j,l)})$;

For $j \in \tilde{\mathcal{S}}_3$, find the number of candidates leading to a similar causal effect estimate with j :

$$V_j = \left| \left\{ l \in \tilde{\mathcal{S}}_3 : |\hat{b}^{(2,j,l)}| / \text{SE}(\hat{b}^{(2,j,l)}) \leq \sqrt{\omega^2 \log n_2} \right\} \right|;$$

Find valid IVs using the plurality rule:

$$\check{\mathcal{S}}_4 = \left\{ j : V_j = \max_{l \in \tilde{\mathcal{S}}_3} V_l \right\}.$$

6. Causal effect estimation:

$$\hat{\beta}_{\text{split}} = \frac{\{\hat{\gamma}_{\check{\mathcal{S}}_3, \check{\mathcal{S}}_4}^{(2)}\}^T \widehat{\mathbf{W}} \hat{\Gamma}_{\check{\mathcal{S}}_3, \check{\mathcal{S}}_4}^{(2)}}{\{\hat{\gamma}_{\check{\mathcal{S}}_3, \check{\mathcal{S}}_4}^{(2)}\}^T \widehat{\mathbf{W}} \hat{\gamma}_{\check{\mathcal{S}}_3, \check{\mathcal{S}}_4}^{(2)}},$$

where $\hat{\gamma}_{\check{\mathcal{S}}_3, \check{\mathcal{S}}_4}^{(2)}$ is a subvector of $\hat{\gamma}_{\tilde{\mathcal{S}}_3}^{(2)}$ indexed by $\check{\mathcal{S}}_4$ and similarly for $\hat{\Gamma}_{\check{\mathcal{S}}_3, \check{\mathcal{S}}_4}^{(2)}$. See (A.2) for the explicit form of the weighting matrix $\widehat{\mathbf{W}}$.

Estimated variance of $\hat{\beta}_{\text{split}}$:

$$\hat{v}_{\text{split}} = \widehat{\text{var}}(\hat{\beta}_{\text{split}}) = \frac{\hat{\Theta}_{11} + \hat{\beta}_{\text{split}}^2 \hat{\Theta}_{22} - 2\hat{\beta}_{\text{split}} \hat{\Theta}_{12}}{\{\hat{\gamma}_{\check{\mathcal{S}}_3, \check{\mathcal{S}}_4}^{(2)}\}^T \widehat{\mathbf{W}} \hat{\gamma}_{\check{\mathcal{S}}_3, \check{\mathcal{S}}_4}^{(2)}},$$

where $\hat{\Theta}_{11}, \hat{\Theta}_{22}, \hat{\Theta}_{12}$ are given in (A.5).

7. $100(1 - \alpha)\%$ confidence interval: $[\hat{\beta}_{\text{split}} - z_{1-\alpha/2} \sqrt{\hat{v}_{\text{split}}/n_2}, \hat{\beta}_{\text{split}} + z_{1-\alpha/2} \sqrt{\hat{v}_{\text{split}}/n_2}]$.

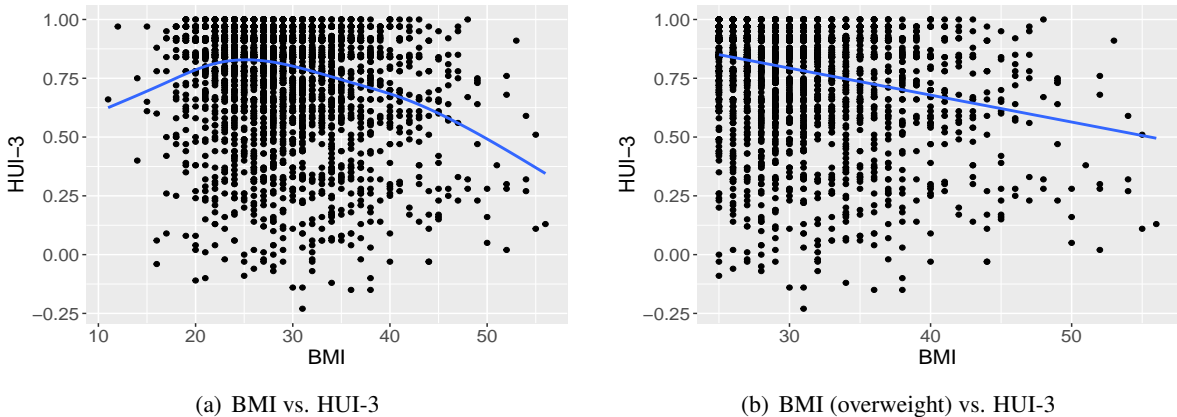


Figure 6: The plot on the left panel depicts the relationship between BMI and Health Utility Index Mark 3 (HUI-3) for the WLS data used in our analysis. On the right panel, we zoom in on BMI above 25 and HUI-3 accordingly.

at biomarkers that are not directly genotyped (Scheet & Stephens, 2006; Marchini et al., 2007; Browning, 2008). The input of missing data imputation are observed variants that meet criterion of quality control: for example, missing call rate $< 2\%$, minor allele frequency (MAF) ≥ 0.01 , Hardy-Weinberg Equilibrium (HWE) p-value $\geq 10^{-4}$, with known and unique positions, etc. See the genotype quality control report attached to Herd et al. (2014), which follows the quality filters described in Laurie et al. (2010). Genotype imputation were performed using IMPUTE2 software (Howie et al., 2009, 2011). To account for uncertainty of the imputation output, we exclude variants with BEAGLE allelic r^2 less than 0.3, which is an assessment of genotype imputation performance (de Bakker et al., 2008; Li et al., 2010).

For the remaining missing values in genotype data after matching with available phenotypes, we replace them by random sampling from the empirical allele distribution. Namely, the missing values at a genetic variant j are sampled from the associated marginal allele empirical distribution. In addition, there might be identical columns in our current SNP matrix, in which rows are indexed by participants considered in our analysis and columns are indexed by genotypes. To proceed, we keep unique ones in our analysis and recheck at the end whether any excluded variants have exactly the same (0,1,2) genotype representation as our estimated valid IVs. If there are any, they will also be identified as valid instruments.

C Notations

For any vector $\mathbf{v} \in \mathbb{R}^p$, v_j represents the j th element of \mathbf{v} . $\|\mathbf{v}\|_1$, $\|\mathbf{v}\|_2$ and $\|\mathbf{v}\|_\infty$ represent the usual 1-, 2- and ∞ - norms respectively. The ℓ_0 norm $\|\mathbf{v}\|_0$ refers to the number of nonzero components in \mathbf{v} . For a set S , $|S|$ denotes its cardinality and S^c is the complement of S . If $S \subset \{1, \dots, p\}$ is an index set, then $\mathbf{v}_S \in \mathbb{R}^{|S|}$ is a subvector of $\mathbf{v} \in \mathbb{R}^p$ indexed by S and $v_{S,l}$ denotes the l th element of \mathbf{v}_S for $1 \leq l \leq |S|$. For an $n \times p$ matrix $\mathbf{A} \in \mathbb{R}^{n \times p}$, we denote the (i, j) th element of \mathbf{A} by A_{ij} , the i th row as \mathbf{A}_i and the j th column as \mathbf{A}_j . \mathbf{A}^T denotes the transpose of \mathbf{A} . $\|\mathbf{A}\|_\infty = \max_{1 \leq i, j \leq p} |A_{ij}|$ represents the maximum of the absolute element of matrix \mathbf{A} and $\|\mathbf{A}\|_1 = \max_{1 \leq j \leq p} \sum_{i=1}^n |A_{ij}|$ is the maximum absolute column sum of

A. For a symmetric matrix \mathbf{A} , let $\lambda_{\min}(\mathbf{A})$ and $\lambda_{\max}(\mathbf{A})$ denote the smallest and the largest eigenvalues respectively. The spectral norm $\|\mathbf{A}\|_2 = \lambda_{\max}(\mathbf{A})$. For functions $f(n)$ and $h(n)$, we write $f(n) = O(h(n))$ if $\lim_{n \rightarrow \infty} f(n)/h(n) = c$, where c is some constant. Particularly, if $h(n) = c$, the notation becomes $f(n) = O(1)$. Similarly, if $\lim_{n \rightarrow \infty} f(n)/h(n) = 0$, we write $f(n) = o(h(n))$. Specifically, if $h(n) = c$, we write $f(n) = o(1)$. The notation $a_n \lesssim c_n$ represents that there exists a constant C such that $a_n \leq Cb_n$ and $a_n \gtrsim b_n$ means that there exists a constant c such that $a_n \geq cb_n$. And $a_n \asymp d_n$ represents $a_n = \tilde{c}b_n$ for some constant \tilde{c} . $\text{cor}(X, Y)$ represents correlation between random variables X and Y , and let $\text{cov}(X, Y)$ denote the associated covariance. If $\mathbf{X} \in \mathbb{R}^p$ and $\mathbf{Y} \in \mathbb{R}^q$ are random vectors, then $\text{cov}(\mathbf{X}, \mathbf{Y}) \in \mathbb{R}^{p \times q}$ is the cross-covariance matrix.

D Technical Details

D.1 Setup for Technical Details

We first revisit some definitions and notations. The index set of candidate instruments passing marginal screening is $\hat{\mathcal{S}}_1 \subset \{1, \dots, p\}$ that has size s . Let $\mathbf{Z}_{\hat{\mathcal{S}}_1}$ denote the subvector of $\mathbf{Z} \in \mathbb{R}^p$ indexed by $\hat{\mathcal{S}}_1$. Consider the models (2.1) and (2.2) with $\mathbf{Z} \in \mathbb{R}^p$ replaced by $\mathbf{Z}_{\hat{\mathcal{S}}_1} \in \mathbb{R}^s$. The parameters $\boldsymbol{\gamma}^*, \boldsymbol{\Gamma}^* \in \mathbb{R}^p$ change accordingly to $\boldsymbol{\gamma}_{\hat{\mathcal{S}}_1}^*, \boldsymbol{\Gamma}_{\hat{\mathcal{S}}_1}^* \in \mathbb{R}^s$. The debiased-lasso estimators of $\boldsymbol{\gamma}_{\hat{\mathcal{S}}_1}^*, \boldsymbol{\Gamma}_{\hat{\mathcal{S}}_1}^*$ under models (2.1) and (2.2) are denoted by $\hat{\boldsymbol{\gamma}}_{\hat{\mathcal{S}}_1}, \hat{\boldsymbol{\Gamma}}_{\hat{\mathcal{S}}_1} \in \mathbb{R}^s$ respectively, and $\tilde{\boldsymbol{\gamma}}_{\hat{\mathcal{S}}_1}, \tilde{\boldsymbol{\Gamma}}_{\hat{\mathcal{S}}_1} \in \mathbb{R}^s$ are the lasso estimators defined after (3.1). The matrix $\mathbf{M} \in \mathbb{R}^{s \times s}$ is given in (G.3) of the main paper and $\mathbb{Z}_{\hat{\mathcal{S}}_1} \in \mathbb{R}^{n \times s}$ is formed by columns of $\mathbb{Z} \in \mathbb{R}^{n \times p}$ indexed by $\hat{\mathcal{S}}_1$.

It follows from (4) and (5) of van de Geer et al. (2014) that the debiased-lasso estimators satisfy the following decomposition

$$\sqrt{n}(\hat{\boldsymbol{\gamma}}_{\hat{\mathcal{S}}_1} - \boldsymbol{\gamma}_{\hat{\mathcal{S}}_1}^*) = \underbrace{\sqrt{n}(\mathbf{M}\hat{\boldsymbol{\Sigma}}_{\hat{\mathcal{S}}_1} - \mathbf{I})(\boldsymbol{\gamma}_{\hat{\mathcal{S}}_1}^* - \tilde{\boldsymbol{\gamma}}_{\hat{\mathcal{S}}_1})}_{\Delta_1} + \frac{1}{\sqrt{n}}\mathbf{M}\mathbb{Z}_{\hat{\mathcal{S}}_1}^T(\mathbf{U}\boldsymbol{\alpha}_D^* + \boldsymbol{\epsilon}_D) \quad (\text{D.1})$$

$$\sqrt{n}(\hat{\boldsymbol{\Gamma}}_{\hat{\mathcal{S}}_1} - \boldsymbol{\Gamma}_{\hat{\mathcal{S}}_1}^*) = \underbrace{\sqrt{n}(\mathbf{M}\hat{\boldsymbol{\Sigma}}_{\hat{\mathcal{S}}_1} - \mathbf{I})(\boldsymbol{\Gamma}_{\hat{\mathcal{S}}_1}^* - \tilde{\boldsymbol{\Gamma}}_{\hat{\mathcal{S}}_1})}_{\Delta_2} + \frac{1}{\sqrt{n}}\mathbf{M}\mathbb{Z}_{\hat{\mathcal{S}}_1}^T\{\mathbf{U}(\boldsymbol{\alpha}_Y^* + \beta^*\boldsymbol{\alpha}_D^*) + (\beta^*\boldsymbol{\epsilon}_D + \boldsymbol{\epsilon}_Y)\}, \quad (\text{D.2})$$

where $\mathbf{U} \in \mathbb{R}^{n \times g}$, $\hat{\boldsymbol{\Sigma}}_{\hat{\mathcal{S}}_1} = \mathbb{Z}_{\hat{\mathcal{S}}_1}^T \mathbb{Z}_{\hat{\mathcal{S}}_1} / n$, and $\mathbf{I} \in \mathbb{R}^{s \times s}$ is an identity matrix. Define $\mathbf{v}_l(\hat{\mathcal{S}}_1) = \mathbb{Z}_{\hat{\mathcal{S}}_1} \mathbf{M}^T \mathbf{e}_l / n \in \mathbb{R}^n$ for $1 \leq l \leq s$, where $\mathbf{e}_l \in \mathbb{R}^s$ is a unit vector with the l th component equal to one and zero otherwise. Hereafter, we use \mathbf{v}_l to refer to $\mathbf{v}_l(\hat{\mathcal{S}}_1)$ for ease of notation. The ℓ_2 norm of \mathbf{v}_l is $\|\mathbf{v}_l\|^2 = [\mathbf{M}\hat{\boldsymbol{\Sigma}}_{\hat{\mathcal{S}}_1} \mathbf{M}^T]_{ll} / n$. Here $[\cdot]_{ll}$ denotes the l th diagonal element of the matrix.

Let $\eta_{max} = 1 \vee B \sup_{\hat{\mathcal{S}}_1: |\hat{\mathcal{S}}_1|=s} \max_{1 \leq j \leq s} \|[\boldsymbol{\Sigma}_{\hat{\mathcal{S}}_1}^{-1}]_{-j,j}\|_1$. Next, we define the events, on which we

establish our theoretical results.

$$\mathcal{A} = \{\mathcal{S}_* \subset \hat{\mathcal{S}}_1\} \quad (\text{D.3})$$

$$\mathcal{B}_1 = \left\{ \sup_{\hat{\mathcal{S}}_1: |\hat{\mathcal{S}}_1|=s} \|\tilde{\boldsymbol{\gamma}}_{\hat{\mathcal{S}}_1} - \boldsymbol{\gamma}_{\hat{\mathcal{S}}_1}^*\|_1 \leq \frac{16s_1^* \lambda_\gamma}{C_L} \right\} \quad (\text{D.4})$$

$$\mathcal{B}_2 = \left\{ \sup_{\hat{\mathcal{S}}_1: |\hat{\mathcal{S}}_1|=s} \|\tilde{\boldsymbol{\Gamma}}_{\hat{\mathcal{S}}_1} - \boldsymbol{\Gamma}_{\hat{\mathcal{S}}_1}^*\|_1 \leq \frac{16s_2^* \lambda_\Gamma}{C_L} \right\} \quad (\text{D.5})$$

$$\mathcal{B}_3 = \left\{ \sup_{\hat{\mathcal{S}}_1: |\hat{\mathcal{S}}_1|=s} \frac{\|\mathbb{Z}_{\hat{\mathcal{S}}_1}(\boldsymbol{\gamma}_{\hat{\mathcal{S}}_1}^* - \tilde{\boldsymbol{\gamma}}_{\hat{\mathcal{S}}_1})\|^2}{n} \leq \frac{16s_1^* \lambda_\gamma^2}{C_L} \right\} \quad (\text{D.6})$$

$$\tilde{\mathcal{B}} = \left\{ \sup_{\hat{\mathcal{S}}_1: |\hat{\mathcal{S}}_1|=s} \left| \frac{1}{n} \|\mathbf{D} - \mathbb{Z}_{\hat{\mathcal{S}}_1} \tilde{\boldsymbol{\gamma}}_{\hat{\mathcal{S}}_1}\|^2 - (\boldsymbol{\alpha}_D^{*\text{T}} \boldsymbol{\Sigma}_U \boldsymbol{\alpha}_D^* + \sigma_D^2) \right| \leq a_4 \sqrt{\frac{\log n}{n}} + \frac{16\lambda_\gamma^2 s_1^*}{C_L} \right\} \quad (\text{D.7})$$

$$\mathcal{C}_1 = \left\{ \sup_{\hat{\mathcal{S}}_1: |\hat{\mathcal{S}}_1|=s} \|\Delta_1\|_\infty \leq \frac{70a_2 s_1^* \sqrt{\log p} \lambda_\gamma}{C_L^2} \eta_{max} \right\} \quad (\text{D.8})$$

$$\mathcal{C}_2 = \left\{ \sup_{\hat{\mathcal{S}}_1: |\hat{\mathcal{S}}_1|=s} \|\Delta_2\|_\infty \leq \frac{70a_2 s_2^* \sqrt{\log p} \lambda_\Gamma}{C_L^2} \eta_{max} \right\} \quad (\text{D.9})$$

$$\mathcal{C}_3 = \left\{ \frac{1}{n} \max_{1 \leq j \leq p} |\mathbf{Z}_j^\text{T} \boldsymbol{\epsilon}| \leq a_5 \sqrt{\frac{\log p}{n}} \right\} \quad (\text{D.10})$$

$$\mathcal{D} = \left\{ \frac{1}{C_R} - \mu \leq n \|\mathbf{v}_l\|^2 \leq \frac{1}{C_L} + \mu, \forall \hat{\mathcal{S}}_1 \text{ with } |\hat{\mathcal{S}}_1| = s \text{ and } \forall 1 \leq l \leq s \right\} \quad (\text{D.11})$$

$$\mathcal{E}_1 = \left\{ \sup_{\hat{\mathcal{S}}_1: |\hat{\mathcal{S}}_1|=s} \|\mathbf{M} \hat{\boldsymbol{\Sigma}}_{\hat{\mathcal{S}}_1} - \mathbf{I}_s\|_\infty \leq \frac{\lambda_{\text{NL}}}{0.99 C_L} \right\} \quad (\text{D.12})$$

$$\mathcal{E}_2 = \left\{ \sup_{\hat{\mathcal{S}}_1: |\hat{\mathcal{S}}_1|=s} \|\mathbf{M}\|_1 \leq \frac{10\eta_{max}}{C_L} \right\}, \quad (\text{D.13})$$

$$\mathcal{E}_3 = \left\{ \sup_{\hat{\mathcal{S}}_1: |\hat{\mathcal{S}}_1|=s} \max_{1 \leq j \leq s} |[M \hat{\boldsymbol{\Sigma}}_{\hat{\mathcal{S}}_1} M^\text{T} - \boldsymbol{\Sigma}_{\hat{\mathcal{S}}_1}^{-1}]_{jj}| \leq \mu \right\}, \quad (\text{D.14})$$

where \mathcal{S}_* denotes the index set of relevant variables to the exposure that is defined on $\{1, \dots, p\}$; s_1^*, s_2^* represent the number of relevant variables to the exposure and the number of invalid instruments, respectively; C_L, C_R lower and upper bound the eigenvalues of $\boldsymbol{\Sigma} \in \mathbb{R}^{p \times p}$ and B is an upper bound placed on $[\boldsymbol{\Sigma}]_{jj}$, as shown in assumption A2; $\lambda_\gamma = C_\gamma \sqrt{(\log p)/n}$ and $\lambda_\Gamma = C_\Gamma \sqrt{(\log p)/n}$ are lasso tuning parameters, where constants $C_\gamma \geq 5.7 \sqrt{B(\boldsymbol{\alpha}_D^{*\text{T}} \boldsymbol{\Sigma}_U \boldsymbol{\alpha}_D^* + \sigma_D^2)}$, and $C_\Gamma \geq 5.7 \sqrt{B\{(\beta^* \boldsymbol{\alpha}_D^* + \boldsymbol{\alpha}_Y^*)^\text{T} \boldsymbol{\Sigma}_U (\beta^* \boldsymbol{\alpha}_D^* + \boldsymbol{\alpha}_Y^*) + \beta^{*2} \sigma_D^2 + \sigma_Y^2\}}$; $\lambda_{\text{NL}} = 4a_2 \eta_{\text{max}} \sqrt{(\log p)/n}$; $\boldsymbol{\Sigma}_{\hat{\mathcal{S}}_1}^{-1}$ denotes the inverse of the submatrix $\boldsymbol{\Sigma}_{\hat{\mathcal{S}}_1}$ formed by deleting rows and columns of $\boldsymbol{\Sigma}$ indexed by $\hat{\mathcal{S}}_1$ and $[\]_{-j,j}$ refers to the j th column without the j th component of the matrix; a_2, a_4, a_5 are positive constants and particularly, $a_2 > 4\sqrt{3}eB\kappa^2$ where κ is the sub-Gaussian norm of $\boldsymbol{\Sigma}^{-1/2} \mathbf{Z}_1$ and is a finite, positive constant, and $a_5 > \sqrt{1.01B\text{var}(\boldsymbol{\epsilon})}$; μ is defined as

$$\mu = \zeta_1 \left(\frac{\log p}{n} \right)^{1/4} \eta_{\text{max}}^2 \quad (\text{D.15})$$

for some constant $\zeta_1 > 0$.

On the event \mathcal{A} , the set of candidates passing marginal screening, $\hat{\mathcal{S}}_1$, includes all relevant variables to the exposure, and the models (2.1) and (2.2) hold with $\mathbf{Z} \in \mathbb{R}^p$ replaced by $\mathbf{Z}_{\hat{\mathcal{S}}_1} \in \mathbb{R}^s$. The events $\mathcal{B}_1, \mathcal{B}_2, \mathcal{B}_3$ provide convergence rates for lasso post marginal screening estimators as well as the prediction error. Control of the variance estimate for $\mathbf{U}^\top \boldsymbol{\alpha}_D^* + \epsilon_D$ using lasso post marginal screening estimators is introduced in the event $\tilde{\mathcal{B}}$. Events $\mathcal{C}_1, \mathcal{C}_2$ give the convergence rates for the error terms Δ_1, Δ_2 as shown in (D.1) and (D.2) uniformly over all possible $\hat{\mathcal{S}}_1$ of size s . The event \mathcal{C}_3 places an upper bound for the maximal correlation between candidate Z_j and a random error term ϵ that is independent of Z_j for all $j = 1, \dots, p$, which is the key ingredient in controlling convergence rates of the lasso type estimators. The error term ϵ will vary place to place to accommodate with different bounds of interest. The bounded support for $n\|\mathbf{v}_l\|^2$ is provided in the event \mathcal{D} , which will be used to explore the order of the joint threshold.

Let \mathcal{E} be the intersection of all events defined in (D.3)–(D.14). Later we will show that there exists a constant $C_1 > 0$ such that when n, p are sufficiently large, we have

$$P(\mathcal{E}) \geq 1 - e^{-C_1 \log(n \wedge p)}. \quad (\text{D.16})$$

D.2 Proof for Theorem 3.1 and Theorem 3.2

In this section, we give proof for the two main theorems. Before proceeding, we first derive the bias of the ratio estimates associated with the candidate instruments passing marginal screening. Under assumptions A3, on the event \mathcal{A} , the difference between the ratio estimate for each candidate instrument in $\hat{\mathcal{S}}_1$ and the true causal effect β^* , i.e., $\hat{\Gamma}_{\hat{\mathcal{S}}_1, l} / \hat{\gamma}_{\hat{\mathcal{S}}_1, l} - \beta^*$ takes the following form

$$\begin{aligned} \frac{\hat{\Gamma}_{\hat{\mathcal{S}}_1, l}}{\hat{\gamma}_{\hat{\mathcal{S}}_1, l}} - \beta^* &= \frac{e_l^\top \sqrt{n}(\hat{\boldsymbol{\Gamma}}_{\hat{\mathcal{S}}_1} - \boldsymbol{\Gamma}_{\hat{\mathcal{S}}_1}^*) + \sqrt{n}\Gamma_{\hat{\mathcal{S}}_1, l}^*}{e_l^\top \sqrt{n}(\hat{\boldsymbol{\gamma}}_{\hat{\mathcal{S}}_1} - \boldsymbol{\gamma}_{\hat{\mathcal{S}}_1}^*) + \sqrt{n}\gamma_{\hat{\mathcal{S}}_1, l}^*} - \beta^* \\ &= \frac{e_l^\top \Delta_2 + e_l^\top \frac{1}{\sqrt{n}} \mathbf{M} \mathbf{Z}_{\hat{\mathcal{S}}_1}^\top \{\beta^*(\mathbf{U}\boldsymbol{\alpha}_D^* + \boldsymbol{\epsilon}_D) + \mathbf{U}\boldsymbol{\alpha}_Y^* + \boldsymbol{\epsilon}_Y\} + \sqrt{n}\Gamma_{\hat{\mathcal{S}}_1, l}^*}{e_l^\top \Delta_1 + e_l^\top \frac{1}{\sqrt{n}} \mathbf{M} \mathbf{Z}_{\hat{\mathcal{S}}_1}^\top (\mathbf{U}\boldsymbol{\alpha}_D^* + \boldsymbol{\epsilon}_D) + \sqrt{n}\gamma_{\hat{\mathcal{S}}_1, l}^*} - \beta^* \\ &= \frac{e_l^\top \Delta_2 + e_l^\top \frac{1}{\sqrt{n}} \mathbf{M} \mathbf{Z}_{\hat{\mathcal{S}}_1}^\top \{\beta^*(\mathbf{U}\boldsymbol{\alpha}_D^* + \boldsymbol{\epsilon}_D) + \mathbf{U}\boldsymbol{\alpha}_Y^* + \boldsymbol{\epsilon}_Y\} + \sqrt{n}(\pi_{\hat{\mathcal{S}}_1, l}^* + \beta^*\gamma_{\hat{\mathcal{S}}_1, l}^*)}{e_l^\top \Delta_1 + e_l^\top \frac{1}{\sqrt{n}} \mathbf{M} \mathbf{Z}_{\hat{\mathcal{S}}_1}^\top (\mathbf{U}\boldsymbol{\alpha}_D^* + \boldsymbol{\epsilon}_D) + \sqrt{n}\gamma_{\hat{\mathcal{S}}_1, l}^*} - \beta^* \\ &= \beta^* + \frac{e_l^\top (\Delta_2 - \beta^* \Delta_1) + e_l^\top \frac{1}{\sqrt{n}} \mathbf{M} \mathbf{Z}_{\hat{\mathcal{S}}_1}^\top (\mathbf{U}\boldsymbol{\alpha}_Y^* + \boldsymbol{\epsilon}_Y) + \sqrt{n}\pi_{\hat{\mathcal{S}}_1, l}^*}{e_l^\top \Delta_1 + e_l^\top \frac{1}{\sqrt{n}} \mathbf{M} \mathbf{Z}_{\hat{\mathcal{S}}_1}^\top (\mathbf{U}\boldsymbol{\alpha}_D^* + \boldsymbol{\epsilon}_D) + \sqrt{n}\gamma_{\hat{\mathcal{S}}_1, l}^*} - \beta^* \\ &= \frac{e_l^\top (\Delta_2 - \beta^* \Delta_1) + \sqrt{n}\mathbf{v}_l^\top (\mathbf{U}\boldsymbol{\alpha}_Y^* + \boldsymbol{\epsilon}_Y) + \sqrt{n}\pi_{\hat{\mathcal{S}}_1, l}^*}{\sqrt{n}\hat{\gamma}_{\hat{\mathcal{S}}_1, l}} \end{aligned} \quad (\text{D.17})$$

for $1 \leq l \leq s$, where the second and the last equality come from the decomposition (D.1) and (D.2); the third equality follows from $\boldsymbol{\Gamma}_{\hat{\mathcal{S}}_1}^* = \boldsymbol{\pi}_{\hat{\mathcal{S}}_1}^* + \beta^*\boldsymbol{\gamma}_{\hat{\mathcal{S}}_1}^*$.

Recall the definition of the set of candidates passing joint thresholding,

$$\hat{\mathcal{S}}_2 = \left\{ l : 1 \leq l \leq s, |\hat{\gamma}_{\hat{\mathcal{S}}_1, l}| \geq \delta_n \|\mathbf{v}_l\| \frac{\|\mathbf{D} - \mathbb{Z}_{\hat{\mathcal{S}}_1} \tilde{\gamma}_{\hat{\mathcal{S}}_1}\|}{\sqrt{n}} \right\}$$

where $\delta_n = \sqrt{\omega \log s}$ and $\omega > 0$ is a constant. In the coming two sections, we explore the behavior of causal estimates for spurious and relevant instruments in $\hat{\mathcal{S}}_2$.

D.2.1 Limiting Behavior of Causal Effect Estimates from Spurious Instruments

Now we give the proof of Theorem 3.1, which claims that bias of causal effect estimates from spurious instruments that pass both marginal screening and joint thresholding concentrate in a region with the center $C_* = \text{cov}(\boldsymbol{\alpha}_D^{*\text{T}} \mathbf{U}, \boldsymbol{\alpha}_Y^{*\text{T}} \mathbf{U}) / \text{var}(\boldsymbol{\alpha}_D^{*\text{T}} \mathbf{U} + \epsilon_D)$. Without loss of generality, assume $\beta^* > 0$.

Proof of Theorem 3.1. Recall the definition of the set of irrelevant variables, $\check{\mathcal{I}} = \{l : 1 \leq l \leq s, \gamma_{\hat{\mathcal{S}}_1, l}^* = 0\}$.

To prove that there exists a constant $d > 0$ such that the causal estimates $\hat{\Gamma}_{\hat{\mathcal{S}}_1, l} / \hat{\gamma}_{\hat{\mathcal{S}}_1, l}$ for $l \in \check{\mathcal{I}} \cap \hat{\mathcal{S}}_2$ concentrate in the interval $[\beta^* + C_* - d, \beta^* + C_* + d]$ simultaneously, we need to control the probability below

$$P\left(\cup_{l \in \check{\mathcal{I}} \cap \hat{\mathcal{S}}_2} \left\{ \left| \frac{\hat{\Gamma}_{\hat{\mathcal{S}}_1, l}}{\hat{\gamma}_{\hat{\mathcal{S}}_1, l}} - \beta^* - C_* \right| > d \right\}\right), \quad (\text{D.18})$$

where $\hat{\Gamma}_{\hat{\mathcal{S}}_1, l}, \hat{\gamma}_{\hat{\mathcal{S}}_1, l}$ denote the debiased-lasso estimators.

It follows from (D.17) and $\pi_{\hat{\mathcal{S}}_1, l}^* = 0$ for irrelevant variables that

$$\begin{aligned} & P\left(\left\{ \exists l \in \check{\mathcal{I}} \cap \hat{\mathcal{S}}_2 : \left| \frac{\hat{\Gamma}_{\hat{\mathcal{S}}_1, l}}{\hat{\gamma}_{\hat{\mathcal{S}}_1, l}} - \beta^* - C_* \right| > d \right\} \cap \mathcal{E}\right) \\ & \leq P\left(\left\{ \exists l \in \check{\mathcal{I}} \cap \hat{\mathcal{S}}_2 : \left| \frac{e_l^{\text{T}}(\Delta_2 - \beta^* \Delta_1) + \sqrt{n} \mathbf{v}_l^{\text{T}}(\mathbf{U} \boldsymbol{\alpha}_Y^* + \epsilon_Y)}{\sqrt{n} \hat{\gamma}_{\hat{\mathcal{S}}_1, l}} - C_* \right| > d \right\} \cap \mathcal{E}\right) \\ & = P\left(\left\{ \exists l \in \check{\mathcal{I}} \cap \hat{\mathcal{S}}_2 : \left| \frac{e_l^{\text{T}}(\Delta_2 - \beta^* \Delta_1)}{\sqrt{n}} + \mathbf{v}_l^{\text{T}}(\mathbf{U} \boldsymbol{\alpha}_Y^* + \epsilon_Y) - C_* \hat{\gamma}_{\hat{\mathcal{S}}_1, l} \right| > d |\hat{\gamma}_{\hat{\mathcal{S}}_1, l}| \right\} \cap \mathcal{E}\right) \\ & = P\left(\left\{ \exists l \in \check{\mathcal{I}} \cap \hat{\mathcal{S}}_2 : \left| \frac{e_l^{\text{T}}\{\Delta_2 - (\beta^* + C_*) \Delta_1\}}{\sqrt{n}} + \mathbf{v}_l^{\text{T}}(\mathbf{U} \boldsymbol{\alpha}_Y^* + \epsilon_Y) \right. \right. \\ & \quad \left. \left. - C_* \mathbf{v}_l^{\text{T}}(\mathbf{U} \boldsymbol{\alpha}_D^* + \epsilon_D) \right| > d |\hat{\gamma}_{\hat{\mathcal{S}}_1, l}| \right\} \cap \mathcal{E}\right) \\ & \leq P\left(\underbrace{\left\{ \exists l \in \check{\mathcal{I}} \cap \hat{\mathcal{S}}_2 : \left| \frac{e_l^{\text{T}}\{\Delta_2 - (\beta^* + C_*) \Delta_1\}}{\sqrt{n}} \right| > \frac{d |\hat{\gamma}_{\hat{\mathcal{S}}_1, l}|}{2} \right\}}_{(\text{D.19})_a} \cap \mathcal{E}\right) \\ & \quad + P\left(\underbrace{\left\{ \exists l \in \check{\mathcal{I}} \cap \hat{\mathcal{S}}_2 : \left| \mathbf{v}_l^{\text{T}}(\mathbf{U} \boldsymbol{\alpha}_Y^* + \epsilon_Y) - C_* \mathbf{v}_l^{\text{T}}(\mathbf{U} \boldsymbol{\alpha}_D^* + \epsilon_D) \right| > \frac{d |\hat{\gamma}_{\hat{\mathcal{S}}_1, l}|}{2} \right\}}_{(\text{D.19})_b} \cap \mathcal{E}\right), \quad (\text{D.19}) \end{aligned}$$

where $e_l \in \mathbb{R}^s$ is the l 'th unit vector in \mathbb{R}^s and $\mathbf{v}_l = \mathbb{Z}_{\hat{\mathcal{S}}_1} \mathbf{M}^\top e_l / n \in \mathbb{R}^n$ for $1 \leq l \leq s$. The second equality comes from the decomposition (D.1) of $\hat{\gamma}_{\hat{\mathcal{S}}_1}$ and the last inequality is from the definition of $\hat{\mathcal{S}}_2$.

We first focus on (D.19)_a. Take $\delta_L = (\boldsymbol{\alpha}_D^{*\top} \Sigma_U \boldsymbol{\alpha}_D^* + \sigma_D^2) / 2$. On the event $\tilde{\mathcal{B}} \subset \mathcal{E}$, under the conditions that $\log p = O(n^{\tau_1})$ for $0 < \tau_1 < 1$ and s_1^* is fixed, we have

$$\frac{1}{n} \|\mathbf{D} - \mathbb{Z}_{\hat{\mathcal{S}}_1} \tilde{\gamma}_{\hat{\mathcal{S}}_1}\|^2 \geq \delta_L \quad (\text{D.20})$$

for all $\hat{\mathcal{S}}_1$ of size s for n, p sufficiently large. As $n \|\mathbf{v}_l\|^2$ is bounded from below and above on the event $\mathcal{D} \subset \mathcal{E}$, we further obtain by the definition of $\hat{\mathcal{S}}_2$

$$|\hat{\gamma}_{\hat{\mathcal{S}}_1, l}| \geq \frac{\delta_n \delta_L^{1/2} (C_R^{-1} - \mu)^{1/2}}{\sqrt{n}} \quad (\text{D.21})$$

for $l \in \tilde{\mathcal{I}} \cap \hat{\mathcal{S}}_2$, with

$$\mu = \zeta_1 \left(\frac{\log p}{n} \right)^{1/4} \eta_{\max}^2$$

for some constant $\zeta_1 > 0$. Under assumption A6 that $\eta_{\max}^2 = o((n/\log p)^{1/4})$, we have $\mu \rightarrow 0$ as $n, p \rightarrow \infty$. Moreover, it follows from assumptions A4 saying s_1^*, s_2^* are fixed, assumption A6 that $\eta_{\max} = o((n/\log p)^{1/4})$ and the condition $(\log p)^{3/4} = o(n^{1/4} \sqrt{\log s})$ that

$$s_1^* \lambda_\gamma \eta_{\max} \sqrt{\log p} = o(d \delta_n (C_R^{-1} - \mu)^{1/2}), \quad (\text{D.22})$$

$$s_2^* \lambda_\Gamma \eta_{\max} \sqrt{\log p} = o(d \delta_n (C_R^{-1} - \mu)^{1/2}) \quad (\text{D.23})$$

with $\lambda_\gamma = C_\gamma \sqrt{(\log p)/n}$, $\lambda_\Gamma = C_\Gamma \sqrt{(\log p)/n}$ and $\delta_n = \sqrt{\omega \log s}$.

Hence, combining (D.21), (D.22) and (D.23), on the event \mathcal{E} , we have

$$\sup_{\hat{\mathcal{S}}_1: |\hat{\mathcal{S}}_1|=s} \|\Delta_1\|_\infty + \sup_{\hat{\mathcal{S}}_1: |\hat{\mathcal{S}}_1|=s} \|\Delta_2\|_\infty = o(\sqrt{n} |\hat{\gamma}_{\hat{\mathcal{S}}_1, l}|),$$

which further implies that for n, p large enough (D.19)_a = 0.

It remains to bound (D.19)_b. Before proceeding, we first derive the conditional distribution of $\mathbf{v}_l^\top (\mathbf{U} \boldsymbol{\alpha}_Y^* + \boldsymbol{\epsilon}_Y)$ given $\mathbb{Z} \in \mathbb{R}^{n \times p}$ and $\mathbf{U} \boldsymbol{\alpha}_D^* + \boldsymbol{\epsilon}_D = \mathbf{y}$. By conditioning on \mathbb{Z} and $\mathbf{U} \boldsymbol{\alpha}_D^* + \boldsymbol{\epsilon}_D$, the observed exposures $\mathbf{D} \in \mathbb{R}^n$ is fixed, so is $\hat{\mathcal{S}}_1$, as the marginal screening is implemented on the exposure only. This implies that \mathbf{v}_l is also fixed for $l = 1, \dots, s$. Then by direct computations, for $1 \leq l \leq s$, we have

$$\mathbf{v}_l^\top (\mathbf{U} \boldsymbol{\alpha}_Y^*) | \mathbb{Z}, \mathbf{U} \boldsymbol{\alpha}_D^* + \boldsymbol{\epsilon}_D = \mathbf{y} \sim N \left(C_* \mathbf{v}_l^\top \mathbf{y}, \left\{ \text{var}(\boldsymbol{\alpha}_Y^{*\top} \mathbf{U}) - \frac{\text{cov}^2(\boldsymbol{\alpha}_Y^{*\top} \mathbf{U}, \boldsymbol{\alpha}_D^{*\top} \mathbf{U})}{\text{var}(\boldsymbol{\alpha}_D^{*\top} \mathbf{U} + \boldsymbol{\epsilon}_D)} \right\} \|\mathbf{v}_l\|^2 \right), \quad (\text{D.24})$$

where $C_* = \text{cov}(\boldsymbol{\alpha}_D^{*\top} \mathbf{U}, \boldsymbol{\alpha}_Y^{*\top} \mathbf{U}) / \text{var}(\boldsymbol{\alpha}_D^{*\top} \mathbf{U} + \boldsymbol{\epsilon}_D)$. Under assumption A1 that $\boldsymbol{\epsilon}_Y$ is independent of

$\mathbf{U}, \mathbf{Z}, \epsilon_D$, we further obtain

$$\begin{aligned} \mathbf{v}_l^\top (\mathbf{U}\boldsymbol{\alpha}_Y^* + \boldsymbol{\epsilon}_Y) | \mathbb{Z}, \mathbf{U}\boldsymbol{\alpha}_D^* + \boldsymbol{\epsilon}_D = \mathbf{y} &\sim \\ N \left(C_* \mathbf{v}_l^\top \mathbf{y}, \left\{ \text{var}(\boldsymbol{\alpha}_Y^* \mathbf{U}) - \frac{\text{cov}^2(\boldsymbol{\alpha}_Y^* \mathbf{U}, \boldsymbol{\alpha}_D^* \mathbf{U})}{\text{var}(\boldsymbol{\alpha}_D^* \mathbf{U} + \boldsymbol{\epsilon}_D)} + \sigma_Y^2 \right\} \|\mathbf{v}_l\|^2 \right). \end{aligned} \quad (\text{D.25})$$

Next, we can bound (D.19)_b by

$$\begin{aligned} (\text{D.19})_b &= P \left(\left\{ \exists l \in \check{\mathcal{I}} \cap \hat{\mathcal{S}}_2 : |\mathbf{v}_l^\top (\mathbf{U}\boldsymbol{\alpha}_Y^* + \boldsymbol{\epsilon}_Y) - C_* \mathbf{v}_l^\top (\mathbf{U}\boldsymbol{\alpha}_D^* + \boldsymbol{\epsilon}_D)| > \frac{d|\hat{\gamma}_{\hat{\mathcal{S}}_1, l}|}{2} \right\} \cap \mathcal{E} \right) \\ &\leq P \left(\exists l \in \{1, \dots, s\} : |\mathbf{v}_l^\top (\boldsymbol{\alpha}_Y^* \mathbf{U} + \boldsymbol{\epsilon}_Y) - C_* \mathbf{v}_l^\top (\mathbf{U}\boldsymbol{\alpha}_D^* + \boldsymbol{\epsilon}_D)| > \frac{d\delta_n \|\mathbf{v}_l\| \delta_L^{1/2}}{2} \right) \\ &\leq \sum_{1 \leq l \leq s} P \left(|\mathbf{v}_l^\top (\mathbf{U}\boldsymbol{\alpha}_Y^* + \boldsymbol{\epsilon}_Y) - C_* \mathbf{v}_l^\top (\mathbf{U}\boldsymbol{\alpha}_D^* + \boldsymbol{\epsilon}_D)| > \frac{d\delta_n \|\mathbf{v}_l\| \delta_L^{1/2}}{2} \right) \\ &= \sum_{1 \leq l \leq s} E \left[P \left(|\mathbf{v}_l^\top (\mathbf{U}\boldsymbol{\alpha}_Y^* + \boldsymbol{\epsilon}_Y) - C_* \mathbf{v}_l^\top (\mathbf{U}\boldsymbol{\alpha}_D^* + \boldsymbol{\epsilon}_D)| > \frac{d\delta_n \|\mathbf{v}_l\| \delta_L^{1/2}}{2} \middle| \mathbb{Z}, \mathbf{U}\boldsymbol{\alpha}_D^* + \boldsymbol{\epsilon}_D \right) \right] \\ &\leq \sum_{1 \leq l \leq s} E \left[2 \exp \left\{ - \frac{d^2 \delta_L \delta_n^2}{8 \left\{ \text{var}(\boldsymbol{\alpha}_Y^* \mathbf{U}) - \frac{\text{cov}^2(\boldsymbol{\alpha}_Y^* \mathbf{U}, \boldsymbol{\alpha}_D^* \mathbf{U})}{\text{var}(\boldsymbol{\alpha}_D^* \mathbf{U} + \boldsymbol{\epsilon}_D)} + \sigma_Y^2 \right\}} \right\} \right] \\ &= 2 \exp \{ (1 - 4d^2 \omega / \tilde{C}^2) \log(s) \}, \end{aligned} \quad (\text{D.26})$$

where

$$\tilde{C} := \frac{8 \left\{ \text{var}(\boldsymbol{\alpha}_Y^* \mathbf{U}) - \frac{\text{cov}^2(\boldsymbol{\alpha}_Y^* \mathbf{U}, \boldsymbol{\alpha}_D^* \mathbf{U})}{\text{var}(\boldsymbol{\alpha}_D^* \mathbf{U} + \boldsymbol{\epsilon}_D)} + \sigma_Y^2 \right\}^{1/2}}{\sqrt{\text{var}(\boldsymbol{\alpha}_D^* \mathbf{U} + \boldsymbol{\epsilon}_D)}}.$$

Here the first inequality is from the definition of $\hat{\mathcal{S}}_2$ and (D.20); the second inequality is simply a union bound; the second equality applies the law of total expectation; the last inequality uses (D.25) and the Gaussian tail bound; the last equality replaces δ_L with its explicit form $(\boldsymbol{\alpha}_D^{*\top} \Sigma_U \boldsymbol{\alpha}_D^* + \sigma_D^2)/2$.

Take $d = \tilde{C}/\sqrt{\omega}$. Then by (D.26) and (D.19)_a = 0 as shown previously,

$$P \left(\left\{ \exists l \in \check{\mathcal{I}} \cap \hat{\mathcal{S}}_2 : \left| \frac{\hat{\Gamma}_{\hat{\mathcal{S}}_1, l}}{\hat{\gamma}_{\hat{\mathcal{S}}_1, l}} - \beta^* - C_* \right| > \frac{\tilde{C}}{\sqrt{\omega}} \right\} \cap \mathcal{E} \right) \leq 2s^{-3}. \quad (\text{D.27})$$

Using (D.27) and (D.16) that accounts for \mathcal{E} completes the proof. \square

D.2.2 Limiting Behavior of Causal Effect Estimates from Relevant Variables

In this section, we establish concentration results for valid and invalid instruments that pass joint thresholding. In particular, the causal effect estimates from valid IVs concentrate around the true causal effect β^* and the causal effect estimates from invalid IVs which violate the exclusion restriction assumption concentrate

around $\beta^* + \pi_{\hat{\mathcal{S}}_1, l}^*/\gamma_{\hat{\mathcal{S}}_1, l}^*$, with $\pi_{\hat{\mathcal{S}}_1, l}^* \neq 0$ for $l \in \hat{\mathcal{S}}_2$.

Proof of Theorem 3.2. The first statement that relevant variables can pass joint thresholding with probability tending to one follows directly from Lemma D.1. Recall the definition of the set of relevant variables $\check{\mathcal{R}} = \{l : 1 \leq l \leq s, \gamma_{\hat{\mathcal{S}}_1, l}^* \neq 0\}$. To prove the concentration statement regarding $(\hat{\Gamma}_{\hat{\mathcal{S}}_1, l}/\hat{\gamma}_{\hat{\mathcal{S}}_1, l}) - (\beta^* + \pi_{\hat{\mathcal{S}}_1, l}^*/\gamma_{\hat{\mathcal{S}}_1, l}^*)$ for relevant variables that survive joint thresholding, it suffices to control

$$P\left(\cup_{l \in \check{\mathcal{R}}} \left\{ \left| \frac{\hat{\Gamma}_{\hat{\mathcal{S}}_1, l}}{\hat{\gamma}_{\hat{\mathcal{S}}_1, l}} - \left(\beta^* + \frac{\pi_{\hat{\mathcal{S}}_1, l}^*}{\gamma_{\hat{\mathcal{S}}_1, l}^*} \right) \right| > \epsilon_n \right\} \right), \quad (\text{D.28})$$

where

$$\epsilon_n = C_2 \sqrt{\frac{\log p}{n} \frac{10\eta_{\max}}{C_L}}$$

for some constant $C_2 > 0$. Define events $\Omega_l = \{|\hat{\gamma}_{\hat{\mathcal{S}}_1, l} - \gamma_{\hat{\mathcal{S}}_1, l}^*| \leq |\gamma_{\hat{\mathcal{S}}_1, l}^*|/2\}$ for $l \in \check{\mathcal{R}}$. Simple calculations give

$$\begin{aligned} P(\cup_{l \in \check{\mathcal{R}}} \Omega_l^c) &= P\left(\exists l \in \check{\mathcal{R}} : |\hat{\gamma}_{\hat{\mathcal{S}}_1, l} - \gamma_{\hat{\mathcal{S}}_1, l}^*| > \frac{|\gamma_{\hat{\mathcal{S}}_1, l}^*|}{2}\right) \\ &\leq P\left(\exists l \in \check{\mathcal{R}} : |\hat{\gamma}_{\hat{\mathcal{S}}_1, l} - \gamma_{\hat{\mathcal{S}}_1, l}^*| > \frac{c_0}{2}\right), \end{aligned} \quad (\text{D.29})$$

where the inequality is from assumption A5 that $|\gamma_{\hat{\mathcal{S}}_1, l}^*| \geq c_0$ for $l \in \check{\mathcal{R}}$.

Applying the triangle inequality, the difference between two ratios satisfies

$$\left| \frac{\hat{\Gamma}_{\hat{\mathcal{S}}_1, l}}{\hat{\gamma}_{\hat{\mathcal{S}}_1, l}} - \frac{\Gamma_{\hat{\mathcal{S}}_1, l}^*}{\gamma_{\hat{\mathcal{S}}_1, l}^*} \right| \leq \frac{|\hat{\Gamma}_{\hat{\mathcal{S}}_1, l} - \Gamma_{\hat{\mathcal{S}}_1, l}^*|}{|\hat{\gamma}_{\hat{\mathcal{S}}_1, l}|} + |\Gamma_{\hat{\mathcal{S}}_1, l}^*| \frac{|\hat{\gamma}_{\hat{\mathcal{S}}_1, l} - \gamma_{\hat{\mathcal{S}}_1, l}^*|}{|\hat{\gamma}_{\hat{\mathcal{S}}_1, l} \gamma_{\hat{\mathcal{S}}_1, l}^*|}. \quad (\text{D.30})$$

On the event Ω_l for $l \in \check{\mathcal{R}}$, observe that $\gamma_{\hat{\mathcal{S}}_1, l}^{*2} \leq 4|\hat{\gamma}_{\hat{\mathcal{S}}_1, l} \gamma_{\hat{\mathcal{S}}_1, l}^*|$ and moreover $|\gamma_{\hat{\mathcal{S}}_1, l}^*| \leq 4|\hat{\gamma}_{\hat{\mathcal{S}}_1, l}|$. Then it follows directly from these two inequalities and assumption A5 that

$$\begin{aligned} (\text{D.30}) &\leq \frac{4}{c_0} |\hat{\Gamma}_{\hat{\mathcal{S}}_1, l} - \Gamma_{\hat{\mathcal{S}}_1, l}^*| + \frac{4(\check{C}_0 + \beta^* C_0)}{c_0^2} |\hat{\gamma}_{\hat{\mathcal{S}}_1, l} - \gamma_{\hat{\mathcal{S}}_1, l}^*| \\ &\leq c_4 (|\hat{\Gamma}_{\hat{\mathcal{S}}_1, l} - \Gamma_{\hat{\mathcal{S}}_1, l}^*| + |\hat{\gamma}_{\hat{\mathcal{S}}_1, l} - \gamma_{\hat{\mathcal{S}}_1, l}^*|), \end{aligned}$$

where $c_4 = \max\{4/c_0, 4(\check{C}_0 + \beta^* C_0)/c_0^2\}$. We further obtain

$$\begin{aligned} &P\left(\exists l \in \check{\mathcal{R}} : \left| \frac{\hat{\Gamma}_{\hat{\mathcal{S}}_1, l}}{\hat{\gamma}_{\hat{\mathcal{S}}_1, l}} - \frac{\Gamma_{\hat{\mathcal{S}}_1, l}^*}{\gamma_{\hat{\mathcal{S}}_1, l}^*} \right| > \epsilon_n \text{ and } |\hat{\gamma}_{\hat{\mathcal{S}}_1, l} - \gamma_{\hat{\mathcal{S}}_1, l}^*| \leq \frac{|\gamma_{\hat{\mathcal{S}}_1, l}^*|}{2}\right) \\ &\leq P\left(\exists l \in \check{\mathcal{R}} : (|\hat{\Gamma}_{\hat{\mathcal{S}}_1, l} - \Gamma_{\hat{\mathcal{S}}_1, l}^*| + |\hat{\gamma}_{\hat{\mathcal{S}}_1, l} - \gamma_{\hat{\mathcal{S}}_1, l}^*|) > \frac{\epsilon_n}{c_4}\right). \end{aligned} \quad (\text{D.31})$$

Under assumption A6 that $\eta_{\max} = o((n/\log p)^{1/4})$, clearly (D.29) can be upper bounded by (D.31). Hence,

bounding (D.31) is sufficient to control (D.28).

Using the decomposition (D.1) and (D.2), we have

$$\begin{aligned} & |\widehat{\Gamma}_{\widehat{\mathcal{S}}_1, l} - \Gamma_{\widehat{\mathcal{S}}_1, l}^*| + |\widehat{\gamma}_{\widehat{\mathcal{S}}_1, l} - \gamma_{\widehat{\mathcal{S}}_1, l}^*| \\ & \leq \frac{e_l^\top \Delta_1}{\sqrt{n}} + \frac{e_l^\top \Delta_2}{\sqrt{n}} + |\mathbf{v}_l^\top (\mathbf{U} \boldsymbol{\alpha}_D^* + \boldsymbol{\epsilon}_D)| + |\mathbf{v}_l^\top \{\mathbf{U}(\boldsymbol{\alpha}_Y^* + \beta^* \boldsymbol{\alpha}_D^*) + \beta^* \boldsymbol{\epsilon}_D + \boldsymbol{\epsilon}_Y\}|, \end{aligned}$$

where $\mathbf{v}_l = \mathbb{Z}_{\widehat{\mathcal{S}}_1} \mathbf{M}^\top e_l / n \in \mathbb{R}^n$ and $e_l \in \mathbb{R}^s$ is a unit vector with the l th component equal to one and zero otherwise. On the event \mathcal{E} , we further obtain

$$\begin{aligned} & \sup_{\widehat{\mathcal{S}}_1: |\widehat{\mathcal{S}}_1|=s} \frac{\|\Delta_1\|_\infty}{\sqrt{n}} + \sup_{\widehat{\mathcal{S}}_1: |\widehat{\mathcal{S}}_1|=s} \frac{\|\Delta_2\|_\infty}{\sqrt{n}} \\ & \leq \frac{140a_2 \sqrt{\log p} \max\{s_1^* \lambda_\gamma, s_2^* \lambda_\Gamma\}}{\sqrt{n} C_L^2} \eta_{\max} \\ & = o(\epsilon_n), \end{aligned} \tag{D.32}$$

where the last statement follows from

$$\sqrt{\log p} \max\{\lambda_\gamma, \lambda_\Gamma\} \eta_{\max} = o(\sqrt{n} \epsilon_n)$$

under A4 that s_1^*, s_2^* are fixed and $\log p = o(n)$. Note by definition of $\mathbf{v}_l = \mathbb{Z}_{\widehat{\mathcal{S}}_1} \mathbf{M}^\top e_l / n \in \mathbb{R}^n$, on the event \mathcal{E} , we also have

$$\begin{aligned} & \sup_{\widehat{\mathcal{S}}_1: |\widehat{\mathcal{S}}_1|=s} \max_{1 \leq l \leq p} |\mathbf{v}_l^\top (\mathbf{U} \boldsymbol{\alpha}_D^* + \boldsymbol{\epsilon}_D)| + \sup_{\widehat{\mathcal{S}}_1: |\widehat{\mathcal{S}}_1|=s} \max_{1 \leq l \leq p} |\mathbf{v}_l^\top \{\mathbf{U}(\boldsymbol{\alpha}_Y^* + \beta^* \boldsymbol{\alpha}_D^*) + \beta^* \boldsymbol{\epsilon}_D + \boldsymbol{\epsilon}_Y\}| \\ & \leq \sup_{\widehat{\mathcal{S}}_1: |\widehat{\mathcal{S}}_1|=s} \|\mathbf{M}\|_1 \sup_{\widehat{\mathcal{S}}_1: |\widehat{\mathcal{S}}_1|=s} \frac{1}{n} \|\mathbb{Z}_{\widehat{\mathcal{S}}_1}^\top (\mathbf{U} \boldsymbol{\alpha}_D^* + \boldsymbol{\epsilon}_D)\|_\infty \\ & \quad + \sup_{\widehat{\mathcal{S}}_1: |\widehat{\mathcal{S}}_1|=s} \|\mathbf{M}\|_1 \sup_{\widehat{\mathcal{S}}_1: |\widehat{\mathcal{S}}_1|=s} \frac{1}{n} \|\mathbb{Z}_{\widehat{\mathcal{S}}_1}^\top \{\mathbf{U}(\boldsymbol{\alpha}_Y^* + \beta^* \boldsymbol{\alpha}_D^*) + \beta^* \boldsymbol{\epsilon}_D + \boldsymbol{\epsilon}_Y\}\|_\infty \\ & \leq \sup_{\widehat{\mathcal{S}}_1: |\widehat{\mathcal{S}}_1|=s} \|\mathbf{M}\|_1 \left[\max_{1 \leq j \leq p} \frac{1}{n} |\mathbf{Z}_j^\top (\mathbf{U} \boldsymbol{\alpha}_D^* + \boldsymbol{\epsilon}_D)| + \max_{1 \leq j \leq p} \frac{1}{n} |\mathbf{Z}_j^\top \{\mathbf{U}(\boldsymbol{\alpha}_Y^* + \beta^* \boldsymbol{\alpha}_D^*) + \beta^* \boldsymbol{\epsilon}_D + \boldsymbol{\epsilon}_Y\}| \right] \\ & \leq \frac{10a_7 \eta_{\max}}{C_L} \sqrt{\frac{\log p}{n}} \end{aligned} \tag{D.33}$$

with

$$a_7 = 2.1 \sqrt{B \max\{\boldsymbol{\alpha}_D^{*\top} \Sigma_U \boldsymbol{\alpha}_D^* + \sigma_D^2, (\boldsymbol{\alpha}_Y^* + \beta^* \boldsymbol{\alpha}_D^*)^\top \Sigma_U (\boldsymbol{\alpha}_Y^* + \beta^* \boldsymbol{\alpha}_D^*) + \beta^{*2} \sigma_D^2 + \sigma_Y^2\}}.$$

The second inequality uses the fact that the maximal correlation between candidates in $\widehat{\mathcal{S}}_1$ and some linear combination of $\mathbf{U}, \boldsymbol{\epsilon}_D, \boldsymbol{\epsilon}_Y$ is no greater than the maximal correlation evaluated on the initial p -dimension candidates whatever $\widehat{\mathcal{S}}_1$ is; the last inequality uses the uniform bound on $\|\mathbf{M}\|_1$ over all $\widehat{\mathcal{S}}_1$ of size s and bounds of the maximal correlations as provided in the event \mathcal{E} .

Combining (D.32) and (D.33), on the event \mathcal{E} , we get

$$\max_{l \in \mathcal{R}} (|\hat{\Gamma}_{\hat{S}_1, l} - \Gamma_{\hat{S}_1, l}^*| + |\hat{\gamma}_{\hat{S}_1, l} - \gamma_{\hat{S}_1, l}^*|) \lesssim \epsilon_n.$$

Then the concentration inequality follows directly from (D.16). \square

D.2.3 Relevant variables can pass joint thresholding

The lemma below shows that relevant variables can pass joint thresholding with high probability.

Lemma D.1. Assume the same conditions as Theorem 3.2. Then with probability tending to one, relevant variables can pass joint thresholding.

Proof of Lemma D.1. Recall the definition of the set of variables passing joint thresholding,

$$\hat{S}_2 = \left\{ l : 1 \leq l \leq s, |\hat{\gamma}_{\hat{S}_1, l}| \geq \delta_n \|\mathbf{v}_l\| \frac{\|\mathbf{D} - \mathbb{Z}_{\hat{S}_1} \tilde{\gamma}_{\hat{S}_1}\|}{\sqrt{n}} \right\},$$

where $\mathbf{v}_l = \mathbb{Z}_{\hat{S}_1} \mathbf{M}^T \mathbf{e}_l / n \in \mathbb{R}^n$ and $\mathbf{e}_l \in \mathbb{R}^s$ is a unit vector with the l th component equal to one and zero otherwise. And $\delta_n = \sqrt{\omega \log s}$ with $\omega > 0$ a constant.

On the event \mathcal{E} , first notice that all variables that are relevant to the exposure can pass marginal screening, that is, \hat{S}_1 includes all relevant variables. By decomposition (D.1), for $l \in \mathcal{R} = \{l : 1 \leq l \leq s, \gamma_{\hat{S}_1, l}^* \neq 0\}$, the index set of relevant variables defined on \hat{S}_1 , we have

$$\begin{aligned} |\hat{\gamma}_{\hat{S}_1, l}| &\geq |\gamma_{\hat{S}_1, l}^*| - \left| \frac{1}{\sqrt{n}} \mathbf{e}_l^T \Delta_1 + \mathbf{v}_l^T (\mathbf{U} \boldsymbol{\alpha}_D^* + \boldsymbol{\epsilon}_D) \right| \\ &\geq \min_{l \in \mathcal{R}} |\gamma_{\hat{S}_1, l}^*| - \max_{l \in \mathcal{R}} \left| \frac{1}{\sqrt{n}} \mathbf{e}_l^T \Delta_1 + \mathbf{v}_l^T (\mathbf{U} \boldsymbol{\alpha}_D^* + \boldsymbol{\epsilon}_D) \right| \\ &\geq c_0 - \sup_{\hat{S}_1: |\hat{S}_1|=s} \frac{\|\Delta_1\|_\infty}{\sqrt{n}} - \sup_{\hat{S}_1: |\hat{S}_1|=s} \max_{1 \leq l \leq p} |\mathbf{v}_l^T (\mathbf{U} \boldsymbol{\alpha}_D^* + \boldsymbol{\epsilon}_D)|, \end{aligned} \quad (\text{D.34})$$

where the last inequality follows from assumption A5. Following similar arguments used to show (D.33), together with assumption A4 and $\log p = o(n)$, on the event \mathcal{E} , we have

$$\begin{aligned} &\sup_{\hat{S}_1: |\hat{S}_1|=s} \frac{\|\Delta_1\|_\infty}{\sqrt{n}} + \sup_{\hat{S}_1: |\hat{S}_1|=s} \max_{1 \leq l \leq p} |\mathbf{v}_l^T (\mathbf{U} \boldsymbol{\alpha}_D^* + \boldsymbol{\epsilon}_D)| \\ &\lesssim \eta_{\max} \sqrt{\frac{\log p}{n}}, \end{aligned} \quad (\text{D.35})$$

which is negligible compared to c_0 under assumption A6 that $\eta_{\max} = o((n/\log p)^{1/4})$ as $n, p \rightarrow \infty$. In addition, on the event \mathcal{E} , the joint threshold satisfies

$$\delta_n \|\mathbf{v}_l\| \frac{\|\mathbf{D} - \mathbb{Z}_{\hat{S}_1} \tilde{\gamma}_{\hat{S}_1}\|}{\sqrt{n}} \lesssim \sqrt{\frac{\log s}{n}}. \quad (\text{D.36})$$

It follows directly from (D.34), (D.35) and (D.36) that relevant variables can pass joint thresholding on the event \mathcal{E} . Then using (D.16) completes the proof. \square

Remark D.2. We can allow the relevance strength to decay, and take c_0 , the minimal relevance strength, to satisfy

$$c_0 \asymp \eta_{\max} \sqrt{\frac{\log p}{n}}.$$

Clearly, $c_0 \gg \sqrt{(\log s)/n}$ and thus relevant variables can still pass joint thresholding.

D.3 Control of Events defined Section D.1

The event \mathcal{A} refers to the so-called sure screening property (Fan & Lv, 2008), which claims that under certain conditions, the set of variables passing marginal screening, denoted by $\hat{\mathcal{S}}_1$ with cardinality s , can include all relevant variables with probability tending to one. For completeness, we present the sure screening property as Lemma D.3 below, which is also Theorem 1 of Fan & Lv (2008).

Lemma D.3. Suppose A1, A2, A5 and $\log p = O(n^{\tau_1})$ for $0 < \tau_1 < 1$ hold. Further assume that there exists $c > 0$ such that $\min_{j:\gamma_j^* \neq 0} |\text{cov}(D/\gamma_j^*, Z_j)| \geq c$. If $n^{\tau_2} = O(s)$ for $0 < \tau_2 < 1$, then

$$P(\mathcal{A}) \geq 1 - \exp\{-Cn/(\log n)\}$$

for some $C > 0$.

Lemma D.4 gives convergence rates for estimation error and prediction error of lasso post marginal screening, which correspond to events $\mathcal{B}_1, \mathcal{B}_2, \mathcal{B}_3$ defined in Section D.1,

$$\begin{aligned} \mathcal{B}_1 &= \left\{ \sup_{\hat{\mathcal{S}}_1: |\hat{\mathcal{S}}_1|=s} \|\tilde{\gamma}_{\hat{\mathcal{S}}_1} - \gamma_{\hat{\mathcal{S}}_1}^*\|_1 \leq \frac{16s_1^* \lambda_\gamma}{C_L} \right\} \\ \mathcal{B}_2 &= \left\{ \sup_{\hat{\mathcal{S}}_1: |\hat{\mathcal{S}}_1|=s} \|\tilde{\Gamma}_{\hat{\mathcal{S}}_1} - \Gamma_{\hat{\mathcal{S}}_1}^*\|_1 \leq \frac{16s_2^* \lambda_\Gamma}{C_L} \right\} \\ \mathcal{B}_3 &= \left\{ \sup_{\hat{\mathcal{S}}_1: |\hat{\mathcal{S}}_1|=s} \frac{\|\mathbb{Z}_{\hat{\mathcal{S}}_1}(\gamma_{\hat{\mathcal{S}}_1}^* - \tilde{\gamma}_{\hat{\mathcal{S}}_1})\|^2}{n} \leq \frac{16s_1^* \lambda_\gamma^2}{C_L} \right\}. \end{aligned}$$

Lemma D.4. Under the same conditions as Lemma D.3, and further assume A1 and A4. Take the lasso penalty parameter $\lambda_\gamma = C_\gamma \sqrt{(\log p)/n}$ with $C_\gamma \geq 5.7 \sqrt{B(\boldsymbol{\alpha}_D^{*\top} \Sigma_U \boldsymbol{\alpha}_D^* + \sigma_D^2)}$. Then there exist constants c_3, c_4 such that the following holds

$$P(\mathcal{B}_1 \cap \mathcal{A}) \geq 1 - (e^{-c_3 n} + e^{-c_4 \log p}). \quad (\text{D.37})$$

and

$$P(\mathcal{B}_3 \cap \mathcal{A}) \geq 1 - (e^{-c_3 n} + e^{-c_4 \log p}). \quad (\text{D.38})$$

Similarly, for the lasso estimator $\tilde{\Gamma}_{\hat{\mathcal{S}}_1}$ regarding the outcome model, taking the lasso penalty parameter

$\lambda_\Gamma = C_\Gamma \sqrt{(\log p)/n}$ with $C_\Gamma \geq 5.7 \sqrt{B\{(\beta^* \boldsymbol{\alpha}_D^* + \boldsymbol{\alpha}_Y^*)^\top \Sigma_U (\beta^* \boldsymbol{\alpha}_D^* + \boldsymbol{\alpha}_Y^*) + \beta^{*2} \sigma_D^2 + \sigma_Y^2\}}$, we have

$$P(\mathcal{B}_2 \cap \mathcal{A}) \geq 1 - (e^{-c_3 n} + e^{-c_5 \log p}) \quad (\text{D.39})$$

for constants $c_3, c_5 > 0$.

Proof of Lemma D.4. We focus on the concentration statement with respect to $\tilde{\gamma}_{\hat{\mathcal{S}}_1}$ and similar arguments can be applied to $\tilde{\Gamma}_{\hat{\mathcal{S}}_1}$. On the event \mathcal{A} that $\hat{\mathcal{S}}_1$, which has cardinality s , includes the true model of the exposure, we have $\mathbf{D} = \mathbb{Z}_{\hat{\mathcal{S}}_1} \boldsymbol{\gamma}_{\hat{\mathcal{S}}_1}^* + \mathbf{U} \boldsymbol{\alpha}_D^* + \boldsymbol{\epsilon}_D$. Let $\mathcal{S}_0 \subset \{1, \dots, s\}$ and $\tilde{\mathcal{S}}_0 \subset \{1, \dots, p\}$ denote the true exposure model, and s_1^* represents the sparsity of the true exposure model.

Before proceeding, we first define the compatibility conditions for $\hat{\Sigma}$ and $\hat{\Sigma}_{\hat{\mathcal{S}}_1}$ respectively in the following

$$\phi_1^2(\hat{\Sigma}, 3) = \min_{\tilde{\boldsymbol{\theta}} \in \mathbb{R}^p} \left\{ \frac{s_1^* \tilde{\boldsymbol{\theta}}^\top \hat{\Sigma} \tilde{\boldsymbol{\theta}}}{\|\tilde{\boldsymbol{\theta}}_{\tilde{\mathcal{S}}_0}\|_1^2} \right\} \text{ s.t. } \|\tilde{\boldsymbol{\theta}}_{\tilde{\mathcal{S}}_0^c}\|_1 \leq 3 \|\tilde{\boldsymbol{\theta}}_{\tilde{\mathcal{S}}_0}\|_1 \quad (\text{D.40})$$

$$\phi_2^2(\hat{\Sigma}_{\hat{\mathcal{S}}_1}, 3) = \min_{\boldsymbol{\theta} \in \mathbb{R}^s} \left\{ \frac{s_1^* \boldsymbol{\theta}^\top \hat{\Sigma}_{\hat{\mathcal{S}}_1} \boldsymbol{\theta}}{\|\boldsymbol{\theta}_{\mathcal{S}_0}\|_1^2} \right\} \text{ s.t. } \|\boldsymbol{\theta}_{\mathcal{S}_0^c}\|_1 \leq 3 \|\boldsymbol{\theta}_{\mathcal{S}_0}\|_1, \quad (\text{D.41})$$

where $\boldsymbol{\theta}_{\mathcal{S}_0}$ and $\boldsymbol{\theta}_{\mathcal{S}_0^c}$ denote the subvectors of $\boldsymbol{\theta} \in \mathbb{R}^s$ indexed by \mathcal{S}_0 and \mathcal{S}_0^c respectively, and similarly for $\tilde{\boldsymbol{\theta}}$. For any $\boldsymbol{\theta} \in \mathbb{R}^s$ satisfying $\|\boldsymbol{\theta}_{\mathcal{S}_0^c}\|_1 \leq 3 \|\boldsymbol{\theta}_{\mathcal{S}_0}\|_1$, take $\boldsymbol{\psi} \in \mathbb{R}^p$ such that $\boldsymbol{\psi}_{\hat{\mathcal{S}}_1} = \boldsymbol{\theta}$ and $\boldsymbol{\psi}_{\hat{\mathcal{S}}_1^c} = \mathbf{0}$. Then (D.41) can be rewritten as

$$\phi_2^2(\hat{\Sigma}_{\hat{\mathcal{S}}_1}, 3) = \min_{\substack{\boldsymbol{\psi} \in \mathbb{R}^p: \\ \boldsymbol{\psi}_{\hat{\mathcal{S}}_1} = \boldsymbol{\theta}, \boldsymbol{\psi}_{\hat{\mathcal{S}}_1^c} = \mathbf{0}}} \left\{ \frac{s_1^* \boldsymbol{\psi}^\top \hat{\Sigma} \boldsymbol{\psi}}{\|\boldsymbol{\psi}_{\tilde{\mathcal{S}}_0}\|_1^2} \right\} \text{ s.t. } \|\boldsymbol{\psi}_{\tilde{\mathcal{S}}_0^c}\|_1 \leq 3 \|\boldsymbol{\psi}_{\tilde{\mathcal{S}}_0}\|_1.$$

Comparing with (D.40), clearly,

$$\phi_2^2(\hat{\Sigma}_{\hat{\mathcal{S}}_1}, 3) \geq \phi_1^2(\hat{\Sigma}, 3). \quad (\text{D.42})$$

Define events

$$\mathcal{G}_3 = \left\{ \sup_{\hat{\mathcal{S}}_1: |\hat{\mathcal{S}}_1|=s} \max_{1 \leq k \leq s} \frac{|\mathbf{Z}_{\hat{\mathcal{S}}_1, k}^\top (\mathbf{U} \boldsymbol{\alpha}_D^* + \boldsymbol{\epsilon}_D)|}{n} \leq \frac{\lambda_\gamma}{4} \right\},$$

$$\mathcal{G}_4 = \left\{ \phi_1^2(\hat{\Sigma}, 3) \geq \frac{C_L}{4} \right\},$$

where $C_L > 0$ lower bounds eigenvalues of the covariance matrix $\Sigma \in \mathbb{R}^{p \times p}$ by assumption A2. Here \mathcal{G}_4 implies that the compatibility condition holds for $\hat{\Sigma}_{\hat{\mathcal{S}}_1}$ and \mathcal{S}_0 . On $\mathcal{G}_3 \cap \mathcal{G}_4$, using Theorem 6.1 in [Bühlmann](#)

& van de Geer (2011), we get

$$\frac{\|\mathbb{Z}_{\hat{\mathcal{S}}_1}(\gamma_{\hat{\mathcal{S}}_1}^* - \tilde{\gamma}_{\hat{\mathcal{S}}_1})\|^2}{n} \leq \frac{4s_1^* \lambda_\gamma^2}{\phi_1^2(\hat{\Sigma}, 3)} \quad (\text{D.43})$$

$$\|\tilde{\gamma}_{\hat{\mathcal{S}}_1} - \gamma_{\hat{\mathcal{S}}_1}^*\|_1 \leq \frac{4s_1^* \lambda_\gamma}{\phi_1^2(\hat{\Sigma}, 3)}. \quad (\text{D.44})$$

Taking supremum over all possible $\hat{\mathcal{S}}_1$ with cardinality s , we then obtain

$$\sup_{\hat{\mathcal{S}}_1: |\hat{\mathcal{S}}_1|=s} \frac{\|\mathbb{Z}_{\hat{\mathcal{S}}_1}(\gamma_{\hat{\mathcal{S}}_1}^* - \tilde{\gamma}_{\hat{\mathcal{S}}_1})\|^2}{n} \leq \frac{16s_1^* \lambda_\gamma^2}{C_L} \quad (\text{D.45})$$

$$\sup_{\hat{\mathcal{S}}_1: |\hat{\mathcal{S}}_1|=s} \|\tilde{\gamma}_{\hat{\mathcal{S}}_1} - \gamma_{\hat{\mathcal{S}}_1}^*\|_1 \leq \frac{16s_1^* \lambda_\gamma}{C_L}. \quad (\text{D.46})$$

To show the concentration inequalities (D.37) and (D.38), it suffices to control $P(\mathcal{G}_3^c)$ and $P(\mathcal{G}_4^c)$.

Using Lemma D.57 with $\epsilon = \mathbf{U}\alpha_D^* + \epsilon_D$ and $a_5 = C_\gamma/4$, we have

$$\begin{aligned} P(\mathcal{G}_3^c) &\leq P\left(\frac{1}{n} \max_{1 \leq j \leq p} |\mathbf{Z}_j^\top (\mathbf{U}\alpha_D^* + \epsilon_D)| > \frac{\lambda_\gamma}{4}\right) \\ &\leq e^{-c_4 \log p} \end{aligned} \quad (\text{D.47})$$

for some constant $c_4 > 0$, where the first inequality uses the fact that the maximal correlation between Z_j and $\mathbf{U}\alpha_D^* + \epsilon_D$ for $1 \leq j \leq p$ is not affected by $\hat{\mathcal{S}}_1$.

Following the proof of Theorem 7.(a) in Javanmard & Montanari (2014), there exists a constant $c_3 > 0$ such that

$$P(\mathcal{G}_4^c) \leq e^{-c_3 n}. \quad (\text{D.48})$$

Combining (D.47) and (D.48) gives (D.37) and (D.38). Similar arguments can be applied to the lasso estimator $\tilde{\Gamma}_{\hat{\mathcal{S}}_1}$. This completes the proof. \square

Lemma D.5 provides uniform concentration inequalities over all possible $\hat{\mathcal{S}}_1$ for $\Delta_1, \Delta_2 \in \mathbb{R}^s$. Recall

$$\begin{aligned} \mathcal{C}_1 &= \left\{ \sup_{\hat{\mathcal{S}}_1: |\hat{\mathcal{S}}_1|=s} \|\Delta_1\|_\infty \leq \frac{70a_2 s_1^* \sqrt{\log p} \lambda_\gamma}{C_L^2} \eta_{\max} \right\} \\ \mathcal{C}_2 &= \left\{ \sup_{\hat{\mathcal{S}}_1: |\hat{\mathcal{S}}_1|=s} \|\Delta_2\|_\infty \leq \frac{70a_2 s_2^* \sqrt{\log p} \lambda_\Gamma}{C_L^2} \eta_{\max} \right\}, \end{aligned}$$

where a_2 is a constant satisfying $a_2 > 4\sqrt{3}eB\kappa^2$.

Lemma D.5. Suppose the same conditions as Lemma D.4 and Lemma D.13. Then we have

$$P(\mathcal{C}_1 \cap \mathcal{A}) \geq 1 - (e^{-c_3 n} + e^{-c_9 \log p}) \quad (\text{D.49})$$

and

$$P(\mathcal{C}_2 \cap \mathcal{A}) \geq 1 - (e^{-c_3 n} + e^{-c_{10} \log p}) \quad (\text{D.50})$$

for some constants $c_3, c_9, c_{10} > 0$.

Proof of Lemma D.5. The error terms Δ_1, Δ_2 take the following form:

$$\begin{aligned} \Delta_1 &= \sqrt{n}(\mathbf{M}\widehat{\boldsymbol{\Sigma}}_{\hat{\mathcal{S}}_1} - \mathbf{I}_s)(\boldsymbol{\gamma}_{\hat{\mathcal{S}}_1}^* - \tilde{\boldsymbol{\gamma}}_{\hat{\mathcal{S}}_1}) \\ \Delta_2 &= \sqrt{n}(\mathbf{M}\widehat{\boldsymbol{\Sigma}}_{\hat{\mathcal{S}}_1} - \mathbf{I}_s)(\boldsymbol{\Gamma}_{\hat{\mathcal{S}}_1}^* - \tilde{\boldsymbol{\Gamma}}_{\hat{\mathcal{S}}_1}). \end{aligned}$$

We focus on the concentration inequality of $\|\Delta_1\|_\infty$ and similar arguments can be applied to $\|\Delta_2\|_\infty$. The max norm of $\Delta_1 \in \mathbb{R}^s$ can be bounded by

$$\|\Delta_1\|_\infty \leq \sqrt{n}\|\mathbf{M}\widehat{\boldsymbol{\Sigma}}_{\hat{\mathcal{S}}_1} - \mathbf{I}_s\|_\infty \|\tilde{\boldsymbol{\gamma}}_{\hat{\mathcal{S}}_1} - \boldsymbol{\gamma}_{\hat{\mathcal{S}}_1}^*\|_1. \quad (\text{D.51})$$

Recall

$$\begin{aligned} \mathcal{E}_1 &= \left\{ \sup_{\hat{\mathcal{S}}_1: |\hat{\mathcal{S}}_1|=s} \|\mathbf{M}\widehat{\boldsymbol{\Sigma}}_{\hat{\mathcal{S}}_1} - \mathbf{I}_s\|_\infty \leq \frac{\lambda_{\text{NL}}}{0.99C_L} \right\}, \\ \mathcal{B}_1 &= \left\{ \sup_{\hat{\mathcal{S}}_1: |\hat{\mathcal{S}}_1|=s} \|\tilde{\boldsymbol{\gamma}}_{\hat{\mathcal{S}}_1} - \boldsymbol{\gamma}_{\hat{\mathcal{S}}_1}^*\|_1 \leq \frac{16s_1^* \lambda_\gamma}{C_L} \right\}, \end{aligned}$$

where $\lambda_{\text{NL}} = 4a_2\eta_{\max}\sqrt{(\log p)/n}$. On the event $\mathcal{E}_1 \cap \mathcal{B}_1$, it follows directly from (D.51) that

$$\sup_{\hat{\mathcal{S}}_1: |\hat{\mathcal{S}}_1|=s} \|\Delta_1\|_\infty \leq \frac{70a_2s_1^*\sqrt{\log p}\lambda_\gamma}{C_L^2}\eta_{\max}. \quad (\text{D.52})$$

Thus we obtain the concentration statement (D.49) by using (D.37) of Lemma D.4 and Lemma D.13. The concentration inequality regarding Δ_2 can be proved in a similar fashion. \square

The lemma below controls the variance estimate of $\mathbf{U}^\text{T}\boldsymbol{\alpha}_D^* + \epsilon_D$ established using lasso estimator, which corresponds to

$$\tilde{\mathcal{B}} = \left\{ \sup_{\hat{\mathcal{S}}_1: |\hat{\mathcal{S}}_1|=s} \left| \frac{1}{n} \|\mathbf{D} - \mathbb{Z}_{\hat{\mathcal{S}}_1} \tilde{\boldsymbol{\gamma}}_{\hat{\mathcal{S}}_1}\|^2 - (\boldsymbol{\alpha}_D^{*\text{T}} \boldsymbol{\Sigma}_U \boldsymbol{\alpha}_D^* + \sigma_D^2) \right| \leq a_4 \sqrt{\frac{\log n}{n}} + \frac{16\lambda_\gamma^2 s_1^*}{C_L} \right\}.$$

Lemma D.6. Suppose the same conditions as Lemma D.4. There exist constants $a_4, c_6 > 0$ such that

$$P(\tilde{\mathcal{B}} \cap \mathcal{A}) \geq 1 - e^{-c_6 \log(n \wedge p)}. \quad (\text{D.53})$$

Proof of Lemma D.6. Using the triangle inequality and the fact that $D = \mathbf{Z}_{\hat{\mathcal{S}}_1}^\text{T} \boldsymbol{\gamma}_{\hat{\mathcal{S}}_1}^* + \mathbf{U}^\text{T} \boldsymbol{\alpha}_D^* + \epsilon_D$ on the

event \mathcal{A} , it is easy to show that

$$\left| \frac{1}{n} \|\mathbf{D} - \mathbb{Z}_{\hat{\mathcal{S}}_1} \tilde{\gamma}_{\hat{\mathcal{S}}_1}\|^2 - \frac{1}{n} \|\mathbf{U}\boldsymbol{\alpha}_D^* + \boldsymbol{\epsilon}_D\|^2 \right| \leq \frac{1}{n} \|\mathbb{Z}_{\hat{\mathcal{S}}_1} (\tilde{\gamma}_{\hat{\mathcal{S}}_1} - \gamma_{\hat{\mathcal{S}}_1}^*)\|^2. \quad (\text{D.54})$$

Again applying the triangle inequality yields

$$\begin{aligned} & \left| \frac{1}{n} \|\mathbf{D} - \mathbb{Z}_{\hat{\mathcal{S}}_1} \tilde{\gamma}_{\hat{\mathcal{S}}_1}\|^2 - (\boldsymbol{\alpha}_D^{*\text{T}} \Sigma_U \boldsymbol{\alpha}_D^* + \sigma_D^2) \right| \\ & \leq \left| \frac{1}{n} \|\mathbf{D} - \mathbb{Z}_{\hat{\mathcal{S}}_1} \tilde{\gamma}_{\hat{\mathcal{S}}_1}\|^2 - \frac{1}{n} \|\mathbf{U}\boldsymbol{\alpha}_D^* + \boldsymbol{\epsilon}_D\|^2 \right| + \left| \frac{1}{n} \|\mathbf{U}\boldsymbol{\alpha}_D^* + \boldsymbol{\epsilon}_D\|^2 - (\boldsymbol{\alpha}_D^{*\text{T}} \Sigma_U \boldsymbol{\alpha}_D^* + \sigma_D^2) \right|. \end{aligned} \quad (\text{D.55})$$

Taking the supremum over all $\hat{\mathcal{S}}_1$ of size s , by (D.54) and (D.55), we have

$$\begin{aligned} & \sup_{\hat{\mathcal{S}}_1: |\hat{\mathcal{S}}_1|=s} \left| \frac{1}{n} \|\mathbf{D} - \mathbb{Z}_{\hat{\mathcal{S}}_1} \tilde{\gamma}_{\hat{\mathcal{S}}_1}\|^2 - (\boldsymbol{\alpha}_D^{*\text{T}} \Sigma_U \boldsymbol{\alpha}_D^* + \sigma_D^2) \right| \\ & \leq \sup_{\hat{\mathcal{S}}_1: |\hat{\mathcal{S}}_1|=s} \frac{1}{n} \|\mathbb{Z}_{\hat{\mathcal{S}}_1} (\tilde{\gamma}_{\hat{\mathcal{S}}_1} - \gamma_{\hat{\mathcal{S}}_1}^*)\|^2 + \left| \frac{1}{n} \|\mathbf{U}\boldsymbol{\alpha}_D^* + \boldsymbol{\epsilon}_D\|^2 - (\boldsymbol{\alpha}_D^{*\text{T}} \Sigma_U \boldsymbol{\alpha}_D^* + \sigma_D^2) \right|. \end{aligned} \quad (\text{D.56})$$

Then applying Lemma D.9 and Lemma D.4 gives the desired result. \square

Lemma D.7 shows that $n\|\mathbf{v}_l\|^2$ has bounded support uniformly over all $\hat{\mathcal{S}}_1$ of size s . Recall

$$\mathcal{D} = \left\{ \frac{1}{C_R} - \mu \leq n\|\mathbf{v}_l\|^2 \leq \frac{1}{C_L} + \mu, \forall \hat{\mathcal{S}}_1 \text{ with } |\hat{\mathcal{S}}_1| = s \text{ and } \forall 1 \leq l \leq s \right\}.$$

Lemma D.7. Suppose assumptions A2 and A6 hold. Then there exists a constant $c_{25} > 0$ such that

$$P(\mathcal{D}) \geq 1 - e^{-c_{25} \log p}.$$

Proof of Lemma D.7. Under assumption A2, on the event

$$\mathcal{E}_3 = \left\{ \sup_{\hat{\mathcal{S}}_1: |\hat{\mathcal{S}}_1|=s} \max_{1 \leq j \leq s} |[M\hat{\Sigma}_{\hat{\mathcal{S}}_1} M^T - \Sigma_{\hat{\mathcal{S}}_1}^{-1}]_{jj}| \leq \mu \right\},$$

direct calculations give

$$\frac{1}{C_R} - \mu \leq [\Sigma_{\hat{\mathcal{S}}_1}^{-1}]_{ll} - \mu \leq n\|\mathbf{v}_l\|^2 = [M\hat{\Sigma}_{\hat{\mathcal{S}}_1} M^T]_{ll} \leq [\Sigma_{\hat{\mathcal{S}}_1}^{-1}]_{ll} + \mu \leq \frac{1}{C_L} + \mu$$

for all $\hat{\mathcal{S}}_1$ of size s and all $1 \leq l \leq s$. We thus finish the proof by using Lemma D.14-(ii). \square

D.4 Concentration results

Recall the event \mathcal{C}_3 defined for the maximal correlation between candidate instrument Z_j and error term ϵ that is independent of Z_j for all $j = 1, \dots, p$:

$$\mathcal{C}_3 = \left\{ \frac{1}{n} \max_{1 \leq j \leq p} |\mathbf{Z}_j^\top \epsilon| \leq a_5 \sqrt{\frac{\log p}{n}} \right\}.$$

Lemma D.8. Suppose assumption A2 and $\log p = o(n)$ hold. If ϵ_i 's follow *i.i.d.* $N(0, \sigma_\epsilon^2)$ and are independent of Z_{ij} for $i = 1, \dots, n$ and $j = 1, \dots, p$, then for $a_5 > \sqrt{1.01B\sigma_\epsilon^2}$, there exists a constant $a_6 > 0$ such that

$$P(\mathcal{C}_3) \geq 1 - e^{-a_6 \log p} \quad (\text{D.57})$$

Proof of Lemma D.8. Define event $\mathcal{G}_5 = \{ \max_{1 \leq j \leq p} \hat{\Sigma}_{jj} \leq K \}$ with $K \geq B + 20\kappa^2 \sqrt{(\log p)/n}$. Then we have the following

$$\begin{aligned} & P\left(\frac{1}{n} \max_{1 \leq j \leq p} |\mathbf{Z}_j^\top \epsilon| > a_5 \sqrt{\frac{\log p}{n}}\right) \\ & \leq P\left(\frac{1}{n} \max_{1 \leq j \leq p} |\mathbf{Z}_j^\top \epsilon| > a_5 \sqrt{\frac{\log p}{n}}, \mathcal{G}_5\right) + P(\mathcal{G}_5^c) \\ & = P\left(\frac{1}{n} \max_{1 \leq j \leq p} \|\mathbf{Z}_j\| |\tilde{\mathbf{Z}}_j^\top \epsilon| > a_5 \sqrt{\frac{\log p}{n}}, \mathcal{G}_5\right) + P(\mathcal{G}_5^c) \\ & \leq P\left(\frac{\sqrt{K}}{\sqrt{n}} \max_{1 \leq j \leq p} |\tilde{\mathbf{Z}}_j^\top \epsilon| > a_5 \sqrt{\frac{\log p}{n}}\right) + P(\mathcal{G}_5^c), \end{aligned} \quad (\text{D.58})$$

where $\tilde{\mathbf{Z}}_j = \mathbf{Z}_j / \|\mathbf{Z}_j\|$ and the second inequality is from the definition of the event \mathcal{G}_5 . Using the law of total expectation,

$$\begin{aligned} & P\left(\frac{\sqrt{K}}{\sqrt{n}} \max_{1 \leq j \leq p} |\tilde{\mathbf{Z}}_j^\top \epsilon| > a_5 \sqrt{\frac{\log p}{n}}\right) \\ & = E_{\mathbb{Z}} \left\{ P\left(\frac{\sqrt{K}}{\sqrt{n}} \max_{1 \leq j \leq p} |\tilde{\mathbf{Z}}_j^\top \epsilon| > a_5 \sqrt{\frac{\log p}{n}} \mid \mathbb{Z}\right) \right\} \\ & \leq 2p \exp\left\{-\frac{a_5^2 \log p}{K\sigma_\epsilon^2}\right\}, \end{aligned} \quad (\text{D.59})$$

where the last inequality comes from the Gaussian tail bound applied to $\tilde{\mathbf{Z}}_j^\top \epsilon | \mathbb{Z}$ which is conditionally normal under assumption A1, and union bound.

Following the proof of Theorem 7.(a) in [Javanmard & Montanari \(2014\)](#), there exists a constant $c_1 > 0$ such that

$$P(\mathcal{G}_5^c) \leq e^{-c_1 n}. \quad (\text{D.60})$$

Under $\log p = o(n)$, for $a_5 > \sqrt{1.01B\sigma_\epsilon^2}$, combining (D.59) and (D.60) gives

$$P\left(\frac{1}{n} \max_{1 \leq j \leq p} |\mathbf{Z}_j^T \boldsymbol{\epsilon}| > a_5 \sqrt{\frac{\log p}{n}}\right) \leq e^{-a_6 \log p}$$

for some constant $a_6 > 0$. □

Lemma D.9. Under assumption A1, there exists a constant $c_8 > 0$ such that for all $0 < t < 6|\boldsymbol{\alpha}_D^*| \|U_1 \boldsymbol{\epsilon}_{1D}\|_{\psi_1} \sqrt{n/\log n}$

$$P\left(\left|\frac{\|\mathbf{U}\boldsymbol{\alpha}_D^* + \boldsymbol{\epsilon}_D\|^2}{n} - (\boldsymbol{\alpha}_D^{*\top} \Sigma_U \boldsymbol{\alpha}_D^* + \sigma_D^2)\right| \leq t \sqrt{\frac{\log n}{n}}\right) \geq 1 - 3e^{-t^2 c_8 \log n}.$$

Proof of Lemma D.9. It follows from $E(U_i) = E(\epsilon_{iD}) = 0$ and $U_i \perp \epsilon_{iD}$ for all $i = 1, \dots, n$ that

$$E\left[\frac{1}{n} \|\mathbf{U}\boldsymbol{\alpha}_D^* + \boldsymbol{\epsilon}_D\|^2\right] = \boldsymbol{\alpha}_D^{*\top} \Sigma_U \boldsymbol{\alpha}_D^* + \sigma_D^2.$$

For any $t_1 > 0$, the concentration inequality regarding $\|\boldsymbol{\alpha}_D^* \mathbf{U} + \boldsymbol{\epsilon}_D\|^2/n$ satisfies

$$\begin{aligned} & P\left(\left|\frac{1}{n} \|\boldsymbol{\alpha}_D^* \mathbf{U} + \boldsymbol{\epsilon}_D\|^2 - (\boldsymbol{\alpha}_D^{*\top} \Sigma_U \boldsymbol{\alpha}_D^* + \sigma_D^2)\right| > t_1\right) \\ &= P\left(\left|\left(\frac{1}{n} \sum_{i=1}^n (\mathbf{U}_i^T \boldsymbol{\alpha}_D^*)^2 - \boldsymbol{\alpha}_D^{*\top} \Sigma_U \boldsymbol{\alpha}_D^*\right) + \left(\frac{1}{n} \sum_{i=1}^n \epsilon_{iD}^2 - \sigma_D^2\right) + \left(\frac{2}{n} \sum_{i=1}^n \epsilon_{iD} (\mathbf{U}_i^T \boldsymbol{\alpha}_D^*)\right)\right| > t_1\right) \\ &\leq P\left(\left|\frac{1}{n} \sum_{i=1}^n (\mathbf{U}_i^T \boldsymbol{\alpha}_D^*)^2 - \boldsymbol{\alpha}_D^{*\top} \Sigma_U \boldsymbol{\alpha}_D^*\right| + \left|\frac{1}{n} \sum_{i=1}^n \epsilon_{iD}^2 - \sigma_D^2\right| + 2\left|\frac{1}{n} \sum_{i=1}^n \epsilon_{iD} (\mathbf{U}_i^T \boldsymbol{\alpha}_D^*)\right| > t_1\right) \\ &\leq P\left(\left|\frac{1}{n} \sum_{i=1}^n (\mathbf{U}_i^T \boldsymbol{\alpha}_D^*)^2 - \boldsymbol{\alpha}_D^{*\top} \Sigma_U \boldsymbol{\alpha}_D^*\right| > \frac{t_1}{3}\right) + P\left(\left|\frac{1}{n} \sum_{i=1}^n \epsilon_{iD}^2 - \sigma_D^2\right| > \frac{t_1}{3}\right) \\ &\quad + P\left(\left|\frac{1}{n} \sum_{i=1}^n \epsilon_{iD} (\mathbf{U}_i^T \boldsymbol{\alpha}_D^*)\right| > \frac{t_1}{6}\right) \\ &= P\left(\left|\frac{1}{n} \sum_{i=1}^n \left\{\frac{(\boldsymbol{\alpha}_D^{*\top} \mathbf{U}_i)^2}{\boldsymbol{\alpha}_D^{*\top} \Sigma_U \boldsymbol{\alpha}_D^*} - 1\right\}\right| > \frac{t_1}{3\boldsymbol{\alpha}_D^{*\top} \Sigma_U \boldsymbol{\alpha}_D^*}\right) + P\left(\left|\frac{1}{n} \sum_{i=1}^n \left(\frac{\epsilon_{iD}^2}{\sigma_D^2} - 1\right)\right| > \frac{t_1}{3\sigma_D^2}\right) \\ &\quad + P\left(\left|\frac{1}{n} \sum_{i=1}^n \epsilon_{iD} (\mathbf{U}_i^T \boldsymbol{\alpha}_D^*)\right| > \frac{t_1}{6}\right) \\ &\leq 2 \exp\left\{-\frac{n}{8} \frac{t_1^2}{(\boldsymbol{\alpha}_D^{*\top} \Sigma_U \boldsymbol{\alpha}_D^*)^2}\right\} + 2 \exp\left\{-\frac{n}{8} \frac{t_1^2}{9\sigma_D^4}\right\} + P\left(\left|\frac{1}{n} \sum_{i=1}^n \epsilon_{iD} (\mathbf{U}_i^T \boldsymbol{\alpha}_D^*)\right| > \frac{t_1}{6}\right), \quad (\text{D.61}) \end{aligned}$$

where the last inequality comes from the fact that $(\boldsymbol{\alpha}_D^{*\top} \mathbf{U}_i)^2 / \boldsymbol{\alpha}_D^{*\top} \Sigma_U \boldsymbol{\alpha}_D^*$ and $\epsilon_{iD}^2 / \sigma_D^2$ are iid χ_1^2 for $i = 1, \dots, n$ by assumption A1 and concentration of chi-square variables (e.g. see Example 2.11 in [Wainwright \(2019\)](#)). It reduces to control the last term in (D.61). Under assumptions A1 that $\mathbf{U}_i, \epsilon_{iD}$ are independently and normally distributed, $(\boldsymbol{\alpha}_D^{*\top} \mathbf{U}_i) \epsilon_{iD}$ is sub-Exponential, which follows from the fact that Gaussian random variable is sub-Gaussian and Lemma 2.7.7 in [Vershynin \(2018\)](#) that product of sub-Gaussians is sub-Exponential. Notice that $E\{(\boldsymbol{\alpha}_D^{*\top} \mathbf{U}_i) \epsilon_{iD}\} = 0$. Take $\kappa_{u\epsilon_D} = \|(\boldsymbol{\alpha}_D^{*\top} \mathbf{U}_1) \epsilon_{1D}\|_{\psi_1}$, the Orlicz norm

of $(\boldsymbol{\alpha}_D^{*\top} \mathbf{U}_1) \epsilon_{1D}$. Then by Bernstein-type inequality in Lemma D.19 (e.g. Proposition 5.16 in Vershynin (2012)) with $\mathbf{a} = (\frac{1}{n}, \dots, \frac{1}{n}) \in \mathbb{R}^n$, we get

$$P\left(\left|\frac{1}{n} \sum_{i=1}^n (\boldsymbol{\alpha}_D^{*\top} \mathbf{U}_i) \epsilon_{iD}\right| > \frac{t_1}{6}\right) \leq 2 \exp\left\{-c_3 n \min\left(\frac{t_1^2}{36\kappa_{u\epsilon_D}^2}, \frac{t_1}{6\kappa_{u\epsilon_D}}\right)\right\} \quad (\text{D.62})$$

where c_3 is a positive constant. Combining with (D.61) yields

$$\begin{aligned} & P\left(\left|\frac{1}{n} \|\mathbf{U}\boldsymbol{\alpha}_D^* + \boldsymbol{\epsilon}_D\|^2 - (\boldsymbol{\alpha}_D^{*\top} \Sigma_U \boldsymbol{\alpha}_D^* + \sigma_D^2)\right| > t_1\right) \\ & \leq 2 \exp\left\{-\frac{n}{8} \frac{t_1^2}{(3\boldsymbol{\alpha}_D^{*\top} \Sigma_U \boldsymbol{\alpha}_D^*)^2}\right\} + 2 \exp\left\{-\frac{n}{8} \frac{t_1^2}{9\sigma_D^4}\right\} \\ & \quad + 2 \exp\left\{-c_3 n \min\left(\frac{t_1^2}{36\kappa_{u\epsilon_D}^2}, \frac{t_1}{6\kappa_{u\epsilon_D}}\right)\right\} \\ & = \begin{cases} 2 \exp\left\{-\frac{n}{8} \frac{t_1^2}{(3\boldsymbol{\alpha}_D^{*\top} \Sigma_U \boldsymbol{\alpha}_D^*)^2}\right\} + 2 \exp\left\{-\frac{n}{8} \frac{t_1^2}{9\sigma_D^4}\right\} + 2 \exp\left\{-c_3 n \frac{t_1^2}{36\kappa_{u\epsilon_D}^2}\right\}, & \text{if } \frac{t_1}{6\kappa_{u\epsilon_D}} \leq 1 \\ 2 \exp\left\{-\frac{n}{8} \frac{t_1^2}{(3\boldsymbol{\alpha}_D^{*\top} \Sigma_U \boldsymbol{\alpha}_D^*)^2}\right\} + 2 \exp\left\{-\frac{n}{8} \frac{t_1^2}{9\sigma_D^4}\right\} + 2 \exp\left\{-c_3 n \frac{t_1}{6\kappa_{u\epsilon_D}}\right\}, & \text{if } \frac{t_1}{6\kappa_{u\epsilon_D}} > 1 \end{cases}. \end{aligned}$$

Taking $t_1 = \tilde{c}_8 \sqrt{(\log n)/n}$, we have

$$\begin{aligned} & P\left(\left|\frac{1}{n} \|\boldsymbol{\alpha}_D^* \mathbf{U} + \boldsymbol{\epsilon}_D\|^2 - (\boldsymbol{\alpha}_D^{*\top} \Sigma_U \boldsymbol{\alpha}_D^* + \sigma_D^2)\right| > \tilde{c}_8 \sqrt{\frac{\log n}{n}}\right) \\ & \leq \exp\left\{-\frac{1}{8} \frac{\tilde{c}_8^2 \log n}{(3\boldsymbol{\alpha}_D^{*\top} \Sigma_U \boldsymbol{\alpha}_D^*)^2}\right\} + \exp\left\{-\frac{1}{8} \frac{\tilde{c}_8^2 \log n}{9\sigma_D^4}\right\} + \exp\left\{-\frac{c_3 \tilde{c}_8^2 \log n}{36\kappa_{u\epsilon_D}^2}\right\} \\ & \leq 3e^{-c_8 \log n}, \end{aligned}$$

where $c_8 = 1/\max\{72(\boldsymbol{\alpha}_D^{*\top} \Sigma_U \boldsymbol{\alpha}_D^*)^2/\tilde{c}_8^2, 72\sigma_D^4/\tilde{c}_8^2, (36\kappa_{u\epsilon_D}^2)/(c_3 \tilde{c}_8^2)\}$. The concentration inequality converges to zero as $n \rightarrow \infty$. We thus finish the proof. \square

Lemma D.10. Suppose assumption A2 holds. Then we have for all $4\sqrt{3}eB\kappa^2 < t \leq \epsilon\kappa'\sqrt{n/\log p}$

$$P\left(\|\hat{\boldsymbol{\Sigma}} - \boldsymbol{\Sigma}\|_\infty > t\sqrt{\frac{\log p}{n}}\right) \leq e^{-a_3(t) \log p} \quad (\text{D.63})$$

where $a_3(t) = \{t^2/(24e^2 B^2 \kappa^4)\} - 2$.

Proof of Lemma D.10. Let $V_i^{(jk)} = Z_{ij}Z_{ik} - \Sigma_{jk}$ for $1 \leq i \leq n$ and $1 \leq j, k \leq p$. It is easy to see that $E\{V_i^{(jk)}\} = 0$ under assumption A2. And the (j, k) -th element of $\hat{\boldsymbol{\Sigma}} - \boldsymbol{\Sigma}$ can be written as

$$[\hat{\boldsymbol{\Sigma}} - \boldsymbol{\Sigma}]_{jk} = \frac{1}{n} \sum_{i=1}^n V_i^{(jk)}.$$

By Lemma 2.7.7 of Vershynin (2018) that product of sub-gaussians is sub-exponential and Remark 5.18 of

Vershynin (2012), we get $\|Z_{ij}Z_{ik}\|_{\psi_1} \leq \|Z_{ij}\|_{\psi_2}\|Z_{ik}\|_{\psi_2}$ and $\|V_i^{(jk)}\|_{\psi_1} \leq 2\|Z_{ij}Z_{ik}\|_{\psi_1}$. Moreover,

$$\|V_i^{(jk)}\|_{\psi_1} \leq 2\|Z_{ij}\|_{\psi_2}\|Z_{ik}\|_{\psi_2}. \quad (\text{D.64})$$

Notice that $\Sigma^{1/2}e_j/\sqrt{\Sigma_{jj}} \in \mathcal{S}^{p-1}$, where e_j is a unit vector with the j th element equal to one and zero otherwise, and \mathcal{S}^{p-1} represents the Euclidean unit sphere in \mathbb{R}^p . Then by definition of sub-gaussian norm (see Definition D.15) and definition of $\kappa = \|\Sigma^{-1/2}\mathbf{Z}_1\|_{\psi_2}$, we get

$$\left\| \frac{Z_{1j}}{\sqrt{\Sigma_{jj}}} \right\|_{\psi_2} = \left\| \left\langle \Sigma^{-1/2}\mathbf{Z}_1, \frac{\Sigma^{1/2}e_j}{\sqrt{\Sigma_{jj}}} \right\rangle \right\|_{\psi_2} \leq \kappa$$

for $1 \leq j \leq p$. Since $\|cX\|_{\psi_2} = c\|X\|_{\psi_2}$, which follows directly from the definition of sub-gaussian norm, we have

$$\|Z_{1j}\|_{\psi_2} \leq \kappa\sqrt{\Sigma_{jj}} \leq \kappa\sqrt{B},$$

where the second inequality is from A2. Hence, $\|V_i^{(jk)}\|_{\psi_2} \leq 2\kappa^2B$ by (D.64). Let $\kappa' = 2\kappa^2B$.

Using the Bernstein-type inequality for centered sub-exponential variable as presented in Lemma D.19 yields

$$P\left(\frac{1}{n}\left|\sum_{i=1}^n V_i^{(jk)}\right| > a_2\sqrt{\frac{\log p}{n}}\right) \leq 2\exp\left[-\frac{n}{6}\min\left\{\left(\frac{a_2\sqrt{\log p}}{e\kappa'\sqrt{n}}\right)^2, \frac{a_2\sqrt{\log p}}{e\kappa'\sqrt{n}}\right\}\right]. \quad (\text{D.65})$$

For a_2 satisfying $a_2\sqrt{\log p}/(e\kappa'\sqrt{n}) \leq 1$ with $\kappa' = 2\kappa^2B$, applying union bound over all (j, k) pairs for $1 \leq j, k \leq p$, together with (D.65), we obtain

$$\begin{aligned} P\left(\|\hat{\Sigma} - \Sigma\|_{\infty} > a_2\sqrt{\frac{\log p}{n}}\right) &\leq \max_{1 \leq j, k \leq p} P\left(\frac{1}{n}\left|\sum_{i=1}^n V_i^{(jk)}\right| \geq a_2\sqrt{\frac{\log p}{n}}\right) \\ &\leq 2\exp\left\{2\log p - \frac{a_2^2 \log p}{24e^2B^2\kappa^4}\right\}, \end{aligned}$$

which converges to zero under as $n, p \rightarrow \infty$ under $a_2 > 4\sqrt{3}eB\kappa^2$. \square

D.5 Technical results used in the proofs for debiased lasso estimators

In this section we collect technical results on the matrix \mathbf{M} and related quantities appearing in the debiased lasso estimator. Define

$$\eta_{max} := 1 \vee B \sup_{\hat{\mathcal{S}}_1: |\hat{\mathcal{S}}_1|=s} \max_{1 \leq j \leq s} \|[\Sigma_{\hat{\mathcal{S}}_1}^{-1}]_{-j,j}\|_1$$

and consider the events

$$\mathcal{E}_1 := \left\{ \sup_{\hat{\mathcal{S}}_1: |\hat{\mathcal{S}}_1|=s} \|\mathbf{M}\hat{\Sigma}_{\hat{\mathcal{S}}_1} - \mathbf{I}_s\|_\infty \leq \frac{\lambda_{\text{NL}}}{0.99C_L} \right\} \quad (\text{D.66})$$

$$\mathcal{E}_2 := \left\{ \sup_{\hat{\mathcal{S}}_1: |\hat{\mathcal{S}}_1|=s} \|\mathbf{M}\|_1 \leq \frac{10\eta_{\text{max}}}{C_L} \right\} \quad (\text{D.67})$$

$$\mathcal{E}_3(\zeta_1) := \left\{ \sup_{\hat{\mathcal{S}}_1: |\hat{\mathcal{S}}_1|=s} \max_{1 \leq j \leq s} |[\mathbf{M}\hat{\Sigma}_{\hat{\mathcal{S}}_1} \mathbf{M}^\text{T} - \Sigma_{\hat{\mathcal{S}}_1}^{-1}]_{jj}| \leq \zeta_1 \left(\frac{\log p}{n} \right)^{1/4} \eta_{\text{max}}^2 \right\}, \quad (\text{D.68})$$

where $\lambda_{\text{NL}} = 4a_2\eta_{\text{max}}\sqrt{(\log p)/n}$ with $a_2 > 4\sqrt{3}eB\kappa^2$. We will show below that there exist constants $\zeta_1, \zeta_2 > 0$ such that when n is sufficiently large we have

$$P\left(\mathcal{E}_1 \cap \mathcal{E}_2 \cap \mathcal{E}_3(\zeta_1)\right) \geq 1 - e^{-\zeta_2(n \wedge p)}.$$

To provide a proof of the above statement we need to introduce additional notation. The best linear predictor model of $Z_{\hat{\mathcal{S}}_1, j} \in \mathbb{R}$ in terms of $\mathbf{Z}_{\hat{\mathcal{S}}_1, -j} \in \mathbb{R}^{s-1}$ takes the following form

$$Z_{\hat{\mathcal{S}}_1, j} = \mathbf{Z}_{\hat{\mathcal{S}}_1, -j}^\text{T} \boldsymbol{\theta}_j^{(\hat{\mathcal{S}}_1)} + \epsilon_{\hat{\mathcal{S}}_1, j} \quad (\text{D.69})$$

for $j = 1, \dots, s$, where $\boldsymbol{\theta}_j^{(\hat{\mathcal{S}}_1)}$ denotes the population regression coefficient. Recall that an estimator $\hat{\boldsymbol{\theta}}_j^{(\hat{\mathcal{S}}_1)}$ is given by solving node-wise lasso problems:

$$\hat{\boldsymbol{\theta}}_j^{(\hat{\mathcal{S}}_1)} = \underset{\boldsymbol{\theta} \in \mathbb{R}^s}{\text{argmin}} \left(\frac{1}{n} \|\mathbf{Z}_{\hat{\mathcal{S}}_1, j} - \mathbb{Z}_{\hat{\mathcal{S}}_1, -j} \boldsymbol{\theta}\|^2 + 2\lambda_j \|\boldsymbol{\theta}\|_1 \right)$$

for $j = 1, \dots, s$, where $\mathbf{Z}_{\hat{\mathcal{S}}_1, j} \in \mathbb{R}^n$ denotes the j th column of the design matrix $\mathbb{Z}_{\hat{\mathcal{S}}_1} \in \mathbb{R}^{n \times s}$ and $\mathbb{Z}_{\hat{\mathcal{S}}_1, -j} \in \mathbb{R}^{n \times (s-1)}$ is formed by columns of $\mathbb{Z}_{\hat{\mathcal{S}}_1}$ indexed by $\{1, \dots, s\} \setminus \{j\}$.

Below we shall prove that

$$\|\mathbf{M}\hat{\Sigma}_{\hat{\mathcal{S}}_1} - \mathbf{I}_s\|_\infty \leq \max_{1 \leq j \leq s} \frac{\lambda_j}{\hat{\tau}_{\hat{\mathcal{S}}_1, j}^2}, \quad (\text{D.70})$$

where $\hat{\tau}_{\hat{\mathcal{S}}_1, j}^2 = \|\mathbf{Z}_{\hat{\mathcal{S}}_1, j} - \mathbb{Z}_{\hat{\mathcal{S}}_1, -j} \hat{\boldsymbol{\theta}}_j^{(\hat{\mathcal{S}}_1)}\|^2/n + \lambda_j \|\hat{\boldsymbol{\theta}}_j^{(\hat{\mathcal{S}}_1)}\|_1$.

Let $\tau_{\hat{\mathcal{S}}_1, j}^2 = 1/[\Sigma_{\hat{\mathcal{S}}_1}^{-1}]_{jj}$. To obtain a good bound on $1/\hat{\tau}_{\hat{\mathcal{S}}_1, j}^2$, we will show that there exist constants $a_3, c_{22} > 0$ such that the following holds

$$P\left(\sup_{\hat{\mathcal{S}}_1: |\hat{\mathcal{S}}_1|=s} \max_{1 \leq j \leq s} |\hat{\tau}_{\hat{\mathcal{S}}_1, j}^2 - \tau_{\hat{\mathcal{S}}_1, j}^2| > c_{22} \left(\frac{\log p}{n} \right)^{1/4} \eta_{\text{max}}^2 \right) \leq 3e^{-a_3 \log p} \quad (\text{D.71})$$

and that

$$C_L \leq \tau_{\hat{\mathcal{S}}_1, j}^2 \leq C_R, \quad (\text{D.72})$$

uniformly over all $j = 1, \dots, s$ and all $\widehat{\mathcal{S}}_1$ of cardinality s . Note that by definition of \mathbf{M} we have

$$\sup_{\widehat{\mathcal{S}}_1:|\widehat{\mathcal{S}}_1|=s} \|\mathbf{M}\|_1 = \sup_{\widehat{\mathcal{S}}_1:|\widehat{\mathcal{S}}_1|=s} \max_{1 \leq j \leq s} \|\mathbf{m}_j\|_1 \leq \sup_{\widehat{\mathcal{S}}_1:|\widehat{\mathcal{S}}_1|=s} \max_{1 \leq j \leq s} \frac{1}{\widehat{\tau}_{\widehat{\mathcal{S}}_1,j}^2} \left(1 + \|\boldsymbol{\theta}_j^{(\widehat{\mathcal{S}}_1)}\|_1 + \|\widehat{\boldsymbol{\theta}}_j^{(\widehat{\mathcal{S}}_1)} - \boldsymbol{\theta}_j^{(\widehat{\mathcal{S}}_1)}\|_1 \right)$$

Finally, we will prove below that

$$\begin{aligned} & \sup_{\widehat{\mathcal{S}}_1:|\widehat{\mathcal{S}}_1|=s} \max_{1 \leq j \leq s} |[\mathbf{M}\widehat{\boldsymbol{\Sigma}}_{\widehat{\mathcal{S}}_1} \mathbf{M}^T - \boldsymbol{\Sigma}_{\widehat{\mathcal{S}}_1}^{-1}]_{jj}| \\ & \leq \sup_{\widehat{\mathcal{S}}_1:|\widehat{\mathcal{S}}_1|=s} \|\mathbf{M}\widehat{\boldsymbol{\Sigma}}_{\widehat{\mathcal{S}}_1} - \mathbf{I}_s\|_\infty \sup_{\widehat{\mathcal{S}}_1:|\widehat{\mathcal{S}}_1|=s} \|\mathbf{M}\|_1 + \sup_{\widehat{\mathcal{S}}_1:|\widehat{\mathcal{S}}_1|=s} \max_{1 \leq j \leq s} \left| \frac{1}{\widehat{\tau}_{\widehat{\mathcal{S}}_1,j}^2} - \frac{1}{\tau_{\widehat{\mathcal{S}}_1,j}^2} \right| \end{aligned} \quad (\text{D.73})$$

To proceed, we first control the estimation and the prediction error rates for node-wise lasso estimators, as presented in Lemma D.11 below.

Lemma D.11. Suppose assumptions A2 and A6. Take the node-wise lasso penalty parameter $\lambda_j = \lambda_{\text{NL}} = 4a_2\eta_{\max}\sqrt{(\log p)/n}$ for $j = 1, \dots, s$ and all $\widehat{\mathcal{S}}_1$ of size s , where $a_2 > 4\sqrt{3}eB\kappa^2$ and $\eta_{\max} = 1 \vee B \sup_{\widehat{\mathcal{S}}_1:|\widehat{\mathcal{S}}_1|=s} \max_{1 \leq j \leq s} \|\boldsymbol{\Sigma}_{\widehat{\mathcal{S}}_1}^{-1}\|_{-j,j}$. Then there exists a constant $a_3 > 0$ such that

$$P\left(\sup_{\widehat{\mathcal{S}}_1:|\widehat{\mathcal{S}}_1|=s} \max_{1 \leq j \leq s} \|\widehat{\boldsymbol{\theta}}_j^{(\widehat{\mathcal{S}}_1)} - \boldsymbol{\theta}_j^{(\widehat{\mathcal{S}}_1)}\|_1 > 4B \left\{ \sup_{\widehat{\mathcal{S}}_1:|\widehat{\mathcal{S}}_1|=s} \max_{1 \leq j \leq s} \|\boldsymbol{\Sigma}_{\widehat{\mathcal{S}}_1}^{-1}\|_{-j,j} \right\} \right) \leq e^{-a_3 \log p} \quad (\text{D.74})$$

and

$$P\left(\sup_{\widehat{\mathcal{S}}_1:|\widehat{\mathcal{S}}_1|=s} \max_{1 \leq j \leq s} \frac{\|\mathbb{Z}_{\widehat{\mathcal{S}}_1,-j}(\widehat{\boldsymbol{\theta}}_j^{(\widehat{\mathcal{S}}_1)} - \boldsymbol{\theta}_j^{(\widehat{\mathcal{S}}_1)})\|^2}{n} > 4\lambda_{\text{NL}}B \left\{ \sup_{\widehat{\mathcal{S}}_1:|\widehat{\mathcal{S}}_1|=s} \max_{1 \leq j \leq s} \|\boldsymbol{\Sigma}_{\widehat{\mathcal{S}}_1}^{-1}\|_{-j,j} \right\} \right) \leq e^{-a_3 \log p}. \quad (\text{D.75})$$

Details of the constant a_3 have been discussed in Lemma D.10.

Proof of Lemma D.11. Given the set $\widehat{\mathcal{S}}_1$ of variables passing marginal screening, recall that the nodewise lasso problems take the following form:

$$\widehat{\boldsymbol{\theta}}_j^{(\widehat{\mathcal{S}}_1)} = \underset{\boldsymbol{\theta} \in \mathbb{R}^{s-1}}{\operatorname{argmin}} \frac{1}{n} \|\mathbf{Z}_{\widehat{\mathcal{S}}_1,j} - \mathbb{Z}_{\widehat{\mathcal{S}}_1,-j} \boldsymbol{\theta}\|^2 + 2\lambda_j \|\boldsymbol{\theta}\|_1$$

for $j = 1, \dots, s$. As $\widehat{\boldsymbol{\theta}}_j^{(\widehat{\mathcal{S}}_1)}$ is the minimizer of the above optimization problem, we then have

$$\begin{aligned} \frac{1}{n} \|\mathbf{Z}_{\widehat{\mathcal{S}}_1,j} - \mathbb{Z}_{\widehat{\mathcal{S}}_1,-j} \widehat{\boldsymbol{\theta}}_j^{(\widehat{\mathcal{S}}_1)}\|^2 + 2\lambda_j \|\widehat{\boldsymbol{\theta}}_j^{(\widehat{\mathcal{S}}_1)}\|_1 & \leq \frac{1}{n} \|\mathbf{Z}_{\widehat{\mathcal{S}}_1,j} - \mathbb{Z}_{\widehat{\mathcal{S}}_1,-j} \boldsymbol{\theta}_j^{(\widehat{\mathcal{S}}_1)}\|^2 + 2\lambda_j \|\boldsymbol{\theta}_j^{(\widehat{\mathcal{S}}_1)}\|_1 \\ & = \frac{1}{n} \|\boldsymbol{\epsilon}_{\widehat{\mathcal{S}}_1,j}\|^2 + 2\lambda_j \|\boldsymbol{\theta}_j^{(\widehat{\mathcal{S}}_1)}\|_1, \end{aligned} \quad (\text{D.76})$$

where $\boldsymbol{\epsilon}_{\widehat{\mathcal{S}}_1,j} \in \mathbb{R}^n$ denotes observations of the random error $\epsilon_{\widehat{\mathcal{S}}_1,j}$ in the linear model (D.69). Rearranging

the quadratic form on the left hand side of (D.76), it is easy to show that

$$\begin{aligned} & \frac{1}{n} \|\boldsymbol{\epsilon}_{\hat{\mathcal{S}}_1, j}\|^2 + \frac{2}{n} \boldsymbol{\epsilon}_{\hat{\mathcal{S}}_1, j}^\top \mathbb{Z}_{\hat{\mathcal{S}}_1, -j} \{\boldsymbol{\theta}_j^{(\hat{\mathcal{S}}_1)} - \hat{\boldsymbol{\theta}}_j^{(\hat{\mathcal{S}}_1)}\} + \frac{1}{n} \|\mathbb{Z}_{\hat{\mathcal{S}}_1, -j} \{\boldsymbol{\theta}_j^{(\hat{\mathcal{S}}_1)} - \hat{\boldsymbol{\theta}}_j^{(\hat{\mathcal{S}}_1)}\}\|^2 + 2\lambda_j \|\hat{\boldsymbol{\theta}}_j^{(\hat{\mathcal{S}}_1)}\|_1 \\ & \leq \frac{1}{n} \|\boldsymbol{\epsilon}_{\hat{\mathcal{S}}_1, j}\|^2 + 2\lambda_j \|\boldsymbol{\theta}_j^{(\hat{\mathcal{S}}_1)}\|_1, \end{aligned} \quad (\text{D.77})$$

which further implies that

$$\frac{1}{n} \|\mathbb{Z}_{\hat{\mathcal{S}}_1, -j} \{\boldsymbol{\theta}_j^{(\hat{\mathcal{S}}_1)} - \hat{\boldsymbol{\theta}}_j^{(\hat{\mathcal{S}}_1)}\}\|^2 + 2\lambda_j \|\hat{\boldsymbol{\theta}}_j^{(\hat{\mathcal{S}}_1)}\|_1 \leq \frac{2}{n} \boldsymbol{\epsilon}_{\hat{\mathcal{S}}_1, j}^\top \mathbb{Z}_{\hat{\mathcal{S}}_1, -j} \{\hat{\boldsymbol{\theta}}_j^{(\hat{\mathcal{S}}_1)} - \boldsymbol{\theta}_j^{(\hat{\mathcal{S}}_1)}\} + 2\lambda_j \|\boldsymbol{\theta}_j^{(\hat{\mathcal{S}}_1)}\|_1, \quad (\text{D.78})$$

and moreover,

$$\begin{aligned} & \frac{1}{n} \|\mathbb{Z}_{\hat{\mathcal{S}}_1, -j} \{\boldsymbol{\theta}_j^{(\hat{\mathcal{S}}_1)} - \hat{\boldsymbol{\theta}}_j^{(\hat{\mathcal{S}}_1)}\}\|^2 + 2\lambda_j \|\hat{\boldsymbol{\theta}}_j^{(\hat{\mathcal{S}}_1)} - \boldsymbol{\theta}_j^{(\hat{\mathcal{S}}_1)}\|_1 \\ & \leq \frac{2}{n} \boldsymbol{\epsilon}_{\hat{\mathcal{S}}_1, j}^\top \mathbb{Z}_{\hat{\mathcal{S}}_1, -j} \{\hat{\boldsymbol{\theta}}_j^{(\hat{\mathcal{S}}_1)} - \boldsymbol{\theta}_j^{(\hat{\mathcal{S}}_1)}\} + 4\lambda_j \|\boldsymbol{\theta}_j^{(\hat{\mathcal{S}}_1)}\|_1 \\ & \leq \frac{2}{n} \max_{\substack{1 \leq k \leq s \\ k \neq j}} |\mathbf{Z}_{\hat{\mathcal{S}}_1, k}^\top \boldsymbol{\epsilon}_{\hat{\mathcal{S}}_1, j}| \|\hat{\boldsymbol{\theta}}_j^{(\hat{\mathcal{S}}_1)} - \boldsymbol{\theta}_j^{(\hat{\mathcal{S}}_1)}\|_1 + 4\lambda_j \|\boldsymbol{\theta}_j^{(\hat{\mathcal{S}}_1)}\|_1 \end{aligned} \quad (\text{D.79})$$

which the first inequality is from applying the reverse triangle inequality to the left hand side of (D.78) and the second inequality uses $|\mathbf{u}_1^\top \mathbf{u}_2| \leq \|\mathbf{u}_1\|_\infty \|\mathbf{u}_2\|_1$ for any vectors $\mathbf{u}_1, \mathbf{u}_2$.

Define $\mathcal{G}_1 = \{\sup_{\hat{\mathcal{S}}_1: |\hat{\mathcal{S}}_1|=s} \max_{1 \leq j \leq s} \max_{\substack{1 \leq k \leq s \\ k \neq j}} 2|\mathbf{Z}_{\hat{\mathcal{S}}_1, k}^\top \boldsymbol{\epsilon}_{\hat{\mathcal{S}}_1, j}|/n \leq \lambda_{\text{NL}}\}$. On the event \mathcal{G}_1 , using (D.79), we get

$$\frac{1}{n} \|\mathbb{Z}_{\hat{\mathcal{S}}_1, -j} \{\boldsymbol{\theta}_j^{(\hat{\mathcal{S}}_1)} - \hat{\boldsymbol{\theta}}_j^{(\hat{\mathcal{S}}_1)}\}\|^2 + (2\lambda_j - \lambda_{\text{NL}}) \|\hat{\boldsymbol{\theta}}_j^{(\hat{\mathcal{S}}_1)} - \boldsymbol{\theta}_j^{(\hat{\mathcal{S}}_1)}\|_1 \leq 4\lambda_j \|\boldsymbol{\theta}_j^{(\hat{\mathcal{S}}_1)}\|_1. \quad (\text{D.80})$$

Under $\lambda_j = \lambda_{\text{NL}}$ and $\|\boldsymbol{\theta}_j^{(\hat{\mathcal{S}}_1)}\|_1 \leq B \|[\boldsymbol{\Sigma}_{\hat{\mathcal{S}}_1}^{-1}]_{-j, j}\|_1$ that has been proved in Lemma D.18, we further obtain

$$\frac{1}{n} \|\mathbb{Z}_{\hat{\mathcal{S}}_1, -j} \{\boldsymbol{\theta}_j^{(\hat{\mathcal{S}}_1)} - \hat{\boldsymbol{\theta}}_j^{(\hat{\mathcal{S}}_1)}\}\|^2 \leq 4\lambda_{\text{NL}} B \|[\boldsymbol{\Sigma}_{\hat{\mathcal{S}}_1}^{-1}]_{-j, j}\|_1, \quad (\text{D.81})$$

$$\|\hat{\boldsymbol{\theta}}_j^{(\hat{\mathcal{S}}_1)} - \boldsymbol{\theta}_j^{(\hat{\mathcal{S}}_1)}\|_1 \leq 4B \|[\boldsymbol{\Sigma}_{\hat{\mathcal{S}}_1}^{-1}]_{-j, j}\|_1. \quad (\text{D.82})$$

Taking supremum over $j = 1, \dots, s$ and $\hat{\mathcal{S}}_1$ of size s , then we have

$$\sup_{\hat{\mathcal{S}}_1: |\hat{\mathcal{S}}_1|=s} \max_{1 \leq j \leq s} \frac{\|\mathbb{Z}_{\hat{\mathcal{S}}_1, -j} \{\hat{\boldsymbol{\theta}}_j^{(\hat{\mathcal{S}}_1)} - \boldsymbol{\theta}_j^{(\hat{\mathcal{S}}_1)}\}\|^2}{n} \leq 4\lambda_{\text{NL}} B \left\{ \sup_{\hat{\mathcal{S}}_1: |\hat{\mathcal{S}}_1|=s} \max_{1 \leq j \leq s} \|[\boldsymbol{\Sigma}_{\hat{\mathcal{S}}_1}^{-1}]_{-j, j}\|_1 \right\}, \quad (\text{D.83})$$

$$\sup_{\hat{\mathcal{S}}_1: |\hat{\mathcal{S}}_1|=s} \max_{1 \leq j \leq s} \|\hat{\boldsymbol{\theta}}_j^{(\hat{\mathcal{S}}_1)} - \boldsymbol{\theta}_j^{(\hat{\mathcal{S}}_1)}\|_1 \leq 4B \left\{ \sup_{\hat{\mathcal{S}}_1: |\hat{\mathcal{S}}_1|=s} \max_{1 \leq j \leq s} \|[\boldsymbol{\Sigma}_{\hat{\mathcal{S}}_1}^{-1}]_{-j, j}\|_1 \right\}. \quad (\text{D.84})$$

Now it is remaining to control the maximal correlation between $\mathbf{Z}_{\hat{\mathcal{S}}_1, k}$ and $\boldsymbol{\epsilon}_{\hat{\mathcal{S}}_1, j}$ in absolute value for $k \neq j$

uniformly over all $j = 1, \dots, s$ and all $\hat{\mathcal{S}}_1$ of cardinality s ,

$$\sup_{\hat{\mathcal{S}}_1: |\hat{\mathcal{S}}_1|=s} \max_{1 \leq j \leq s} \max_{\substack{1 \leq k \leq s \\ k \neq j}} \frac{1}{n} |\mathbf{Z}_{\hat{\mathcal{S}}_1, k}^T \boldsymbol{\epsilon}_{\hat{\mathcal{S}}_1, j}|. \quad (\text{D.85})$$

We first reformulate (D.85) in terms of the covariance matrix $\hat{\boldsymbol{\Sigma}}_{\hat{\mathcal{S}}_1} = (\mathbf{Z}_{\hat{\mathcal{S}}_1}^T \mathbf{Z}_{\hat{\mathcal{S}}_1})/n$. Rewrite $\boldsymbol{\epsilon}_{\hat{\mathcal{S}}_1, j}$ in terms of $\mathbf{Z}_{\hat{\mathcal{S}}_1}$ and plug in the explicit form of $\boldsymbol{\theta}_j^{(\hat{\mathcal{S}}_1)}$ given by $\boldsymbol{\theta}_j^{(\hat{\mathcal{S}}_1)} = \{[\boldsymbol{\Sigma}_{\hat{\mathcal{S}}_1}]_{-j, -j}\}^{-1} [\boldsymbol{\Sigma}_{\hat{\mathcal{S}}_1}]_{-j, j}$, then we get

$$\begin{aligned} (\text{D.85}) &= \sup_{\hat{\mathcal{S}}_1: |\hat{\mathcal{S}}_1|=s} \max_{1 \leq j \leq s} \max_{\substack{1 \leq k \leq s \\ k \neq j}} \left| [\hat{\boldsymbol{\Sigma}}_{\hat{\mathcal{S}}_1}]_{kj} - [\hat{\boldsymbol{\Sigma}}_{\hat{\mathcal{S}}_1}]_{k, -j} \{[\boldsymbol{\Sigma}_{\hat{\mathcal{S}}_1}]_{-j, -j}\}^{-1} [\boldsymbol{\Sigma}_{\hat{\mathcal{S}}_1}]_{-j, j} \right| \\ &= \sup_{\hat{\mathcal{S}}_1: |\hat{\mathcal{S}}_1|=s} \max_{1 \leq j \leq s} \max_{\substack{1 \leq k \leq s \\ k \neq j}} \left| [\hat{\boldsymbol{\Sigma}}_{\hat{\mathcal{S}}_1}]_{kj} - [\boldsymbol{\Sigma}_{\hat{\mathcal{S}}_1}]_{kj} + [\boldsymbol{\Sigma}_{\hat{\mathcal{S}}_1}]_{kj} - [\hat{\boldsymbol{\Sigma}}_{\hat{\mathcal{S}}_1}]_{k, -j} \{[\boldsymbol{\Sigma}_{\hat{\mathcal{S}}_1}]_{-j, -j}\}^{-1} [\boldsymbol{\Sigma}_{\hat{\mathcal{S}}_1}]_{-j, j} \right| \\ &\leq \|\hat{\boldsymbol{\Sigma}} - \boldsymbol{\Sigma}\|_\infty + \sup_{\hat{\mathcal{S}}_1: |\hat{\mathcal{S}}_1|=s} \max_{1 \leq j \leq s} \max_{\substack{1 \leq k \leq s \\ k \neq j}} \left| [\boldsymbol{\Sigma}_{\hat{\mathcal{S}}_1}]_{kj} - [\hat{\boldsymbol{\Sigma}}_{\hat{\mathcal{S}}_1}]_{k, -j} \{[\boldsymbol{\Sigma}_{\hat{\mathcal{S}}_1}]_{-j, -j}\}^{-1} [\boldsymbol{\Sigma}_{\hat{\mathcal{S}}_1}]_{-j, j} \right| \\ &= \|\hat{\boldsymbol{\Sigma}} - \boldsymbol{\Sigma}\|_\infty + \sup_{\hat{\mathcal{S}}_1: |\hat{\mathcal{S}}_1|=s} \max_{1 \leq j \leq s} \left\| [\boldsymbol{\Sigma}_{\hat{\mathcal{S}}_1}]_{-j, j} - [\hat{\boldsymbol{\Sigma}}_{\hat{\mathcal{S}}_1}]_{-j, -j} \{[\boldsymbol{\Sigma}_{\hat{\mathcal{S}}_1}]_{-j, -j}\}^{-1} [\boldsymbol{\Sigma}_{\hat{\mathcal{S}}_1}]_{-j, j} \right\|_\infty. \quad (\text{D.86}) \end{aligned}$$

On the event $\mathcal{G}_2 = \{\|\hat{\boldsymbol{\Sigma}} - \boldsymbol{\Sigma}\|_\infty \leq a_2 \sqrt{(\log p)/n}\}$, with a_2 the same constant as in λ_{NL} , in addition to the bound on the max norm of the covariance matrix, we also have

$$\begin{aligned} &\sup_{\hat{\mathcal{S}}_1: |\hat{\mathcal{S}}_1|=s} \max_{1 \leq j \leq s} \left\| [\boldsymbol{\Sigma}_{\hat{\mathcal{S}}_1}]_{-j, j} - [\hat{\boldsymbol{\Sigma}}_{\hat{\mathcal{S}}_1}]_{-j, -j} \{[\boldsymbol{\Sigma}_{\hat{\mathcal{S}}_1}]_{-j, -j}\}^{-1} [\boldsymbol{\Sigma}_{\hat{\mathcal{S}}_1}]_{-j, j} \right\|_\infty \\ &= \sup_{\hat{\mathcal{S}}_1: |\hat{\mathcal{S}}_1|=s} \max_{1 \leq j \leq s} \left\| \left([\boldsymbol{\Sigma}_{\hat{\mathcal{S}}_1}]_{-j, -j} - [\hat{\boldsymbol{\Sigma}}_{\hat{\mathcal{S}}_1}]_{-j, -j} \right) \{[\boldsymbol{\Sigma}_{\hat{\mathcal{S}}_1}]_{-j, -j}\}^{-1} [\boldsymbol{\Sigma}_{\hat{\mathcal{S}}_1}]_{-j, j} \right\|_\infty \\ &\leq \|\hat{\boldsymbol{\Sigma}} - \boldsymbol{\Sigma}\|_\infty \sup_{\hat{\mathcal{S}}_1: |\hat{\mathcal{S}}_1|=s} \max_{1 \leq j \leq s} \left\| \{[\boldsymbol{\Sigma}_{\hat{\mathcal{S}}_1}]_{-j, -j}\}^{-1} [\boldsymbol{\Sigma}_{\hat{\mathcal{S}}_1}]_{-j, j} \right\|_1 \\ &\leq \left(a_2 B \sqrt{\frac{\log p}{n}} \right) \sup_{\hat{\mathcal{S}}_1: |\hat{\mathcal{S}}_1|=s} \max_{1 \leq j \leq s} \left\| [\boldsymbol{\Sigma}_{\hat{\mathcal{S}}_1}^{-1}]_{-j, j} \right\|_1, \quad (\text{D.87}) \end{aligned}$$

where the first inequality bounds the max norm of the matrix product by the max norm of one matrix and the ℓ_1 norm of the other, and the second inequality comes from the definition of \mathcal{G}_2 and $\|\boldsymbol{\theta}_j^{(\hat{\mathcal{S}}_1)}\|_1 \leq B \left\| [\boldsymbol{\Sigma}_{\hat{\mathcal{S}}_1}^{-1}]_{-j, j} \right\|_1$ that has been proved in Lemma D.18.

Combining (D.86) and (D.87), we get

$$\sup_{\hat{\mathcal{S}}_1: |\hat{\mathcal{S}}_1|=s} \max_{1 \leq j \leq s} \max_{\substack{1 \leq k \leq s \\ k \neq j}} \frac{1}{n} |\mathbf{Z}_{\hat{\mathcal{S}}_1, k}^T \boldsymbol{\epsilon}_{\hat{\mathcal{S}}_1, j}| \leq \underbrace{2a_2 \eta_{\max} \sqrt{\frac{\log p}{n}}}_{\frac{\lambda_{\text{NL}}}{2}}. \quad (\text{D.88})$$

Hence, we can bound $P(\mathcal{G}_1^c)$ as follows

$$P(\mathcal{G}_1^c) \leq P(\mathcal{G}_2^c) \leq e^{-a_3 \log p} \quad (\text{D.89})$$

for some constant $a_3 > 0$, where the second inequality follows from Lemma D.10. As (D.83) and (D.84) hold on the event \mathcal{G}_1 , then the concentration inequalities (D.74) and (D.75) follow directly from (D.89). This completes the proof. \square

Before presenting Lemma D.12 below that refers to the claim in (D.71), we introduce some additional notations. Let $\tau_{\hat{\mathcal{S}}_1, j}^2$ be a shorthand of $[\boldsymbol{\Sigma}_{\hat{\mathcal{S}}_1}]_{j,j} - [\boldsymbol{\Sigma}_{\hat{\mathcal{S}}_1}]_{j,-j} \{[\boldsymbol{\Sigma}_{\hat{\mathcal{S}}_1}]_{-j,-j}\}^{-1} [\boldsymbol{\Sigma}_{\hat{\mathcal{S}}_1}]_{-j,j}$, where $\boldsymbol{\Sigma}_{\hat{\mathcal{S}}_1}$ is the covariance matrix of candidate instruments in $\hat{\mathcal{S}}_1$; $[\boldsymbol{\Sigma}_{\hat{\mathcal{S}}_1}]_{j,j}$ represents the (j, j) th element of $\boldsymbol{\Sigma}_{\hat{\mathcal{S}}_1} \in \mathbb{R}^{s \times s}$, $[\boldsymbol{\Sigma}_{\hat{\mathcal{S}}_1}]_{j,-j}$ is the j th row of $\boldsymbol{\Sigma}_{\hat{\mathcal{S}}_1}$ with the j th component deleted, and similarly $[\boldsymbol{\Sigma}_{\hat{\mathcal{S}}_1}]_{-j,j}$ denotes the j th column of $\boldsymbol{\Sigma}_{\hat{\mathcal{S}}_1}$ with the j th component deleted, and $\{[\boldsymbol{\Sigma}_{\hat{\mathcal{S}}_1}]_{-j,-j}\}^{-1}$ is the inverse of the matrix $[\boldsymbol{\Sigma}_{\hat{\mathcal{S}}_1}]_{-j,-j}$ formed by rows and columns of $\boldsymbol{\Sigma}_{\hat{\mathcal{S}}_1}$ that are indexed by $\{1, \dots, s\} \setminus \{j\}$.

The Lemma D.12 says that with probability tending to one, $\hat{\tau}_{\hat{\mathcal{S}}_1, j}^2 = \|\mathbf{Z}_{\hat{\mathcal{S}}_1, j} - \mathbb{Z}_{\hat{\mathcal{S}}_1, -j} \hat{\boldsymbol{\theta}}_j^{(\hat{\mathcal{S}}_1)}\|^2/n + \lambda_j \|\hat{\boldsymbol{\theta}}_j^{(\hat{\mathcal{S}}_1)}\|_1$ has bounded support uniformly over all $j = 1, \dots, s$ and $\hat{\mathcal{S}}_1$, by bounding the difference between $\hat{\tau}_{\hat{\mathcal{S}}_1, j}^2$ and $\tau_{\hat{\mathcal{S}}_1, j}^2$.

Lemma D.12. Assume the same conditions as Lemma D.11. There exist constants $a_3, c_{22} > 0$ such that the following holds

$$P\left(\sup_{\hat{\mathcal{S}}_1: |\hat{\mathcal{S}}_1|=s} \max_{1 \leq j \leq s} |\hat{\tau}_{\hat{\mathcal{S}}_1, j}^2 - \tau_{\hat{\mathcal{S}}_1, j}^2| > c_{22} \eta_{\max}^2 \left(\frac{\log p}{n}\right)^{1/4}\right) \leq 3e^{-a_3 \log p}, \quad (\text{D.90})$$

where $\eta_{\max} = 1 \vee B \sup_{\hat{\mathcal{S}}_1: |\hat{\mathcal{S}}_1|=s} \max_{1 \leq j \leq s} \|[\boldsymbol{\Sigma}_{\hat{\mathcal{S}}_1}^{-1}]_{-j,j}\|_1$. Moreover, we have

$$P\left(\sup_{\hat{\mathcal{S}}_1: |\hat{\mathcal{S}}_1|=s} \max_{1 \leq j \leq s} \frac{1}{\hat{\tau}_{\hat{\mathcal{S}}_1, j}^2} > \frac{1}{0.99C_L}\right) \leq 3e^{-a_3 \log p} \quad (\text{D.91})$$

when n, p are sufficiently large.

Proof of Lemma D.12. We first bound $\tau_{\hat{\mathcal{S}}_1, j}^2 = [\boldsymbol{\Sigma}_{\hat{\mathcal{S}}_1}]_{j,j} - [\boldsymbol{\Sigma}_{\hat{\mathcal{S}}_1}]_{j,-j} \{[\boldsymbol{\Sigma}_{\hat{\mathcal{S}}_1}]_{-j,-j}\}^{-1} [\boldsymbol{\Sigma}_{\hat{\mathcal{S}}_1}]_{-j,j}$. It has been shown in (D.125) in the proof of Lemma D.18 that $\tau_{\hat{\mathcal{S}}_1, j}^2 = 1/[\boldsymbol{\Sigma}_{\hat{\mathcal{S}}_1}^{-1}]_{jj}$. In addition, as the matrix $[\boldsymbol{\Sigma}_{\hat{\mathcal{S}}_1}]_{-j,-j}$ is positive definite and we thus have $[\boldsymbol{\Sigma}_{\hat{\mathcal{S}}_1}]_{j,-j} \{[\boldsymbol{\Sigma}_{\hat{\mathcal{S}}_1}]_{-j,-j}\}^{-1} [\boldsymbol{\Sigma}_{\hat{\mathcal{S}}_1}]_{-j,j} > 0$, which implies that $\tau_{\hat{\mathcal{S}}_1, j}^2 \leq [\boldsymbol{\Sigma}_{\hat{\mathcal{S}}_1}]_{j,j}$. Then under assumption A2 that eigenvalues of the covariance matrix $\boldsymbol{\Sigma} \in \mathbb{R}^{p \times p}$ have bounded support, it is easy to see that

$$C_L \leq \tau_{\hat{\mathcal{S}}_1, j}^2 \leq C_R, \quad (\text{D.92})$$

which holds uniformly over all $j = 1, \dots, s$ and all $\hat{\mathcal{S}}_1$ of cardinality s .

Next, writing $\hat{\tau}_{\hat{\mathcal{S}}_1, j}^2 = \|\mathbf{Z}_{\hat{\mathcal{S}}_1, j} - \mathbb{Z}_{\hat{\mathcal{S}}_1, -j} \hat{\boldsymbol{\theta}}_j^{(\hat{\mathcal{S}}_1)}\|^2/n + \lambda_j \|\hat{\boldsymbol{\theta}}_j^{(\hat{\mathcal{S}}_1)}\|_1$ explicitly, we have

$$\begin{aligned} & \hat{\tau}_{\hat{\mathcal{S}}_1, j}^2 - \tau_{\hat{\mathcal{S}}_1, j}^2 \\ &= \left(\frac{1}{n} \|\mathbf{Z}_{\hat{\mathcal{S}}_1, j} - \mathbb{Z}_{\hat{\mathcal{S}}_1, -j} \boldsymbol{\theta}_j^{(\hat{\mathcal{S}}_1)}\|^2 - \tau_{\hat{\mathcal{S}}_1, j}^2 \right) + \frac{1}{n} \|\mathbb{Z}_{\hat{\mathcal{S}}_1, -j} (\hat{\boldsymbol{\theta}}_j^{(\hat{\mathcal{S}}_1)} - \boldsymbol{\theta}_j^{(\hat{\mathcal{S}}_1)})\|^2 \\ & \quad - \frac{2}{n} (\mathbf{Z}_{\hat{\mathcal{S}}_1, j} - \mathbb{Z}_{\hat{\mathcal{S}}_1, -j} \boldsymbol{\theta}_j^{(\hat{\mathcal{S}}_1)}) \mathbb{Z}_{\hat{\mathcal{S}}_1, -j} (\hat{\boldsymbol{\theta}}_j^{(\hat{\mathcal{S}}_1)} - \boldsymbol{\theta}_j^{(\hat{\mathcal{S}}_1)}) + \lambda_j \|\hat{\boldsymbol{\theta}}_j^{(\hat{\mathcal{S}}_1)}\|_1 \end{aligned} \quad (\text{D.93})$$

Before proceeding, define the following events,

$$\begin{aligned}\mathcal{H}_3 &= \left\{ \sup_{\hat{\mathcal{S}}_1:|\hat{\mathcal{S}}_1|=s} \max_{1 \leq j \leq s} \frac{\|\mathbb{Z}_{\hat{\mathcal{S}}_1,-j}(\hat{\boldsymbol{\theta}}_j^{(\hat{\mathcal{S}}_1)} - \boldsymbol{\theta}_j^{(\hat{\mathcal{S}}_1)})\|^2}{n} \leq 4\lambda_{\text{NL}}B \left(\sup_{\hat{\mathcal{S}}_1:|\hat{\mathcal{S}}_1|=s} \max_{1 \leq j \leq s} \|[\boldsymbol{\Sigma}_{\hat{\mathcal{S}}_1}^{-1}]_{-j,j}\|_1 \right) \right\}, \\ \mathcal{H}_4 &= \left\{ \sup_{\hat{\mathcal{S}}_1:|\hat{\mathcal{S}}_1|=s} \max_{1 \leq j \leq s} \|\hat{\boldsymbol{\theta}}_j^{(\hat{\mathcal{S}}_1)} - \boldsymbol{\theta}_j^{(\hat{\mathcal{S}}_1)}\|_1 \leq 4B \left(\sup_{\hat{\mathcal{S}}_1:|\hat{\mathcal{S}}_1|=s} \max_{1 \leq j \leq s} \|[\boldsymbol{\Sigma}_{\hat{\mathcal{S}}_1}^{-1}]_{-j,j}\|_1 \right) \right\} \\ \mathcal{H}_5 &= \left\{ \sup_{\hat{\mathcal{S}}_1:|\hat{\mathcal{S}}_1|=s} \max_{1 \leq j \leq s} \left| \frac{1}{n} \|\boldsymbol{\epsilon}_{\hat{\mathcal{S}}_1,j}\|^2 - \tau_{\hat{\mathcal{S}}_1,j}^2 \right| \leq 6a_2\eta_{\text{max}}^2 \sqrt{\frac{\log p}{n}} \right\},\end{aligned}$$

where $\boldsymbol{\epsilon}_{\hat{\mathcal{S}}_1,j} = \mathbf{Z}_{\hat{\mathcal{S}}_1,j} - \mathbb{Z}_{\hat{\mathcal{S}}_1,-j}\boldsymbol{\theta}_j^{(\hat{\mathcal{S}}_1)}$. Here the constant a_2 is the same as Lemma D.11. On the event \mathcal{H}_4 , we get

$$\begin{aligned}\sup_{\hat{\mathcal{S}}_1:|\hat{\mathcal{S}}_1|=s} \max_{1 \leq j \leq s} \lambda_j \|\hat{\boldsymbol{\theta}}_j^{(\hat{\mathcal{S}}_1)}\|_1 &\leq \sup_{\hat{\mathcal{S}}_1:|\hat{\mathcal{S}}_1|=s} \max_{1 \leq j \leq s} \left\{ \lambda_j \|\boldsymbol{\theta}_j^{(\hat{\mathcal{S}}_1)}\|_1 + \lambda_j \|\hat{\boldsymbol{\theta}}_j^{(\hat{\mathcal{S}}_1)} - \boldsymbol{\theta}_j^{(\hat{\mathcal{S}}_1)}\|_1 \right\} \\ &\leq 5B\lambda_{\text{NL}} \sup_{\hat{\mathcal{S}}_1:|\hat{\mathcal{S}}_1|=s} \max_{1 \leq j \leq s} \|[\boldsymbol{\Sigma}_{\hat{\mathcal{S}}_1}^{-1}]_{-j,j}\|_1,\end{aligned}\tag{D.94}$$

which uses $\|\boldsymbol{\theta}_j^{(\hat{\mathcal{S}}_1)}\|_1 \leq B\|[\boldsymbol{\Sigma}_{\hat{\mathcal{S}}_1}^{-1}]_{-j,j}\|_1$ as shown in Lemma D.18. Then on the event $\mathcal{H}_3 \cap \mathcal{H}_4 \cap \mathcal{H}_5$, we can bound $|\hat{\tau}_{\hat{\mathcal{S}}_1,j}^2 - \tau_{\hat{\mathcal{S}}_1,j}^2|$ uniformly over all $j = 1, \dots, s$ and $\hat{\mathcal{S}}_1$ by

$$\begin{aligned}&\sup_{\hat{\mathcal{S}}_1:|\hat{\mathcal{S}}_1|=s} \max_{1 \leq j \leq s} |\hat{\tau}_{\hat{\mathcal{S}}_1,j}^2 - \tau_{\hat{\mathcal{S}}_1,j}^2| \\ &\leq \sup_{\hat{\mathcal{S}}_1:|\hat{\mathcal{S}}_1|=s} \max_{1 \leq j \leq s} \left| \frac{1}{n} \|\boldsymbol{\epsilon}_{\hat{\mathcal{S}}_1,j}\|^2 - \tau_{\hat{\mathcal{S}}_1,j}^2 \right| + \sup_{\hat{\mathcal{S}}_1:|\hat{\mathcal{S}}_1|=s} \max_{1 \leq j \leq s} \frac{\|\mathbb{Z}_{\hat{\mathcal{S}}_1,-j}(\hat{\boldsymbol{\theta}}_j^{(\hat{\mathcal{S}}_1)} - \boldsymbol{\theta}_j^{(\hat{\mathcal{S}}_1)})\|^2}{n} \\ &\quad + \frac{2}{n} \sup_{\hat{\mathcal{S}}_1:|\hat{\mathcal{S}}_1|=s} \max_{1 \leq j \leq s} \left\{ \|\boldsymbol{\epsilon}_{\hat{\mathcal{S}}_1,j}\| \|\mathbb{Z}_{\hat{\mathcal{S}}_1,-j}(\hat{\boldsymbol{\theta}}_j^{(\hat{\mathcal{S}}_1)} - \boldsymbol{\theta}_j^{(\hat{\mathcal{S}}_1)})\| \right\} + \sup_{\hat{\mathcal{S}}_1:|\hat{\mathcal{S}}_1|=s} \max_{1 \leq j \leq s} \lambda_j \|\hat{\boldsymbol{\theta}}_j^{(\hat{\mathcal{S}}_1)}\|_1 \\ &\leq c_{22}\eta_{\text{max}}^2 \left(\frac{\log p}{n} \right)^{1/4}\end{aligned}\tag{D.95}$$

for some constant $c_{22} > 0$. The first inequality is from (D.93) and Cauchy-Schwartz inequality; by plugging the explicit form of $\lambda_{\text{NL}} = 4a_2\eta_{\text{max}}\sqrt{(\log p)/n}$, the second inequality comes from (D.94), definitions of $\mathcal{H}_3, \mathcal{H}_5$ and $\log p = o(n)$.

Under assumption A6 that $\eta_{\text{max}} = o((n/\log p)^{1/4})$, applying (D.92) and (D.95), we have

$$0.99C_L \leq \hat{\tau}_{\hat{\mathcal{S}}_1,j}^2 \leq 1.01C_R$$

as $n, p \rightarrow \infty$, which holds uniformly over all $j = 1, \dots, s$ and $\hat{\mathcal{S}}_1$ of size s .

To prove the statements (D.90) and (D.91), bounding $P(\mathcal{H}_3^c), P(\mathcal{H}_4^c)$ and $P(\mathcal{H}_5^c)$ suffices. Recall that $\boldsymbol{\epsilon}_{\hat{\mathcal{S}}_1,j} = \mathbf{Z}_{\hat{\mathcal{S}}_1,j} - \mathbb{Z}_{\hat{\mathcal{S}}_1,-j}\boldsymbol{\theta}_j^{(\hat{\mathcal{S}}_1)}$ and $\tau_{\hat{\mathcal{S}}_1,j}^2 = [\boldsymbol{\Sigma}_{\hat{\mathcal{S}}_1}]_{j,j} - [\boldsymbol{\Sigma}_{\hat{\mathcal{S}}_1}]_{j,-j} \{ [\boldsymbol{\Sigma}_{\hat{\mathcal{S}}_1}]_{-j,-j} \}^{-1} [\boldsymbol{\Sigma}_{\hat{\mathcal{S}}_1}]_{-j,j}$. Using the explicit

forms of $\epsilon_{\hat{\mathcal{S}}_1, j}$ and $\tau_{\hat{\mathcal{S}}_1, j}^2$, as well as $\boldsymbol{\theta}_j^{(\hat{\mathcal{S}}_1)} = [\boldsymbol{\Sigma}_{\hat{\mathcal{S}}_1}]_{-j, -j}^{-1} [\boldsymbol{\Sigma}_{\hat{\mathcal{S}}_1}]_{-j, j}$, we get

$$\begin{aligned} & \left| \frac{1}{n} \|\epsilon_{\hat{\mathcal{S}}_1, j}\|^2 - \tau_{\hat{\mathcal{S}}_1, j}^2 \right| \\ &= |([\hat{\boldsymbol{\Sigma}}_{\hat{\mathcal{S}}_1}]_{jj} - [\boldsymbol{\Sigma}_{\hat{\mathcal{S}}_1}]_{jj}) + [\{\boldsymbol{\theta}_j^{(\hat{\mathcal{S}}_1)}\}^T [\hat{\boldsymbol{\Sigma}}_{\hat{\mathcal{S}}_1}]_{-j, -j} \boldsymbol{\theta}_j^{(\hat{\mathcal{S}}_1)} + [\boldsymbol{\Sigma}_{\hat{\mathcal{S}}_1}]_{j, -j} \boldsymbol{\theta}_j^{(\hat{\mathcal{S}}_1)} - 2[\hat{\boldsymbol{\Sigma}}_{\hat{\mathcal{S}}_1}]_{j, -j} \boldsymbol{\theta}_j^{(\hat{\mathcal{S}}_1)}]| \\ &\leq |[\hat{\boldsymbol{\Sigma}}_{\hat{\mathcal{S}}_1}]_{jj} - [\boldsymbol{\Sigma}_{\hat{\mathcal{S}}_1}]_{jj}| + |[\{\boldsymbol{\theta}_j^{(\hat{\mathcal{S}}_1)}\}^T [\hat{\boldsymbol{\Sigma}}_{\hat{\mathcal{S}}_1}]_{-j, -j} \boldsymbol{\theta}_j^{(\hat{\mathcal{S}}_1)} + [\boldsymbol{\Sigma}_{\hat{\mathcal{S}}_1}]_{j, -j} \boldsymbol{\theta}_j^{(\hat{\mathcal{S}}_1)} - 2[\hat{\boldsymbol{\Sigma}}_{\hat{\mathcal{S}}_1}]_{j, -j} \boldsymbol{\theta}_j^{(\hat{\mathcal{S}}_1)}]| \end{aligned} \quad (\text{D.96})$$

for $j = 1 \dots, s$. Simple calculations yield

$$\begin{aligned} & |[\{\boldsymbol{\theta}_j^{(\hat{\mathcal{S}}_1)}\}^T [\hat{\boldsymbol{\Sigma}}_{\hat{\mathcal{S}}_1}]_{-j, -j} \boldsymbol{\theta}_j^{(\hat{\mathcal{S}}_1)} + [\boldsymbol{\Sigma}_{\hat{\mathcal{S}}_1}]_{j, -j} \boldsymbol{\theta}_j^{(\hat{\mathcal{S}}_1)} - 2[\hat{\boldsymbol{\Sigma}}_{\hat{\mathcal{S}}_1}]_{j, -j} \boldsymbol{\theta}_j^{(\hat{\mathcal{S}}_1)}]| \\ &= |[\{\boldsymbol{\theta}_j^{(\hat{\mathcal{S}}_1)}\}^T ([\hat{\boldsymbol{\Sigma}}_{\hat{\mathcal{S}}_1}]_{-j, -j} - [\boldsymbol{\Sigma}_{\hat{\mathcal{S}}_1}]_{-j, -j}) \boldsymbol{\theta}_j^{(\hat{\mathcal{S}}_1)} + 2([\hat{\boldsymbol{\Sigma}}_{\hat{\mathcal{S}}_1}]_{j, -j} - [\boldsymbol{\Sigma}_{\hat{\mathcal{S}}_1}]_{j, -j}) \boldsymbol{\theta}_j^{(\hat{\mathcal{S}}_1)}]| \\ &\leq |[\{\boldsymbol{\theta}_j^{(\hat{\mathcal{S}}_1)}\}^T ([\hat{\boldsymbol{\Sigma}}_{\hat{\mathcal{S}}_1}]_{-j, -j} - [\boldsymbol{\Sigma}_{\hat{\mathcal{S}}_1}]_{-j, -j}) \boldsymbol{\theta}_j^{(\hat{\mathcal{S}}_1)}]| + 2|([\hat{\boldsymbol{\Sigma}}_{\hat{\mathcal{S}}_1}]_{j, -j} - [\boldsymbol{\Sigma}_{\hat{\mathcal{S}}_1}]_{j, -j}) \boldsymbol{\theta}_j^{(\hat{\mathcal{S}}_1)}| \\ &\leq \|[\hat{\boldsymbol{\Sigma}}_{\hat{\mathcal{S}}_1}]_{-j, -j} - [\boldsymbol{\Sigma}_{\hat{\mathcal{S}}_1}]_{-j, -j}\|_\infty \|\boldsymbol{\theta}_j^{(\hat{\mathcal{S}}_1)}\|_1^2 + 2\|[\hat{\boldsymbol{\Sigma}}_{\hat{\mathcal{S}}_1}]_{j, -j} - [\boldsymbol{\Sigma}_{\hat{\mathcal{S}}_1}]_{j, -j}\|_\infty \|\boldsymbol{\theta}_j^{(\hat{\mathcal{S}}_1)}\|_1. \end{aligned} \quad (\text{D.97})$$

On the event $\mathcal{G}_2 = \{\|\hat{\boldsymbol{\Sigma}} - \boldsymbol{\Sigma}\|_\infty \leq a_2 \sqrt{(\log p)/n}\}$ for some constant $a_2 > 0$, using (D.96), (D.97) and Lemma D.18, we get

$$\begin{aligned} & \sup_{\hat{\mathcal{S}}_1: |\hat{\mathcal{S}}_1|=s} \max_{1 \leq j \leq s} \left| \frac{1}{n} \|\epsilon_{\hat{\mathcal{S}}_1, j}\|^2 - \tau_{\hat{\mathcal{S}}_1, j}^2 \right| \\ &\leq \|\hat{\boldsymbol{\Sigma}} - \boldsymbol{\Sigma}\|_\infty + \|\hat{\boldsymbol{\Sigma}} - \boldsymbol{\Sigma}\|_\infty \|\boldsymbol{\theta}_j^{(\hat{\mathcal{S}}_1)}\|_1^2 + 2\|\hat{\boldsymbol{\Sigma}} - \boldsymbol{\Sigma}\|_\infty \|\boldsymbol{\theta}_j^{(\hat{\mathcal{S}}_1)}\|_1 \\ &\leq 6a_2 \eta_{\max}^2 \sqrt{\frac{\log p}{n}}. \end{aligned} \quad (\text{D.98})$$

Then we can obtain

$$P(\mathcal{H}_5^c) \leq P(\mathcal{G}_2^c) \leq e^{-a_3 \log p}, \quad (\text{D.99})$$

where the second inequality is from Lemma D.10. Details of the constant $a_3 > 0$ can be found in Lemma D.10. Applying Lemma D.11, together with (D.99) we get

$$P(\mathcal{H}_3^c) + P(\mathcal{H}_4^c) + P(\mathcal{H}_5^c) \leq 3e^{-a_3 \log p}. \quad (\text{D.100})$$

We thus finish the proof. \square

Lemma D.13 ($P(\mathcal{E}_1^c)$). Suppose the same conditions as Lemma D.11. Then we have the following

$$P\left(\sup_{\hat{\mathcal{S}}_1: |\hat{\mathcal{S}}_1|=s} \|\mathbf{M} \hat{\boldsymbol{\Sigma}}_{\hat{\mathcal{S}}_1} - \mathbf{I}_s\|_\infty > \frac{\lambda_{\text{NL}}}{0.99C_L}\right) \leq 3e^{-a_3 \log p} \quad (\text{D.101})$$

for some $a_3 > 0$ when n, p are sufficiently large.

Proof of Lemma D.13. Let $\mathbf{m}_j^T \in \mathbb{R}^{1 \times s}$ denote the j th row of \mathbf{M} for $j = 1, \dots, s$. Then $\|\mathbf{M} \hat{\boldsymbol{\Sigma}}_{\hat{\mathcal{S}}_1} - \mathbf{I}_s\|_\infty$

can be rewritten as $\max_{1 \leq j \leq s} \|\widehat{\Sigma}_{\widehat{S}_1} \mathbf{m}_j - e_j\|_\infty$, where $e_j \in \mathbb{R}^s$ is unit vector with the j th element equal to one and zero otherwise. Write $\widehat{\Sigma}_{\widehat{S}_1} \mathbf{m}_j - e_j$ explicitly,

$$\begin{aligned} \widehat{\Sigma}_{\widehat{S}_1} \mathbf{m}_j - e_j &= \frac{1}{n} \mathbb{Z}_{\widehat{S}_1}^T \mathbb{Z}_{\widehat{S}_1} \mathbf{m}_j - e_j \\ &= \begin{pmatrix} \mathbf{Z}_{\widehat{S}_1,1}^T \frac{1}{n} \mathbb{Z}_{\widehat{S}_1} \mathbf{m}_j \\ \vdots \\ \mathbf{Z}_{\widehat{S}_1,j}^T \frac{1}{n} \mathbb{Z}_{\widehat{S}_1} \mathbf{m}_j \\ \vdots \\ \mathbf{Z}_{\widehat{S}_1,s}^T \frac{1}{n} \mathbb{Z}_{\widehat{S}_1} \mathbf{m}_j \end{pmatrix} - \begin{pmatrix} 0 \\ \vdots \\ 1 \\ \vdots \\ 0 \end{pmatrix}, \end{aligned}$$

where $\mathbf{Z}_{\widehat{S}_1,j} \in \mathbb{R}^n$ represents the n observations of candidate $Z_{\widehat{S}_1,j}$ for $j = 1, \dots, s$, which implies that the k th component of $\widehat{\Sigma}_{\widehat{S}_1} \mathbf{m}_j - e_j$, denoted by $[\widehat{\Sigma}_{\widehat{S}_1} \mathbf{m}_j - e_j]_k$ for $1 \leq k \leq s$, satisfies

$$[\widehat{\Sigma}_{\widehat{S}_1} \mathbf{m}_j - e_j]_k = \begin{cases} \mathbf{Z}_{\widehat{S}_1,k}^T \frac{1}{n} \mathbb{Z}_{\widehat{S}_1} \mathbf{m}_j, & k \neq j \\ \mathbf{Z}_{\widehat{S}_1,k}^T \frac{1}{n} \mathbb{Z}_{\widehat{S}_1} \mathbf{m}_j - 1, & k = j \end{cases}. \quad (\text{D.102})$$

Let $\widehat{\kappa}_j$ denote the subdifferential of $\|\boldsymbol{\theta}_j\|_1$ in the node-wise lasso problems (G.1) in the main paper, which takes the following form

$$\widehat{\kappa}_{j,k} = \begin{cases} \text{sign}(\widehat{\theta}_{j,k}^{(\widehat{S}_1)}), & \text{if } \widehat{\theta}_{j,k}^{(\widehat{S}_1)} \neq 0 \\ \in (-1, 1), & \text{if } \widehat{\theta}_{j,k}^{(\widehat{S}_1)} = 0. \end{cases}$$

It follows from the KKT condition of the node-wise lasso that

$$\lambda_j \widehat{\kappa}_j = \frac{1}{n} \mathbb{Z}_{\widehat{S}_1,-j}^T (\mathbf{Z}_{\widehat{S}_1,j} - \mathbb{Z}_{\widehat{S}_1,-j} \widehat{\boldsymbol{\theta}}_j^{(\widehat{S}_1)}). \quad (\text{D.103})$$

Recall that $\widehat{\tau}_{\widehat{S}_1,j}^2 = \|\mathbf{Z}_{\widehat{S}_1,j} - \mathbb{Z}_{\widehat{S}_1,-j} \widehat{\boldsymbol{\theta}}_j^{(\widehat{S}_1)}\|^2/n + \lambda_j \|\widehat{\boldsymbol{\theta}}_j^{(\widehat{S}_1)}\|_1$. Using (D.103) and $\widehat{\kappa}_j^T \widehat{\boldsymbol{\theta}}_j^{(\widehat{S}_1)} = \|\widehat{\boldsymbol{\theta}}_j^{(\widehat{S}_1)}\|_1$, simple calculation yields

$$\begin{aligned} \widehat{\tau}_{\widehat{S}_1,j}^2 &= \frac{1}{n} \mathbf{Z}_{\widehat{S}_1,j}^T (\mathbf{Z}_{\widehat{S}_1,j} - \mathbb{Z}_{\widehat{S}_1,-j} \widehat{\boldsymbol{\theta}}_j^{(\widehat{S}_1)}) - \{\widehat{\boldsymbol{\theta}}_j^{(\widehat{S}_1)}\}^T \frac{\mathbb{Z}_{\widehat{S}_1,-j}^T (\mathbf{Z}_{\widehat{S}_1,j} - \mathbb{Z}_{\widehat{S}_1,-j} \widehat{\boldsymbol{\theta}}_j^{(\widehat{S}_1)})}{n} + \lambda_j \|\widehat{\boldsymbol{\theta}}_j^{(\widehat{S}_1)}\|_1 \\ &= \frac{1}{n} \mathbf{Z}_{\widehat{S}_1,j}^T (\mathbf{Z}_{\widehat{S}_1,j} - \mathbb{Z}_{\widehat{S}_1,-j} \widehat{\boldsymbol{\theta}}_j^{(\widehat{S}_1)}). \end{aligned} \quad (\text{D.104})$$

Then based on the construction that $\mathbf{m}_j^T = e_j^T \widehat{\mathbf{N}} / \widehat{\tau}_{\widehat{\mathcal{S}}_1, j}^2$ from (G.3) in the main paper, we have

$$\begin{aligned} \frac{1}{n} \mathbf{Z}_{\widehat{\mathcal{S}}_1, j}^T \mathbb{Z}_{\widehat{\mathcal{S}}_1} \mathbf{m}_j &= \frac{1}{n} \mathbf{Z}_{\widehat{\mathcal{S}}_1, j}^T \mathbb{Z}_{\widehat{\mathcal{S}}_1} \frac{\widehat{\mathbf{N}}^T e_j}{\widehat{\tau}_{\widehat{\mathcal{S}}_1, j}^2} \\ &= \frac{1}{\widehat{\tau}_{\widehat{\mathcal{S}}_1, j}^2} \frac{1}{n} \mathbf{Z}_{\widehat{\mathcal{S}}_1, j}^T (\mathbf{Z}_{\widehat{\mathcal{S}}_1, j} - \mathbb{Z}_{\widehat{\mathcal{S}}_1, -j} \widehat{\boldsymbol{\theta}}_j^{(\widehat{\mathcal{S}}_1)}) \\ &= 1, \end{aligned} \tag{D.105}$$

where the last equality is from (D.104). In addition, it also follows from (D.103) that

$$\begin{aligned} \frac{1}{n} \mathbb{Z}_{\widehat{\mathcal{S}}_1, -j}^T \mathbb{Z}_{\widehat{\mathcal{S}}_1} \mathbf{m}_j &= \frac{1}{\widehat{\tau}_{\widehat{\mathcal{S}}_1, j}^2} \frac{1}{n} \mathbb{Z}_{\widehat{\mathcal{S}}_1, -j}^T (\mathbf{Z}_{\widehat{\mathcal{S}}_1, j} - \mathbb{Z}_{\widehat{\mathcal{S}}_1, -j} \widehat{\boldsymbol{\theta}}_j^{(\widehat{\mathcal{S}}_1)}) \\ &= \frac{\lambda_j}{\widehat{\tau}_{\widehat{\mathcal{S}}_1, j}^2} \widehat{\boldsymbol{\kappa}}_j. \end{aligned} \tag{D.106}$$

Combining (D.105) and (D.106), the claim in (D.70) follows, that is,

$$\|\mathbf{M} \widehat{\boldsymbol{\Sigma}}_{\widehat{\mathcal{S}}_1} - \mathbf{I}_s\|_\infty \leq \max_{1 \leq j \leq s} \frac{\lambda_j}{\widehat{\tau}_{\widehat{\mathcal{S}}_1, j}^2}.$$

Using $\lambda_j = \lambda_{\text{NL}}$ for all $j = 1, \dots, s$ and $\widehat{\mathcal{S}}_1$ of size s and applying Lemma D.12 give the desired result. \square

Lemma D.14 ($P(\mathcal{E}_2^c)$ and $P(\mathcal{E}_3^c)$). Suppose assumptions A2 and A6 hold. Then we have

(i) Further assume the conditions in Lemma D.12. The following holds

$$P\left(\sup_{\widehat{\mathcal{S}}_1: |\widehat{\mathcal{S}}_1|=s} \|\mathbf{M}\|_1 > \frac{10\eta_{\max}}{C_L}\right) \leq 4e^{-a_3 \log p}. \tag{D.107}$$

Details of the constant $a_3 > 0$ have been discussed in Lemma D.10.

(ii) Under the same conditions as Lemma D.14-(i), then we have

$$P\left(\sup_{\widehat{\mathcal{S}}_1: |\widehat{\mathcal{S}}_1|=s} \max_{1 \leq j \leq s} |[\mathbf{M} \widehat{\boldsymbol{\Sigma}}_{\widehat{\mathcal{S}}_1} \mathbf{M}^T - \boldsymbol{\Sigma}_{\widehat{\mathcal{S}}_1}^{-1}]_{jj}| > \zeta_1 \left(\frac{\log p}{n}\right)^{1/4} \eta_{\max}^2\right) \leq e^{-c_{25} \log p} \tag{D.108}$$

for some constants $\zeta_1, c_{25} > 0$.

Proof of (i) in Lemma D.14: Recall that $\mathbf{m}_j^T \in \mathbb{R}^{1 \times s}$ denotes the j th row of $\mathbf{M} \in \mathbb{R}^{s \times s}$ for $j = 1, \dots, s$.

Based on the construction of the inverse matrix estimation \mathbf{M} as shown in (G.3) of the main paper, we have

$$\begin{aligned}\|\mathbf{m}_j\|_1 &= \frac{1}{\widehat{\tau}_{\widehat{\mathcal{S}}_1, j}^2} (1 + \|\widehat{\boldsymbol{\theta}}_j^{(\widehat{\mathcal{S}}_1)}\|_1) \\ &\leq \frac{1}{\widehat{\tau}_{\widehat{\mathcal{S}}_1, j}^2} \left(1 + \|\boldsymbol{\theta}_j^{(\widehat{\mathcal{S}}_1)}\|_1 + \|\widehat{\boldsymbol{\theta}}_j^{(\widehat{\mathcal{S}}_1)} - \boldsymbol{\theta}_j^{(\widehat{\mathcal{S}}_1)}\|_1 \right).\end{aligned}\tag{D.109}$$

Recall definitions of the events \mathcal{H}_1 and \mathcal{H}_4 ,

$$\begin{aligned}\mathcal{H}_1 &= \left\{ \sup_{\widehat{\mathcal{S}}_1: |\widehat{\mathcal{S}}_1|=s} \max_{1 \leq j \leq s} \frac{1}{\widehat{\tau}_{\widehat{\mathcal{S}}_1, j}^2} \leq \frac{1}{0.99C_L} \right\} \\ \mathcal{H}_4 &= \left\{ \sup_{\widehat{\mathcal{S}}_1: |\widehat{\mathcal{S}}_1|=s} \max_{1 \leq j \leq s} \|\widehat{\boldsymbol{\theta}}_j^{(\widehat{\mathcal{S}}_1)} - \boldsymbol{\theta}_j^{(\widehat{\mathcal{S}}_1)}\|_1 \leq 4B \left(\sup_{\widehat{\mathcal{S}}_1: |\widehat{\mathcal{S}}_1|=s} \max_{1 \leq j \leq s} \|[\boldsymbol{\Sigma}_{\widehat{\mathcal{S}}_1}^{-1}]_{-j, j}\|_1 \right) \right\}.\end{aligned}$$

Using $\|\boldsymbol{\theta}_j^{(\widehat{\mathcal{S}}_1)}\|_1 \leq B \|[\boldsymbol{\Sigma}_{\widehat{\mathcal{S}}_1}^{-1}]_{-j, j}\|_1$ that has been proved in Lemma D.18, on the event $\mathcal{H}_1 \cap \mathcal{H}_4$, then we get

$$\begin{aligned}\sup_{\widehat{\mathcal{S}}_1: |\widehat{\mathcal{S}}_1|=s} \|\mathbf{M}\|_1 &= \sup_{\widehat{\mathcal{S}}_1: |\widehat{\mathcal{S}}_1|=s} \max_{1 \leq j \leq s} \|\mathbf{m}_j\|_1 \\ &\leq \frac{10\eta_{max}}{C_L}.\end{aligned}\tag{D.110}$$

Hence, the statement of Lemma D.14-(i) follows from Lemma D.11 and Lemma D.12. \square

Proof of (ii) in Lemma D.14: Simple calculations yield

$$\begin{aligned}& \sup_{\widehat{\mathcal{S}}_1: |\widehat{\mathcal{S}}_1|=s} \max_{1 \leq j \leq s} |[M\widehat{\boldsymbol{\Sigma}}_{\widehat{\mathcal{S}}_1} M^T - \boldsymbol{\Sigma}_{\widehat{\mathcal{S}}_1}^{-1}]_{jj}| \\ &= \sup_{\widehat{\mathcal{S}}_1: |\widehat{\mathcal{S}}_1|=s} \max_{1 \leq j \leq s} |[(M\widehat{\boldsymbol{\Sigma}}_{\widehat{\mathcal{S}}_1} - \mathbf{I})M^T]_{jj} + [M^T - \boldsymbol{\Sigma}_{\widehat{\mathcal{S}}_1}^{-1}]_{jj}| \\ &\leq \sup_{\widehat{\mathcal{S}}_1: |\widehat{\mathcal{S}}_1|=s} \|(M\widehat{\boldsymbol{\Sigma}}_{\widehat{\mathcal{S}}_1} - \mathbf{I})M^T\|_\infty + \sup_{\widehat{\mathcal{S}}_1: |\widehat{\mathcal{S}}_1|=s} \max_{1 \leq j \leq s} |[M^T - \boldsymbol{\Sigma}_{\widehat{\mathcal{S}}_1}^{-1}]_{jj}| \\ &\leq \sup_{\widehat{\mathcal{S}}_1: |\widehat{\mathcal{S}}_1|=s} \|M\widehat{\boldsymbol{\Sigma}}_{\widehat{\mathcal{S}}_1} - \mathbf{I}_s\|_\infty \sup_{\widehat{\mathcal{S}}_1: |\widehat{\mathcal{S}}_1|=s} \|\mathbf{M}\|_1 + \sup_{\widehat{\mathcal{S}}_1: |\widehat{\mathcal{S}}_1|=s} \max_{1 \leq j \leq s} |[M^T - \boldsymbol{\Sigma}_{\widehat{\mathcal{S}}_1}^{-1}]_{jj}| \\ &\leq \left(\sup_{\widehat{\mathcal{S}}_1: |\widehat{\mathcal{S}}_1|=s} \max_{1 \leq j \leq s} \frac{\lambda_j}{\widehat{\tau}_{\widehat{\mathcal{S}}_1, j}^2} \right) \left(\sup_{\widehat{\mathcal{S}}_1: |\widehat{\mathcal{S}}_1|=s} \|\mathbf{M}\|_1 \right) + \sup_{\widehat{\mathcal{S}}_1: |\widehat{\mathcal{S}}_1|=s} \max_{1 \leq j \leq s} |[M^T - \boldsymbol{\Sigma}_{\widehat{\mathcal{S}}_1}^{-1}]_{jj}|\end{aligned}\tag{D.111}$$

where $\mathbf{I}_s \in \mathbb{R}^{s \times s}$ is an identity matrix and the last inequality is from (D.70).

By definition of the matrix \mathbf{M} , we have $M_{jj} = 1/\widehat{\tau}_{\widehat{\mathcal{S}}_1, j}^2$. Additionally, we have shown in (D.125) in the proof of Lemma D.18 that $\tau_{\widehat{\mathcal{S}}_1, j}^2 = 1/[\boldsymbol{\Sigma}_{\widehat{\mathcal{S}}_1}^{-1}]_{jj}$. Now the approximation error regarding diagonal elements of

\mathbf{M} and $\Sigma_{\hat{\mathcal{S}}_1}^{-1}$ in (D.111) can be bounded in the following

$$\begin{aligned}
& \sup_{\hat{\mathcal{S}}_1:|\hat{\mathcal{S}}_1|=s} \max_{1 \leq j \leq s} |[\mathbf{M}^T - \Sigma_{\hat{\mathcal{S}}_1}^{-1}]_{jj}| \\
&= \sup_{\hat{\mathcal{S}}_1:|\hat{\mathcal{S}}_1|=s} \max_{1 \leq j \leq s} \left| \frac{1}{\hat{\tau}_{\hat{\mathcal{S}}_1,j}^2} - \frac{1}{\tau_{\hat{\mathcal{S}}_1,j}^2} \right| \\
&\leq \left(\sup_{\hat{\mathcal{S}}_1:|\hat{\mathcal{S}}_1|=s} \max_{1 \leq j \leq s} |\hat{\tau}_{\hat{\mathcal{S}}_1,j}^2 - \tau_{\hat{\mathcal{S}}_1,j}^2| \right) \left(\sup_{\hat{\mathcal{S}}_1:|\hat{\mathcal{S}}_1|=s} \max_{1 \leq j \leq s} \frac{1}{\hat{\tau}_{\hat{\mathcal{S}}_1,j}^2} \right) \left(\sup_{\hat{\mathcal{S}}_1:|\hat{\mathcal{S}}_1|=s} \max_{1 \leq j \leq s} \frac{1}{\tau_{\hat{\mathcal{S}}_1,j}^2} \right) \\
&\leq \frac{1}{C_L} \left(\sup_{\hat{\mathcal{S}}_1:|\hat{\mathcal{S}}_1|=s} \max_{1 \leq j \leq s} |\hat{\tau}_{\hat{\mathcal{S}}_1,j}^2 - \tau_{\hat{\mathcal{S}}_1,j}^2| \right) \left(\sup_{\hat{\mathcal{S}}_1:|\hat{\mathcal{S}}_1|=s} \max_{1 \leq j \leq s} \frac{1}{\hat{\tau}_{\hat{\mathcal{S}}_1,j}^2} \right), \tag{D.112}
\end{aligned}$$

where the last inequality is from Assumption A2.

Combining (D.111) and (D.112), under the condition on node-wise lasso tuning parameters $\lambda_j \asymp \eta_{\max} \sqrt{(\log p)/n}$ for all $j = 1, \dots, s$ and all $\hat{\mathcal{S}}_1$ of size s , then (D.108) follows from Lemma D.12 and Lemma D.14-(i). \square

D.6 Auxiliary Results

We first introduce definitions of sub-gaussian and sub-exponential norms of a random variable $X \in \mathbb{R}$ and a random vector $\mathbf{X} \in \mathbb{R}^p$ respectively, which are also Definition 5.7, 5.22 and 5.13 in Vershynin (2012).

Definition D.15. The sub-gaussian norm of a random variable X , denoted by $\|X\|_{\psi_2}$, is defined as

$$\|X\|_{\psi_2} = \sup_{q \geq 1} q^{-1/2} (E|X|^q)^{1/q}.$$

The sub-gaussian norm of a random vector $\mathbf{X} \in \mathbb{R}^p$ is defined as

$$\|\mathbf{X}\|_{\psi_2} = \sup_{x \in \mathcal{S}^{p-1}} \|\langle \mathbf{X}, x \rangle\|_{\psi_2},$$

where $\mathcal{S}^{p-1} = \{\mathbf{u} \in \mathbb{R}^p \mid \|\mathbf{u}\|_2 = 1\}$ is the Euclidean unit sphere in \mathbb{R}^p .

Definition D.16. The sub-exponential norm of a random variable X , denoted by $\|X\|_{\psi_1}$, is defined as

$$\|X\|_{\psi_1} = \sup_{q \geq 1} q^{-1} (E|X|^q)^{1/q}.$$

The sub-gaussian norm of a random vector $\mathbf{X} \in \mathbb{R}^p$ is defined as

$$\|\mathbf{X}\|_{\psi_1} = \sup_{x \in \mathcal{S}^{p-1}} \|\langle \mathbf{X}, x \rangle\|_{\psi_1}.$$

Lemma D.17. Suppose assumption A2 holds. The normalized design matrix $\mathbb{Z}\Sigma^{-1/2}$ has independent and identical sub-gaussian rows. Let $\mathcal{I} \subset \{1, \dots, p\}$ denote an index set with cardinality s . Let $\Sigma_{\mathcal{I}} \in \mathbb{R}^{s \times s}$ denote the principal submatrix of Σ indexed by \mathcal{I} , i.e., the submatrix formed by deleting rows and columns

from \mathcal{I}^c , which is also the covariance matrix of $\mathbf{Z}_{\mathcal{I}} \in \mathbb{R}^s$, the subvector of $\mathbf{Z} \in \mathbb{R}^p$ indexed by \mathcal{I} . Then $\mathbb{Z}_{\mathcal{I}}\Sigma_{\mathcal{I}}^{-1/2}$ also has independent and identical sub-gaussian rows, where $\mathbb{Z}_{\mathcal{I}} \in \mathbb{R}^{n \times s}$ is the design matrix associated with $\mathbf{Z}_{\mathcal{I}}$. The sub-gaussian norm $\kappa_{\mathcal{I}} = \|\Sigma_{\mathcal{I}}^{-1/2}\mathbf{Z}_{\mathcal{I}}\|_{\psi_2}$ satisfies $\kappa_{\mathcal{I}} \leq \sqrt{C_R/C_L}\kappa$, where $\kappa = \|\Sigma^{-1/2}\mathbf{Z}\|_{\psi_2}$.

Proof of Lemma D.17. By definition of sub-gaussian vector, for any $\mathbf{d} \in \mathbb{R}^p$,

$$E[e^{\mathbf{d}^T \mathbf{Z}}] \leq \exp\left\{\frac{\sigma^2 \|\mathbf{d}\|^2}{2}\right\}. \quad (\text{D.113})$$

Define $\tilde{\mathbf{d}} \in \mathbb{R}^p$ such that $\tilde{\mathbf{d}} = \Sigma^{-1/2}\mathbf{y}$ where $\mathbf{y} \in \mathbb{R}^p$ is arbitrary. Then for any $\mathbf{y} \in \mathbb{R}^p$, we have

$$\begin{aligned} E[e^{\mathbf{y}^T(\Sigma^{-1/2}\mathbf{Z})}] &= E[e^{\tilde{\mathbf{d}}^T \mathbf{Z}}] \\ &\leq \exp\left\{\frac{\sigma^2 \|\tilde{\mathbf{d}}\|^2}{2}\right\} \\ &= \exp\left\{\frac{\sigma^2 \|\Sigma^{-1/2}\mathbf{y}\|^2}{2}\right\} \\ &\leq \exp\left\{\frac{\sigma^2 \lambda_{\max}(\Sigma^{-1})\|\mathbf{y}\|^2}{2}\right\} \\ &\leq \exp\left\{\frac{\sigma^2 \|\mathbf{y}\|^2}{2C_L}\right\}, \end{aligned} \quad (\text{D.114})$$

where the first inequality comes from (D.113); the second inequality is from the definition of matrix operator norm; the last inequality uses $\lambda_{\min}(\Sigma) \geq C_L$ under assumption A2. (D.114) implies that $\Sigma^{-1/2}\mathbf{Z} \sim \text{subG}_p(\sigma^2/C_L)$.

For any $\mathbf{u} \in \mathbb{R}^s$, define $\check{\mathbf{d}} \in \mathbb{R}^p$ such that $\check{\mathbf{d}}_{\mathcal{I}} = \mathbf{u}$ and $\check{\mathbf{d}}_{\mathcal{I}^c} = \mathbf{0}$. Then it follows directly from (D.113) that

$$E[e^{\mathbf{u}^T \mathbf{Z}}] = E[e^{\check{\mathbf{d}}^T \mathbf{Z}}] \leq \exp\left\{\frac{\sigma^2 \|\mathbf{u}\|^2}{2}\right\}.$$

Applying similar arguments used to show (D.114), we have $\Sigma_{\mathcal{I}}^{-1/2}\mathbf{Z}_{\mathcal{I}} \sim \text{subG}_s(\sigma^2/C_L)$.

Next, we explore the relationship between the $\kappa_{\mathcal{I}} = \|\Sigma_{\mathcal{I}}^{-1/2}\mathbf{Z}_{\mathcal{I}}\|_{\psi_2}$ and $\kappa = \|\Sigma^{-1/2}\mathbf{Z}\|_{\psi_2}$. By definition of the sub-gaussian norm (see Definition D.15), we get

$$\kappa = \sup_{\mathbf{x}_1 \in \mathcal{S}^{p-1}} \left[\sup_{q \geq 1} q^{-1/2} \{E(|\mathbf{x}_1^T \Sigma^{-1/2} \mathbf{Z}|^q)\}^{1/q} \right]. \quad (\text{D.115})$$

For any $\mathbf{x}_2 \in \mathcal{S}^{s-1}$, the sub-gaussian norm of $\mathbf{x}_2^T \boldsymbol{\Sigma}_{\mathcal{I}}^{-1/2} \mathbf{Z}_{\mathcal{I}}$ can be bounded by

$$\begin{aligned} \|\mathbf{x}_2^T \boldsymbol{\Sigma}_{\mathcal{I}}^{-1/2} \mathbf{Z}_{\mathcal{I}}\|_{\psi_2} &= \sup_{q \geq 1} q^{-1/2} \{E(|(\boldsymbol{\Sigma}_{\mathcal{I}}^{-1/2} \mathbf{x}_2)^T \mathbf{Z}_{\mathcal{I}}|^q)\}^{1/q} \\ &= \sup_{q \geq 1} q^{-1/2} \left\{ E \left(\left| \frac{(\boldsymbol{\Sigma}_{\mathcal{I}}^{-1/2} \mathbf{x}_2)^T \mathbf{Z}_{\mathcal{I}}}{\|\boldsymbol{\Sigma}_{\mathcal{I}}^{-1/2} \mathbf{x}_2\|} \right|^q \right) \right\}^{1/q} \\ &\leq C_L^{-1/2} \sup_{q \geq 1} q^{-1/2} \{E(|\tilde{\mathbf{x}}_2^T \mathbf{Z}_{\mathcal{I}}|^q)\}^{1/q}, \end{aligned} \quad (\text{D.116})$$

where $\tilde{\mathbf{x}}_2 = \boldsymbol{\Sigma}_{\mathcal{I}}^{-1/2} \mathbf{x}_2 / \|\boldsymbol{\Sigma}_{\mathcal{I}}^{-1/2} \mathbf{x}_2\|$. The inequality is from $\|\boldsymbol{\Sigma}_{\mathcal{I}}^{-1/2} \mathbf{x}_2\|^2 \leq 1/C_L$, which follows directly from the definition of matrix operator norm and assumption A2. Define $\tilde{\mathbf{x}}_1 \in \mathbb{R}^p$ such that the elements indexed by \mathcal{I} are $\tilde{\mathbf{x}}_2 \in \mathbb{R}^s$ and zero otherwise. Then the sub-gaussian norm $\kappa_{\mathcal{I}}$ satisfies

$$\begin{aligned} \kappa_{\mathcal{I}} &= \sup_{\mathbf{x}_2 \in \mathcal{S}^{s-1}} \|\mathbf{x}_2^T \boldsymbol{\Sigma}_{\mathcal{I}}^{-1/2} \mathbf{Z}_{\mathcal{I}}\|_{\psi_2} \\ &\leq C_L^{-1/2} \sup_{\mathbf{x}_2 \in \mathcal{S}^{s-1}} \left[\sup_{q \geq 1} q^{-1/2} \{E(|\tilde{\mathbf{x}}_2^T \mathbf{Z}_{\mathcal{I}}|^q)\}^{1/q} \right] \\ &= C_L^{-1/2} \sup_{\substack{\tilde{\mathbf{x}}_1 \in \mathbb{R}^p: \|\tilde{\mathbf{x}}_1\|=1 \\ [\tilde{\mathbf{x}}_1]_{\mathcal{I}} = \tilde{\mathbf{x}}_2, [\tilde{\mathbf{x}}_1]_{\mathcal{I}^c} = \mathbf{0}}} \left[\sup_{q \geq 1} q^{-1/2} \{E(|\tilde{\mathbf{x}}_1^T \mathbf{Z}|^q)\}^{1/q} \right] \\ &= C_L^{-1/2} \sup_{\substack{\tilde{\mathbf{x}}_1 \in \mathbb{R}^p: \|\tilde{\mathbf{x}}_1\|=1 \\ [\tilde{\mathbf{x}}_1]_{\mathcal{I}} = \tilde{\mathbf{x}}_2, [\tilde{\mathbf{x}}_1]_{\mathcal{I}^c} = \mathbf{0}}} \left[\sup_{q \geq 1} q^{-1/2} \left\{ E \left(\left| \frac{(\boldsymbol{\Sigma}^{1/2} \tilde{\mathbf{x}}_1)^T \boldsymbol{\Sigma}^{-1/2} \mathbf{Z}}{\|\boldsymbol{\Sigma}^{1/2} \tilde{\mathbf{x}}_1\|} \right|^q \right) \right\}^{1/q} \right] \\ &\leq \sqrt{\frac{C_R}{C_L}} \sup_{\substack{\tilde{\mathbf{x}}_1 \in \mathbb{R}^p: \|\tilde{\mathbf{x}}_1\|=1 \\ [\tilde{\mathbf{x}}_1]_{\mathcal{I}} = \tilde{\mathbf{x}}_2, [\tilde{\mathbf{x}}_1]_{\mathcal{I}^c} = \mathbf{0}}} \left[\sup_{q \geq 1} q^{-1/2} \left\{ E \left(\left| \frac{(\boldsymbol{\Sigma}^{1/2} \tilde{\mathbf{x}}_1)^T \boldsymbol{\Sigma}^{-1/2} \mathbf{Z}}{\|\boldsymbol{\Sigma}^{1/2} \tilde{\mathbf{x}}_1\|} \right|^q \right) \right\}^{1/q} \right] \end{aligned} \quad (\text{D.117})$$

where $[\tilde{\mathbf{x}}_1]_{\mathcal{I}}$ denotes the subvector of $\tilde{\mathbf{x}}_1$ indexed by \mathcal{I} and similar for $[\tilde{\mathbf{x}}_1]_{\mathcal{I}^c}$. The inequality is from (D.116) and the second equality follows from the construction of $\tilde{\mathbf{x}}_1$; the second inequality comes from $\|\boldsymbol{\Sigma}^{1/2} \tilde{\mathbf{x}}_1\|^2 \leq C_R$ using $\|\tilde{\mathbf{x}}_1\| = 1$ together with the definition of matrix operator norm and assumption A2. One can see that (D.117) takes supremum over a subset of \mathcal{S}^{s-1} , then comparing (D.117) with (D.115), we obtain

$$\kappa_{\mathcal{I}} \leq \sqrt{\frac{C_R}{C_L}} \kappa.$$

□

Lemma D.18. The population version of the nodewise regression coefficient $\boldsymbol{\theta}_j^{(\hat{\mathcal{S}}_1)}$ and the inverse covariance matrix $\boldsymbol{\Sigma}_{\hat{\mathcal{S}}_1}^{-1}$ satisfies

$$\boldsymbol{\theta}_j^{(\hat{\mathcal{S}}_1)} = -\{[\boldsymbol{\Sigma}_{\hat{\mathcal{S}}_1}]_{j,j} - [\boldsymbol{\Sigma}_{\hat{\mathcal{S}}_1}]_{j,-j} \{[\boldsymbol{\Sigma}_{\hat{\mathcal{S}}_1}]_{-j,-j}\}^{-1} [\boldsymbol{\Sigma}_{\hat{\mathcal{S}}_1}]_{-j,j}\} [\boldsymbol{\Sigma}_{\hat{\mathcal{S}}_1}^{-1}]_{-j,j}. \quad (\text{D.118})$$

Moreover, under assumption A2, we have

$$\|\boldsymbol{\theta}_j^{(\hat{\mathcal{S}}_1)}\|_1 \leq B\|\boldsymbol{\Sigma}_{\hat{\mathcal{S}}_1}^{-1}\|_{-j,j}. \quad (\text{D.119})$$

Proof of Lemma D.18. Recall that the population nodewise regression coefficient $\boldsymbol{\theta}_j^{(\hat{\mathcal{S}}_1)}$ in the model (D.69) is given by

$$\boldsymbol{\theta}_j^{(\hat{\mathcal{S}}_1)} = \{[\boldsymbol{\Sigma}_{\hat{\mathcal{S}}_1}]_{-j,-j}\}^{-1}[\boldsymbol{\Sigma}_{\hat{\mathcal{S}}_1}]_{-j,j}$$

for $j = 1, \dots, s$, where $[\boldsymbol{\Sigma}_{\hat{\mathcal{S}}_1}]_{-j,j}$ denotes the j th column of $\boldsymbol{\Sigma}_{\hat{\mathcal{S}}_1}$ with the j th component deleted, and $\{[\boldsymbol{\Sigma}_{\hat{\mathcal{S}}_1}]_{-j,-j}\}^{-1}$ is the inverse of the matrix $[\boldsymbol{\Sigma}_{\hat{\mathcal{S}}_1}]_{-j,-j}$ that is formed by rows and columns of $\boldsymbol{\Sigma}_{\hat{\mathcal{S}}_1}$ indexed by $\{1, \dots, s\} \setminus \{j\}$. Define matrix $\tilde{\boldsymbol{\Sigma}}_{\hat{\mathcal{S}}_1}$ as

$$\tilde{\boldsymbol{\Sigma}}_{\hat{\mathcal{S}}_1} = \begin{pmatrix} [\boldsymbol{\Sigma}_{\hat{\mathcal{S}}_1}]_{jj} & [\boldsymbol{\Sigma}_{\hat{\mathcal{S}}_1}]_{j,-j} \\ [\boldsymbol{\Sigma}_{\hat{\mathcal{S}}_1}]_{-j,j} & [\boldsymbol{\Sigma}_{\hat{\mathcal{S}}_1}]_{-j,-j} \end{pmatrix}$$

Applying the Schur complement to calculate the inverse of $\tilde{\boldsymbol{\Sigma}}_{\hat{\mathcal{S}}_1}$, we can show that the first row of $\tilde{\boldsymbol{\Sigma}}_{\hat{\mathcal{S}}_1}^{-1}$ satisfies

$$\begin{cases} [\tilde{\boldsymbol{\Sigma}}_{\hat{\mathcal{S}}_1}^{-1}]_{11} = \{[\boldsymbol{\Sigma}_{\hat{\mathcal{S}}_1}]_{jj} - [\boldsymbol{\Sigma}_{\hat{\mathcal{S}}_1}]_{j,-j}\{[\boldsymbol{\Sigma}_{\hat{\mathcal{S}}_1}]_{-j,-j}\}^{-1}[\boldsymbol{\Sigma}_{\hat{\mathcal{S}}_1}]_{-j,j}\}^{-1}, \\ [\tilde{\boldsymbol{\Sigma}}_{\hat{\mathcal{S}}_1}^{-1}]_{1,-1} = -[\tilde{\boldsymbol{\Sigma}}_{\hat{\mathcal{S}}_1}^{-1}]_{11}\{\boldsymbol{\theta}_j^{(\hat{\mathcal{S}}_1)}\}^T. \end{cases} \quad (\text{D.120})$$

It follows directly from (D.120) that $\{\boldsymbol{\theta}_j^{(\hat{\mathcal{S}}_1)}\}^T$ differs from $[\tilde{\boldsymbol{\Sigma}}_{\hat{\mathcal{S}}_1}^{-1}]_{1,-1}$ up to a scale. Observe that $\tilde{\boldsymbol{\Sigma}}_{\hat{\mathcal{S}}_1}$ can be written as

$$\tilde{\boldsymbol{\Sigma}}_{\hat{\mathcal{S}}_1} = \boldsymbol{P}_r \boldsymbol{\Sigma}_{\hat{\mathcal{S}}_1} \boldsymbol{P}_c, \quad (\text{D.121})$$

where $\boldsymbol{P}_r, \boldsymbol{P}_c \in \mathbb{R}^{s \times s}$ are permutation matrices, which permute the rows and the columns respectively. More specifically,

$$\boldsymbol{P}_r = \begin{pmatrix} e_j^T \\ e_1^T \\ \vdots \\ e_{j-1}^T \\ e_{j+1}^T \\ \vdots \\ e_s^T \end{pmatrix} \text{ and } \boldsymbol{P}_c = (e_j \ e_1 \ \cdots \ e_{j-1} \ e_{j+1} \ \cdots \ e_s), \quad (\text{D.122})$$

where $e_j \in \mathbb{R}^s$ is a unit vector with the j th component equal to one and zero otherwise. Then by symmetry of $\boldsymbol{\Sigma}_{\hat{\mathcal{S}}_1}^{-1}$ and (D.121), we get

$$\tilde{\boldsymbol{\Sigma}}_{\hat{\mathcal{S}}_1}^{-1} = \boldsymbol{P}_c^{-1}(\boldsymbol{P}_r \boldsymbol{\Sigma}_{\hat{\mathcal{S}}_1}^{-1})^T. \quad (\text{D.123})$$

Left multiplying \boldsymbol{P}_c on both sides of (D.123) yields

$$\tilde{\boldsymbol{\Sigma}}_{\hat{\mathcal{S}}_1}^{-1} \boldsymbol{P}_c^T = \boldsymbol{P}_r \boldsymbol{\Sigma}_{\hat{\mathcal{S}}_1}^{-1}, \quad (\text{D.124})$$

which further implies that $e_1^T(\tilde{\Sigma}_{\hat{\mathcal{S}}_1}^{-1} \mathbf{P}_c^T) = e_j^T \Sigma_{\hat{\mathcal{S}}_1}^{-1}$. Combining with (D.120), we have

$$\begin{cases} [\Sigma_{\hat{\mathcal{S}}_1}^{-1}]_{jj} = \{[\Sigma_{\hat{\mathcal{S}}_1}]_{jj} - [\Sigma_{\hat{\mathcal{S}}_1}]_{j,-j} \{[\Sigma_{\hat{\mathcal{S}}_1}]_{-j,-j}\}^{-1} [\Sigma_{\hat{\mathcal{S}}_1}]_{-j,j}\}^{-1}, \\ [\Sigma_{\hat{\mathcal{S}}_1}^{-1}]_{j,-j} = -[\tilde{\Sigma}_{\hat{\mathcal{S}}_1}^{-1}]_{11} \{\boldsymbol{\theta}_j^{(\hat{\mathcal{S}}_1)}\}^T, \end{cases} \quad (\text{D.125})$$

and then (D.118) follows directly. Moreover,

$$\begin{aligned} \|\boldsymbol{\theta}_j^{(\hat{\mathcal{S}}_1)}\|_1 &= |[\Sigma_{\hat{\mathcal{S}}_1}]_{jj} - [\Sigma_{\hat{\mathcal{S}}_1}]_{j,-j} \{[\Sigma_{\hat{\mathcal{S}}_1}]_{-j,-j}\}^{-1} [\Sigma_{\hat{\mathcal{S}}_1}]_{-j,j}| \|[\Sigma_{\hat{\mathcal{S}}_1}^{-1}]_{-j,j}\|_1 \\ &\leq [\Sigma_{\hat{\mathcal{S}}_1}]_{jj} \|[\Sigma_{\hat{\mathcal{S}}_1}^{-1}]_{-j,j}\|_1 \\ &\leq B \|[\Sigma_{\hat{\mathcal{S}}_1}^{-1}]_{-j,j}\|_1, \end{aligned} \quad (\text{D.126})$$

where the first inequality uses the fact that $\{[\Sigma_{\hat{\mathcal{S}}_1}]_{-j,-j}\}^{-1}$ is positive definite by assumption A2 and hence, the quadratic term within the absolute value is positive, and moreover $[\Sigma_{\hat{\mathcal{S}}_1}^{-1}]_{jj} > 0$ since diagonal elements of any positive definite matrix is strictly positive; the second inequality is from $\max_{1 \leq j \leq p} \Sigma_{jj} \leq B$. This completes the proof. \square

Lemma D.19. Let X_1, \dots, X_n be independent centered subexponential random variables and $K = \max_{1 \leq i \leq n} \|X_i\|_{\psi_1}$. Then for every $\mathbf{a} \in \mathbb{R}^n$ and every $t > 0$, we have

$$P\left(\left|\sum_{i=1}^n a_i X_i\right| \geq t\right) \leq 2 \exp\left\{-c \min\left(\frac{t^2}{K^2 \|\mathbf{a}\|^2}, \frac{t}{K \|\mathbf{a}\|_\infty}\right)\right\},$$

where c is a positive constant.

E Standard error of bias estimate in Algorithm S1 and Algorithm 1

We derive the standard error of bias estimate used for our mode-finding algorithm in the context of sample splitting, and similar arguments can be applied to Algorithm 2 implemented on full data. The OLS estimates $\hat{\boldsymbol{\gamma}}_{\check{\mathcal{S}}_3}^{(2)}$ and $\hat{\boldsymbol{\Gamma}}_{\check{\mathcal{S}}_3}^{(2)} \in \mathbb{R}^q$ take the following form

$$\begin{aligned} \sqrt{n_2}(\hat{\boldsymbol{\gamma}}_{\check{\mathcal{S}}_3}^{(2)} - \boldsymbol{\gamma}_{\check{\mathcal{S}}_3}) &= [\hat{\Sigma}_{\check{\mathcal{S}}_3}^{(2)}]^{-1} \frac{1}{\sqrt{n_2}} \{\mathbb{Z}_{\check{\mathcal{S}}_3}^{(2)}\}^T (\mathbf{U}^{(2)} \boldsymbol{\alpha}_D^* + \boldsymbol{\epsilon}_D^{(2)}) \\ \sqrt{n_2}(\hat{\boldsymbol{\Gamma}}_{\check{\mathcal{S}}_3}^{(2)} - \boldsymbol{\Gamma}_{\check{\mathcal{S}}_3}) &= [\hat{\Sigma}_{\check{\mathcal{S}}_3}^{(2)}]^{-1} \frac{1}{\sqrt{n_2}} \{\mathbb{Z}_{\check{\mathcal{S}}_3}^{(2)}\}^T \{\mathbf{U}^{(2)} (\boldsymbol{\alpha}_Y^* + \beta^* \boldsymbol{\alpha}_D^*) + (\beta^* \boldsymbol{\epsilon}_D^{(2)} + \boldsymbol{\epsilon}_Y^{(2)})\}, \end{aligned} \quad (\text{E.1})$$

where $\mathbf{U}^{(2)}, \boldsymbol{\epsilon}_D^{(2)}, \boldsymbol{\epsilon}_Y^{(2)}$ are collections of $\mathbf{U}, \epsilon_D, \epsilon_Y$ on the second subsample H_2 . To proceed, let Θ_{11} be shorthand of the variance of $(\boldsymbol{\alpha}_Y^* + \beta^* \boldsymbol{\alpha}_D^*)^T \mathbf{U} + (\beta^* \epsilon_D + \epsilon_Y)$ and Θ_{22} denotes the variance of $\boldsymbol{\alpha}_D^{*T} \mathbf{U} + \epsilon_D$, and the covariance between these two is Θ_{12} . The population covariance matrix of candidate instruments associated with $\check{\mathcal{S}}_3$ is denoted by $\Sigma_{\check{\mathcal{S}}_3}$.

Since H_2 is independent of $\check{\mathcal{S}}_3$ and we have assumed that $\check{\mathcal{S}}_3$ includes all relevant instruments (see Section A.1 for more discussion on this assumption), which implies that the models (2.1) and (2.2) still hold

with \mathbf{Z} replaced by $\mathbf{Z}_{\tilde{\mathcal{S}}_3}$. The following consistency can be established by the weak law of large numbers

$$\hat{\gamma}_{\tilde{\mathcal{S}}_3}^{(2)} \xrightarrow{p} \gamma_{\tilde{\mathcal{S}}_3}^*, \quad \hat{\Gamma}_{\tilde{\mathcal{S}}_3}^{(2)} \xrightarrow{p} \Gamma_{\tilde{\mathcal{S}}_3}^*. \quad (\text{E.2})$$

Under assumptions A1 and A2, we can also obtain the asymptotic distribution below

$$\sqrt{n_2} \left(\begin{pmatrix} \hat{\gamma}_{\tilde{\mathcal{S}}_3}^{(2)} \\ \hat{\Gamma}_{\tilde{\mathcal{S}}_3}^{(2)} \end{pmatrix} - \begin{pmatrix} \gamma_{\tilde{\mathcal{S}}_3}^* \\ \Gamma_{\tilde{\mathcal{S}}_3}^* \end{pmatrix} \right) \xrightarrow{d} N \left(\mathbf{0}, \begin{pmatrix} \Theta_{22} \Sigma_{\tilde{\mathcal{S}}_3}^{-1} & \Theta_{12} \Sigma_{\tilde{\mathcal{S}}_3}^{-1} \\ \Theta_{12} \Sigma_{\tilde{\mathcal{S}}_3}^{-1} & \Theta_{11} \Sigma_{\tilde{\mathcal{S}}_3}^{-1} \end{pmatrix} \right). \quad (\text{E.3})$$

Recall that the bias estimate $\hat{b}^{(2,j,l)} = \hat{\beta}^{(2,l)} - \hat{\beta}^{(2,j)}$ for $j, l \in \tilde{\mathcal{S}}_3$, where $\hat{\beta}^{(2,l)} = \hat{\Gamma}_{\tilde{\mathcal{S}}_3}^{(2)} / \hat{\gamma}_{\tilde{\mathcal{S}}_3}^{(2)}$ and “(2)” in the superscript emphasizes that the estimate is obtained from the subsample H_2 . The estimate $\hat{\beta}^{(2,j)}$ is defined in similar fashion. It follows from (E.3) that

$$\sqrt{n_2} \left(\begin{pmatrix} \hat{\gamma}_{\tilde{\mathcal{S}}_3,j}^{(2)} \\ \hat{\gamma}_{\tilde{\mathcal{S}}_3,l}^{(2)} \\ \hat{\Gamma}_{\tilde{\mathcal{S}}_3,j}^{(2)} \\ \hat{\Gamma}_{\tilde{\mathcal{S}}_3,l}^{(2)} \end{pmatrix} - \begin{pmatrix} \gamma_{\tilde{\mathcal{S}}_3,j}^* \\ \gamma_{\tilde{\mathcal{S}}_3,l}^* \\ \Gamma_{\tilde{\mathcal{S}}_3,j}^* \\ \Gamma_{\tilde{\mathcal{S}}_3,l}^* \end{pmatrix} \right) \xrightarrow{d} N \left(\mathbf{0}, \begin{pmatrix} \Theta_{22} [\Sigma_{\tilde{\mathcal{S}}_3}^{-1}]_{jj} & \Theta_{22} [\Sigma_{\tilde{\mathcal{S}}_3}^{-1}]_{jl} & \Theta_{12} [\Sigma_{\tilde{\mathcal{S}}_3}^{-1}]_{jj} & \Theta_{12} [\Sigma_{\tilde{\mathcal{S}}_3}^{-1}]_{jl} \\ \Theta_{22} [\Sigma_{\tilde{\mathcal{S}}_3}^{-1}]_{jl} & \Theta_{22} [\Sigma_{\tilde{\mathcal{S}}_3}^{-1}]_{ll} & \Theta_{12} [\Sigma_{\tilde{\mathcal{S}}_3}^{-1}]_{jl} & \Theta_{12} [\Sigma_{\tilde{\mathcal{S}}_3}^{-1}]_{ll} \\ \Theta_{12} [\Sigma_{\tilde{\mathcal{S}}_3}^{-1}]_{jj} & \Theta_{12} [\Sigma_{\tilde{\mathcal{S}}_3}^{-1}]_{jl} & \Theta_{11} [\Sigma_{\tilde{\mathcal{S}}_3}^{-1}]_{jj} & \Theta_{11} [\Sigma_{\tilde{\mathcal{S}}_3}^{-1}]_{jl} \\ \Theta_{12} [\Sigma_{\tilde{\mathcal{S}}_3}^{-1}]_{jl} & \Theta_{12} [\Sigma_{\tilde{\mathcal{S}}_3}^{-1}]_{ll} & \Theta_{11} [\Sigma_{\tilde{\mathcal{S}}_3}^{-1}]_{jl} & \Theta_{11} [\Sigma_{\tilde{\mathcal{S}}_3}^{-1}]_{ll} \end{pmatrix} \right).$$

By delta method, we get

$$\sqrt{n_2} \left(\begin{pmatrix} \hat{\beta}^{(2,j)} \\ \hat{\beta}^{(2,l)} \end{pmatrix} - \begin{pmatrix} \frac{\Gamma_{\tilde{\mathcal{S}}_3,j}^*}{\gamma_{\tilde{\mathcal{S}}_3,j}^*} \\ \frac{\Gamma_{\tilde{\mathcal{S}}_3,l}^*}{\gamma_{\tilde{\mathcal{S}}_3,l}^*} \end{pmatrix} \right) \xrightarrow{d} N \left(\mathbf{0}, \begin{pmatrix} v_{jj} & v_{jl} \\ v_{jl} & v_{ll} \end{pmatrix} \right),$$

where

$$\begin{aligned} v_{jj} &= \frac{[\Sigma_{\tilde{\mathcal{S}}_3}^{-1}]_{jj}}{\gamma_{\tilde{\mathcal{S}}_3,j}^{*2}} \left\{ \Theta_{11} - \frac{2\Gamma_{\tilde{\mathcal{S}}_3,j}^*}{\gamma_{\tilde{\mathcal{S}}_3,j}^*} \Theta_{12} + \left(\frac{\Gamma_{\tilde{\mathcal{S}}_3,j}^*}{\gamma_{\tilde{\mathcal{S}}_3,j}^*} \right)^2 \Theta_{22} \right\} \\ v_{ll} &= \frac{[\Sigma_{\tilde{\mathcal{S}}_3}^{-1}]_{ll}}{\gamma_{\tilde{\mathcal{S}}_3,l}^{*2}} \left\{ \Theta_{11} - \frac{2\Gamma_{\tilde{\mathcal{S}}_3,l}^*}{\gamma_{\tilde{\mathcal{S}}_3,l}^*} \Theta_{12} + \left(\frac{\Gamma_{\tilde{\mathcal{S}}_3,l}^*}{\gamma_{\tilde{\mathcal{S}}_3,l}^*} \right)^2 \Theta_{22} \right\} \\ v_{jl} &= \frac{[\Sigma_{\tilde{\mathcal{S}}_3}^{-1}]_{jl}}{(\gamma_{\tilde{\mathcal{S}}_3,j}^*)(\gamma_{\tilde{\mathcal{S}}_3,l}^*)} \left\{ \Theta_{11} - \left(\frac{\Gamma_{\tilde{\mathcal{S}}_3,j}^*}{\gamma_{\tilde{\mathcal{S}}_3,j}^*} + \frac{\Gamma_{\tilde{\mathcal{S}}_3,l}^*}{\gamma_{\tilde{\mathcal{S}}_3,l}^*} \right) \Theta_{12} + \left(\frac{\Gamma_{\tilde{\mathcal{S}}_3,j}^*}{\gamma_{\tilde{\mathcal{S}}_3,j}^*} \right) \left(\frac{\Gamma_{\tilde{\mathcal{S}}_3,l}^*}{\gamma_{\tilde{\mathcal{S}}_3,l}^*} \right) \Theta_{22} \right\}. \end{aligned}$$

Applying the delta method again yields

$$\sqrt{n_2} \left\{ \hat{b}^{(2,j,l)} - \left(\frac{\Gamma_{\tilde{\mathcal{S}}_3,l}^*}{\gamma_{\tilde{\mathcal{S}}_3,l}^*} - \frac{\Gamma_{\tilde{\mathcal{S}}_3,j}^*}{\gamma_{\tilde{\mathcal{S}}_3,j}^*} \right) \right\} \xrightarrow{d} N(0, v_{jj} - 2v_{jl} + v_{ll}). \quad (\text{E.4})$$

Then the variance of $\sqrt{n_2}\{\hat{b}^{(2,j,l)}\}$ can be estimated by $\hat{v}_{jj} - 2\hat{v}_{jl} + \hat{v}_{ll}$, where

$$\hat{v}_{jj} = \frac{\{[\hat{\Sigma}_{\tilde{\mathcal{S}}_3}^{(2)}]^{-1}\}_{jj}}{\{\hat{\gamma}_{\tilde{\mathcal{S}}_3,j}^{(2)}\}^2} \left\{ \hat{\Theta}_{11} - \frac{2\hat{\Gamma}_{\tilde{\mathcal{S}}_3,j}^{(2)}}{\hat{\gamma}_{\tilde{\mathcal{S}}_3,j}^{(2)}} \hat{\Theta}_{12} + \left(\frac{\hat{\Gamma}_{\tilde{\mathcal{S}}_3,j}^{(2)}}{\hat{\gamma}_{\tilde{\mathcal{S}}_3,j}^{(2)}} \right)^2 \hat{\Theta}_{22} \right\} \quad (\text{E.5})$$

$$\hat{v}_{ll} = \frac{\{[\hat{\Sigma}_{\tilde{\mathcal{S}}_3}^{(2)}]^{-1}\}_{ll}}{\{\hat{\gamma}_{\tilde{\mathcal{S}}_3,l}^{(2)}\}^2} \left\{ \hat{\Theta}_{11} - \frac{2\hat{\Gamma}_{\tilde{\mathcal{S}}_3,l}^{(2)}}{\hat{\gamma}_{\tilde{\mathcal{S}}_3,l}^{(2)}} \hat{\Theta}_{12} + \left(\frac{\hat{\Gamma}_{\tilde{\mathcal{S}}_3,l}^{(2)}}{\hat{\gamma}_{\tilde{\mathcal{S}}_3,l}^{(2)}} \right)^2 \hat{\Theta}_{22} \right\} \quad (\text{E.6})$$

$$\hat{v}_{jl} = \frac{\{[\hat{\Sigma}_{\tilde{\mathcal{S}}_3}^{(2)}]^{-1}\}_{jl}}{\{\hat{\gamma}_{\tilde{\mathcal{S}}_3,j}^{(2)}\}\{\hat{\gamma}_{\tilde{\mathcal{S}}_3,l}^{(2)}\}} \left\{ \hat{\Theta}_{11} - \left(\frac{\hat{\Gamma}_{\tilde{\mathcal{S}}_3,j}^{(2)}}{\hat{\gamma}_{\tilde{\mathcal{S}}_3,j}^{(2)}} + \frac{\hat{\Gamma}_{\tilde{\mathcal{S}}_3,l}^{(2)}}{\hat{\gamma}_{\tilde{\mathcal{S}}_3,l}^{(2)}} \right) \hat{\Theta}_{12} + \left(\frac{\hat{\Gamma}_{\tilde{\mathcal{S}}_3,j}^{(2)}}{\hat{\gamma}_{\tilde{\mathcal{S}}_3,j}^{(2)}} \right) \left(\frac{\hat{\Gamma}_{\tilde{\mathcal{S}}_3,l}^{(2)}}{\hat{\gamma}_{\tilde{\mathcal{S}}_3,l}^{(2)}} \right) \hat{\Theta}_{22} \right\} \quad (\text{E.7})$$

and $\hat{\Theta}_{11}, \hat{\Theta}_{12}, \hat{\Theta}_{22}$ are given in (A.5). And $\text{SE}(\hat{b}^{(2,j,l)})$ is $\sqrt{(\hat{v}_{jj} - 2\hat{v}_{jl} + \hat{v}_{ll})/n_2}$.

For Algorithm 2 implemented on the full data, $\text{SE}(\hat{b}^{(j,l)})$ can be constructed similarly, by replacing $[\hat{\Sigma}_{\tilde{\mathcal{S}}_3}^{(2)}]^{-1}$ with \mathbf{M} estimated by (G.3) using all n observations in the main paper, replacing n_2 with n , and substituting $\hat{\gamma}_{\tilde{\mathcal{S}}_3}^{(2)}, \hat{\Gamma}_{\tilde{\mathcal{S}}_3}^{(2)}$ with the debiased lasso estimators $\hat{\gamma}_{\tilde{\mathcal{S}}_1}$ and $\hat{\Gamma}_{\tilde{\mathcal{S}}_1}$ respectively. And $\hat{\Theta}_{11}, \hat{\Theta}_{12}, \hat{\Theta}_{22}$ take the following form

$$\hat{\Theta}_{11} = \frac{1}{n} \left\| \mathbf{Y} - \tilde{\mathbf{Z}}_{\tilde{\mathcal{S}}_1} \tilde{\mathbf{\Gamma}}_{\tilde{\mathcal{S}}_1} \right\|_2^2, \quad \hat{\Theta}_{22} = \frac{1}{n} \left\| \mathbf{D} - \tilde{\mathbf{Z}}_{\tilde{\mathcal{S}}_1} \tilde{\boldsymbol{\gamma}}_{\tilde{\mathcal{S}}_1} \right\|_2^2, \quad \hat{\Theta}_{12} = \frac{1}{n} (\mathbf{Y} - \tilde{\mathbf{Z}}_{\tilde{\mathcal{S}}_1} \tilde{\mathbf{\Gamma}}_{\tilde{\mathcal{S}}_1})^\top (\mathbf{D} - \tilde{\mathbf{Z}}_{\tilde{\mathcal{S}}_1} \tilde{\boldsymbol{\gamma}}_{\tilde{\mathcal{S}}_1}).$$

F Additional Simulations

To further examine the performance and show the robustness of the proposed procedure, we consider additional settings in numerical experiments. Under the same setting as the simulation in the main paper, we evaluate the proposed procedure and other competing methods when there are larger number of candidate instruments to begin with in Section F.1. We then consider the setting where some irrelevant variables are allowed to be correlated with valid instruments in Section F.2 as well as the setting that some irrelevant variables are correlated with each other in Section F.3. A typical example of such scenarios would be the linkage disequilibrium in genetic studies. Simulation study under multivariate unmeasured confounders is presented in Section F.4. Additionally, finite sample performances of the proposed method in comparison with several other approaches in the presence of weak instruments are collected in Section F.5. In Section F.6, we carry out numerical studies, in which the ‘‘independence’’ IV assumption is violated, that is, invalid instrument can be correlated with the unobserved confounding U . Furthermore, we compare our proposed method with other competing methods in the econometric literature that deal with weak instruments in Section F.7.

F.1 Higher dimension of candidate instruments – simulation 1

In this simulation study, we consider the same data generating setting as the numerical experiment in the main paper and only change the dimension of candidate instruments p from 50,000 to 100,000. Our comparison includes the proposed method using full data– Proposed (full), proposed sample splitting method– Proposed (split), the naive Algorithm 1–Naive, and the oracle method (Oracle) by assuming that we know the valid instruments a priori. We evaluate the performance in terms of bias, efficiency and validity of in-

ference, and summarize the simulation results in Tables 3 and 4. The histogram of causal effect estimates under $\sigma_D^2 = 0$ is displayed in Figure 7.

Table 3: Performance summary for various methods and σ_D^2 under simulation 1 across 1000 Monte Carlo runs with $n = 500$ and $p = 100,000$. We make the numbers bold for the method with the best performance except the oracle estimate. Standard errors are presented in the bracket if applicable. For $SE < 0.005$, we report as $SE = 0.00$

| | Method | Bias $\times 10$ (SE $\times 10$) | RMSE $\times 10$ | Coverage (Nominal = 95%) |
|------------------|------------------|------------------------------------|------------------|--------------------------|
| $\sigma_D^2 = 0$ | Proposed (full) | -0.09(0.02) | 0.55 | 0.94 |
| | Proposed (split) | -0.30(0.07) | 2.28 | 0.89 |
| | Naive | -2.07(0.01) | 2.12 | 0.01 |
| | Oracle | -0.02(0.01) | 0.28 | 0.94 |
| $\sigma_D^2 = 2$ | Proposed (full) | -0.06(0.01) | 0.38 | 0.95 |
| | Proposed (split) | -0.35(0.08) | 2.53 | 0.86 |
| | Naive | -1.78(0.02) | 1.87 | 0.04 |
| | Oracle | -0.02(0.01) | 0.27 | 0.94 |
| $\sigma_D^2 = 4$ | Proposed (full) | -0.13(0.03) | 0.95 | 0.92 |
| | Proposed (split) | -0.23(0.09) | 2.98 | 0.81 |
| | Naive | -1.17(0.02) | 1.32 | 0.17 |
| | Oracle | -0.02(0.01) | 0.27 | 0.94 |

The simulation results suggest that the Proposed (full) outperforms competing methods in terms of bias, efficiency and validity of inference. For the sample splitting–Proposed (split), the bias and RMSE are much larger compared to the ones obtained by the proposed method using full data, especially when σ_D^2 is small. And estimates by “Naive” are biased. When the variance of the random error in the exposure ϵ_D increases, the performance of “Proposed (full)” remains similar, which indicates that our approach using full data works even when the variance of unobserved confounding is relatively small compared to that of the random error ϵ_D . For the sample splitting method, one can see the RMSE increases and the coverage probability decreases further below the nominal level when ϵ_D increases.

The results in Table 4 show that “Naive” misidentifies spurious instruments as valid and miss many or almost all the valid instruments. The sample splitting procedure can find most valid instruments when the variance σ_D^2 is small. However, the estimated set of valid instruments will include some invalid ones since we only use part of the data and the estimates have larger variation than those obtained using the full sample. Consequently, the resulting causal effect estimate has moderate bias and the empirical coverage deviates from the nominal level. In comparison, “Proposed (full)” can locate spurious instruments with the help of pseudo variables and correctly identify most valid instruments even if σ_D^2 is large.

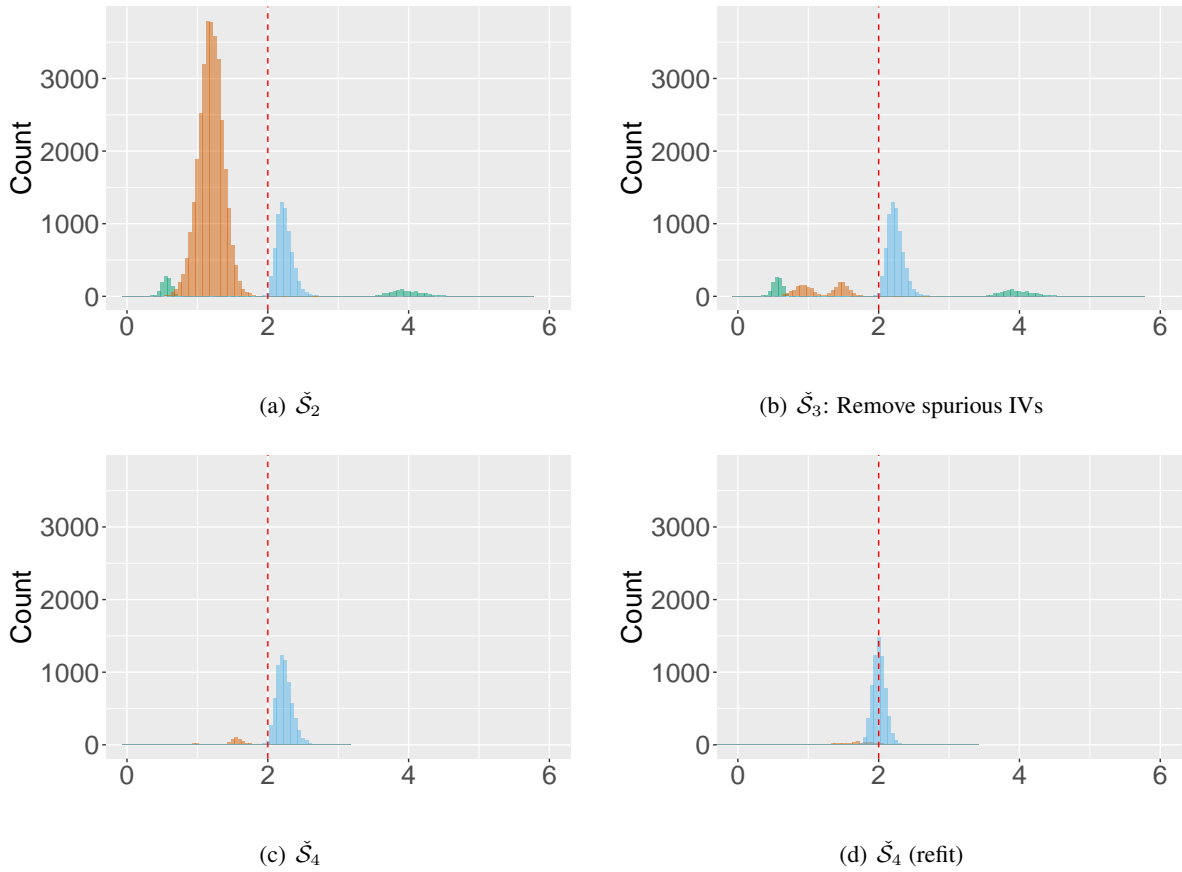


Figure 7: Plots (a)-(c) correspond to the simulation 1 for higher dimension in Section F.1. Plots (a)-(c) are histograms of causal effect estimates from valid, invalid and spurious instruments in $\tilde{\mathcal{S}}_2$, $\tilde{\mathcal{S}}_3$ and $\tilde{\mathcal{S}}_4$ respectively obtained from Algorithm 2–Proposed (full) across 1000 Monte Carlo runs. The blue pile represents causal estimates from valid IVs; the green pile refers to invalid IVs; the orange pile is causal estimates from irrelevant variables, including both irrelevant variables from the initial candidate set and pseudo ones. The red dashed line is the true causal effect $\beta^* = 2$. The results are based on $(n, p, \sigma_D^2) = (500, 50, 000, 0)$. Plot (d) gives the distribution of effect estimates from refitted model.

Table 4: Average number of invalid, valid IVs and irrelevant variables in $\check{\mathcal{S}}_2$, $\check{\mathcal{S}}_3$ and $\check{\mathcal{S}}_4$ under simulation 1 respectively across 1000 Monte Carlo runs. Note that “Naive” is applied without including pseudo variables. The results are based on $n = 500$ and $p = 100,000$. “–” stands for “inapplicable”

| | | $\check{\mathcal{S}}_2$ | | | $\check{\mathcal{S}}_3$ | | | $\check{\mathcal{S}}_4$ | | |
|------------------|------------------|-------------------------|-------|------------|-------------------------|-------|------------|-------------------------|-------|------------|
| Method | | Invalid | Valid | Irrelevant | Invalid | Valid | Irrelevant | Invalid | Valid | Irrelevant |
| $\sigma_D^2 = 0$ | Proposed (full) | 2.00 | 7.00 | 32.41 | 1.99 | 6.99 | 1.97 | 0.00 | 6.67 | 0.52 |
| | Proposed (split) | 1.89 | 7.00 | 51.38 | 1.80 | 6.65 | 2.16 | 0.21 | 6.64 | 0.11 |
| | Naive | 2.00 | 7.00 | 15.66 | – | – | – | 0.00 | 0.03 | 15.65 |
| $\sigma_D^2 = 2$ | Proposed (full) | 2.00 | 7.00 | 37.76 | 1.97 | 6.98 | 2.07 | 0.00 | 6.85 | 1.07 |
| | Proposed (split) | 1.88 | 7.00 | 56.76 | 1.78 | 6.36 | 2.07 | 0.28 | 6.33 | 0.12 |
| | Naive | 2.00 | 7.00 | 18.44 | – | – | – | 0.00 | 0.48 | 18.44 |
| $\sigma_D^2 = 4$ | Proposed (full) | 2.00 | 7.00 | 42.17 | 1.98 | 6.68 | 2.08 | 0.04 | 6.57 | 1.21 |
| | Proposed (split) | 1.87 | 7.00 | 62.37 | 1.78 | 5.33 | 2.13 | 0.36 | 5.25 | 0.17 |
| | Naive | 2.00 | 7.00 | 21.37 | – | – | – | 0.00 | 2.41 | 21.36 |

F.2 Some irrelevant variables are correlated with valid instruments – simulation 2

To further evaluate the performance of our method, we consider the scenario where noise variables can be correlated with valid instruments. In the simulations, we set $p = 50,000$ and there are 9 relevant instruments generated from independent standard normal, two of which are invalid that have direct effect on the outcome. For each $j = 3, \dots, 7$, we generate 10 irrelevant variables which follow $N(0, 1)$ and are correlated with valid instrument Z_j . In our numerical experiments, we consider weak and moderate correlations, which are 0.2 and 0.6 respectively. All the other irrelevant variables, the unobserved confounding U and random error ϵ_Y are independently generated from $N(0, 1)$. Random error ϵ_D follows $N(0, \sigma_D^2)$ with $\sigma_D^2 = 0, 2, 4$. We set the true causal effect $\beta^* = 2$. Coefficient parameters of the true models are given by

$$\begin{aligned}\gamma^* &= (3, 3, 3, 3, 3, 3, 3, 3, 3, 0, \dots, 0)^T \\ \pi^* &= (3.5, 3.5, 0, 0, \dots, 0)^T \\ \alpha_D^* &= 4; \alpha_Y^* = -3.\end{aligned}$$

Our comparison includes the proposed method using full data—Proposed (full), sample splitting—Proposed (split), the naive Algorithm 1—Naive, and the oracle method (Oracle) by assuming that we know the valid instruments a priori. We evaluate the performance in terms of bias, efficiency and validity of inference, and summarize the simulation results in Tables 5 and 6. Histograms of causal effect estimates for weak and moderate correlation are displayed in Figure 8 and Figure 9 respectively.

In the presence of irrelevant variables correlated with valid instruments, “Proposed (full)” is comparable with the oracle estimate. However, “Proposed (split)” and “Naive” perform badly. Comparing the number of valid, invalid and spurious instruments in the estimated set of valid instruments $\check{\mathcal{S}}_4$ as shown in Table 6, one can see that “Proposed (full)” can correctly identify most valid instruments. The sample splitting fails to identify invalid IVs due to the fact that only part of the data is used and the associated estimates have larger variances. For “Naive”, it misses most valid IVs and misuses many spurious instruments as valid ones.

Table 5: Performance summary for various methods and σ_D^2 under simulation 2 across 1000 Monte Carlo runs with $n = 500$ and $p = 50,000$. We make the numbers bold for the method with the best performance except the oracle estimate. Standard errors are presented in the bracket if applicable. For $SE < 0.005$, we report as $SE = 0.00$

| | Method | Bias $\times 10$ (SE $\times 10$) | RMSE $\times 10$ | Coverage (Nominal = 95%) |
|-----------------------------|------------------|------------------------------------|------------------|--------------------------|
| Weak Correlation | | | | |
| $\sigma_D^2 = 0$ | Proposed (full) | 0.01(0.01) | 0.39 | 0.95 |
| | Proposed (split) | 0.52(0.06) | 2.10 | 0.84 |
| | Naive | -7.61(0.01) | 7.62 | 0.00 |
| | Oracle | 0.02(0.01) | 0.33 | 0.96 |
| $\sigma_D^2 = 2$ | Proposed (full) | 0.04(0.01) | 0.46 | 0.95 |
| | Proposed (split) | 1.49(0.10) | 3.53 | 0.69 |
| | Naive | -6.77(0.03) | 6.83 | 0.00 |
| | Oracle | 0.01(0.01) | 0.33 | 0.95 |
| $\sigma_D^2 = 4$ | Proposed (full) | 0.33(0.06) | 1.80 | 0.92 |
| | Proposed (split) | 3.49(0.14) | 5.60 | 0.43 |
| | Naive | -4.86(0.07) | 5.33 | 0.02 |
| | Oracle | 0.01(0.01) | 0.33 | 0.95 |
| Moderate Correlation | | | | |
| $\sigma_D^2 = 0$ | Proposed (full) | 0.02(0.01) | 0.43 | 0.95 |
| | Proposed (split) | 0.53(0.06) | 1.91 | 0.82 |
| | Naive | -7.56(0.01) | 7.57 | 0.00 |
| | Oracle | 0.02(0.01) | 0.33 | 0.96 |
| $\sigma_D^2 = 2$ | Proposed (full) | 0.04(0.02) | 0.52 | 0.95 |
| | Proposed (split) | 1.27(0.09) | 3.09 | 0.68 |
| | Naive | -6.49(0.04) | 6.62 | 0.00 |
| | Oracle | 0.01(0.01) | 0.33 | 0.95 |
| $\sigma_D^2 = 4$ | Proposed (full) | 0.25(0.05) | 1.47 | 0.93 |
| | Proposed (split) | 3.15(0.13) | 5.15 | 0.45 |
| | Naive | -3.88(0.07) | 4.48 | 0.05 |
| | Oracle | 0.01(0.01) | 0.33 | 0.95 |

Table 6: Average number of invalid, valid IVs and irrelevant variables in \check{S}_2 , \check{S}_3 and \check{S}_4 under simulation 2 respectively across 1000 Monte Carlo runs. Note that “Naive” is applied without including pseudo variables. The results are based on $n = 500$ and $p = 50,000$. “–” stands for “inapplicable”

| | | \check{S}_2 | | | \check{S}_3 | | | \check{S}_4 | | |
|-----------------------------|------------------|---------------|-------|------------|---------------|-------|------------|---------------|-------|------------|
| | Method | Invalid | Valid | Irrelevant | Invalid | Valid | Irrelevant | Invalid | Valid | Irrelevant |
| Weak Correlation | | | | | | | | | | |
| $\sigma_D^2 = 0$ | Proposed (full) | 2.00 | 7.00 | 39.55 | 2.00 | 7.00 | 2.04 | 0.00 | 6.75 | 0.57 |
| | Proposed (split) | 2.00 | 6.96 | 77.75 | 1.99 | 6.69 | 2.07 | 0.22 | 6.67 | 0.04 |
| | Naive | 2.00 | 7.00 | 31.49 | – | – | – | 0.00 | 0.00 | 31.48 |
| $\sigma_D^2 = 2$ | Proposed (full) | 2.00 | 7.00 | 45.25 | 2.00 | 6.96 | 2.01 | 0.00 | 6.89 | 1.01 |
| | Proposed (split) | 2.00 | 6.95 | 83.21 | 1.99 | 5.79 | 1.88 | 0.46 | 5.66 | 0.03 |
| | Naive | 2.00 | 7.00 | 36.09 | – | – | – | 0.00 | 0.04 | 36.06 |
| $\sigma_D^2 = 4$ | Proposed (full) | 2.00 | 7.00 | 50.49 | 2.00 | 6.61 | 2.07 | 0.06 | 6.55 | 1.17 |
| | Proposed (split) | 2.00 | 6.95 | 89.15 | 1.99 | 4.03 | 2.02 | 0.84 | 3.72 | 0.12 |
| | Naive | 2.00 | 7.00 | 40.09 | – | – | – | 0.00 | 0.74 | 40.06 |
| Moderate Correlation | | | | | | | | | | |
| $\sigma_D^2 = 0$ | Proposed (full) | 2.00 | 7.00 | 37.39 | 2.00 | 7.00 | 2.17 | 0.00 | 6.61 | 0.71 |
| | Proposed (split) | 2.00 | 6.96 | 76.13 | 1.99 | 6.72 | 2.28 | 0.25 | 6.70 | 0.03 |
| | Naive | 2.00 | 7.00 | 31.06 | – | – | – | 0.00 | 0.00 | 31.04 |
| $\sigma_D^2 = 2$ | Proposed (full) | 2.00 | 7.00 | 42.15 | 2.00 | 6.96 | 2.08 | 0.00 | 6.89 | 1.08 |
| | Proposed (split) | 1.99 | 6.95 | 82.50 | 1.99 | 5.88 | 2.13 | 0.48 | 5.72 | 0.04 |
| | Naive | 2.00 | 7.00 | 35.26 | – | – | – | 0.00 | 0.13 | 35.24 |
| $\sigma_D^2 = 4$ | Proposed (full) | 2.00 | 7.00 | 47.33 | 2.00 | 6.57 | 2.25 | 0.04 | 6.42 | 1.26 |
| | Proposed (split) | 1.99 | 6.94 | 88.12 | 1.99 | 4.18 | 2.18 | 0.83 | 3.76 | 0.09 |
| | Naive | 2.00 | 7.00 | 38.96 | – | – | – | 0.00 | 1.52 | 38.93 |

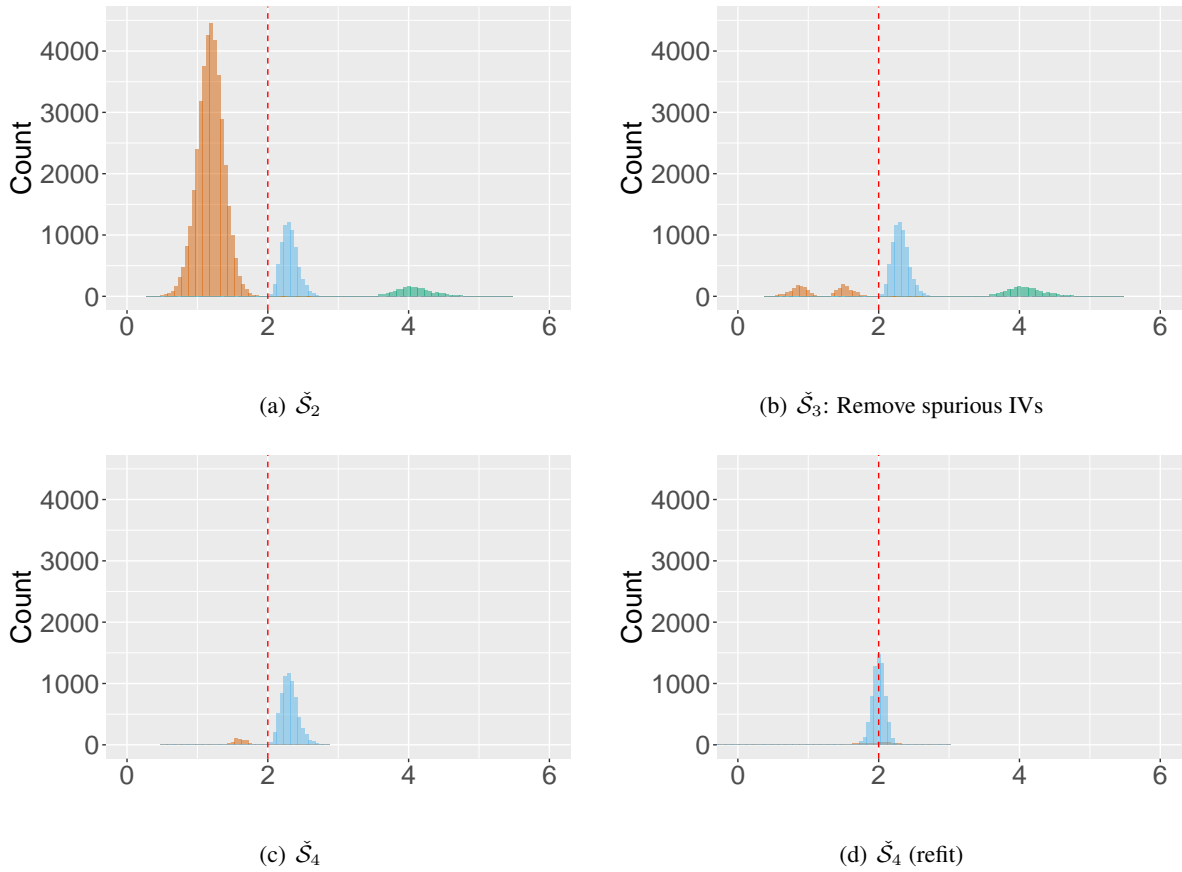


Figure 8: Plots (a)-(c) correspond to the simulation 2 for weak correlation in Section F.2. Plots (a)-(c) are histograms of causal effect estimates from valid, invalid and spurious instruments in $\tilde{\mathcal{S}}_2$, $\tilde{\mathcal{S}}_3$ and $\tilde{\mathcal{S}}_4$ respectively obtained from Algorithm 2–Proposed (full) across 1000 Monte Carlo runs. The blue pile represents causal estimates from valid IVs; the green pile refers to invalid IVs; the orange pile is causal estimates from irrelevant variables, including both irrelevant variables from the initial candidate set and pseudo ones. The red dashed line is the true causal effect $\beta^* = 2$. The results are based on $(n, p, \sigma_D^2) = (500, 50, 000, 0)$. Plot (d) gives the distribution of effect estimates from refitted model.

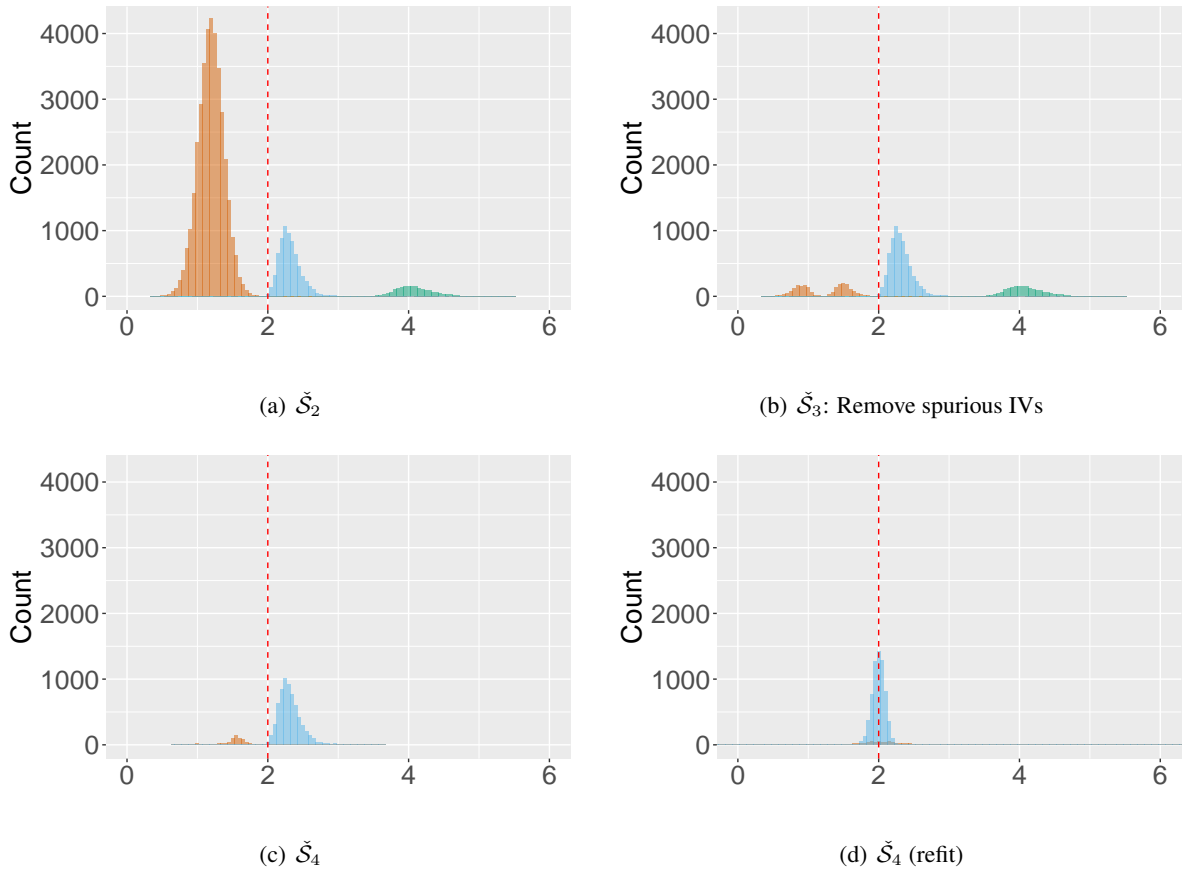


Figure 9: Plots (a)-(c) correspond to the simulation 2 for moderate correlation in Section F.2. Plots (a)-(c) are histograms of causal effect estimates from valid, invalid and spurious instruments in \tilde{S}_2 , \tilde{S}_3 and \tilde{S}_4 respectively obtained from Algorithm 2–Proposed (full) across 1000 Monte Carlo runs. The blue pile represents causal estimates from valid IVs; the green pile refers to invalid IVs; the orange pile is causal estimates from irrelevant variables, including both irrelevant variables from the initial candidate set and pseudo ones. The red dashed line is the true causal effect $\beta^* = 2$. The results are based on $(n, p, \sigma_D^2) = (500, 50, 000, 0)$. Plot (d) gives the distribution of effect estimates from refitted model.

F.3 Correlated irrelevant variables – simulation 3

In practice, irrelevant variables might also be correlated with each other. For example, in genetic data, neighbouring SNPs may have large correlation, formally called haplotypes. If a SNP has nonnegligible sample correlation with the risk factor due to pure chance and is estimated to be relevant, then the SNPs that are highly correlated with this one have more chance to enter the model. To assess how the proposed method performs under this setting, we mimic the aforementioned data structure by generating correlated irrelevant variables having different correlation magnitude: low, medium and high. Specifically, we generate $p = 50,000$ candidate instruments from $N(0, 1)$, where Z_1, Z_2 have direct effects on the outcome, Z_3, \dots, Z_9 are valid instruments and Z_j 's are noise variables for $j \geq 10$. We group irrelevant variables into 200 blocks. In the first block, irrelevant variables Z_{10}, \dots, Z_{250} are independent. While for the remaining 199 blocks, each block consists of 250 irrelevant variables, where the first half are weakly correlated with correlation 0.2 and the second half have moderate correlation equal to 0.5. Same as before, the unmeasured confounder U and random error ϵ_Y follow $N(0, 1)$. The random error ϵ_D is generated from $N(0, \sigma_D^2)$ with $\sigma_D^2 = 0, 2, 4$. We set the true causal estimate $\beta^* = 2$. The other parameters in the risk factor and the outcome models (2.1) and (2.2) are given by

$$\begin{aligned}\gamma^* &= (3, 3, 3, 3, 3, 3, 3, 3, 0, \dots, 0)^T \\ \pi^* &= (3.5, 3.5, 0, 0, \dots, 0)^T \\ \alpha_D^* &= 4; \alpha_Y^* = -3.\end{aligned}$$

Our comparison includes the proposed method using full data–Proposed (full), sample splitting–Proposed (split), the naive Algorithm 1–Naive, and the oracle method (Oracle) by assuming that we know the valid instruments a priori. We evaluate the performance in terms of bias, efficiency and validity of inference, and summarize the simulation results in Table 7. We present in 8 the average number of valid, invalid and spurious instruments passing joint thresholding, after spurious IVs removal, and also in the estimated set of valid instruments, respectively. See Figure 10 for the histogram of causal effect estimates under $\sigma_D^2 = 0$.

The “Proposed (full)” still performs well under the setting that some irrelevant variables are correlated. The sample splitting only uses part of the samples and some invalid instruments are estimated as valid due to the loss of efficiency and its performance is getting worse as σ_D^2 increases. Consequently, the resulting causal effect estimate has moderate bias and the empirical coverage deviates from the nominal level. The “Naive” gives biased causal estimate as it has misidentified valid as invalid and misused many spurious instruments as valid ones. As a result, the empirical coverage of “Naive” is far from the nominal level and average bias of causal estimate is large in comparison with other methods.

F.4 Numerical experiment under multivariate unmeasured confounding – simulation 4

In this section, we consider multivariate unmeasured confounders $U \in \mathbb{R}^2$. The direct effects of U on the exposure and the outcome are set to

$$\alpha_D^* = (2, 2)^T; \alpha_Y^* = (-2, -2)^T.$$

Table 7: Performance summary for various methods and σ_D^2 under simulation 3 across 1000 Monte Carlo runs with $n = 500$ and $p = 50,000$. We make the numbers bold for the method with the best performance except the oracle estimate. Standard errors are presented in the bracket if applicable. For $SE < 0.005$, we report as $SE = 0.00$

| | Method | Bias $\times 10$ (SE $\times 10$) | RMSE $\times 10$ | Coverage (Nominal = 95%) |
|------------------|------------------|------------------------------------|------------------|--------------------------|
| $\sigma_D^2 = 0$ | Proposed (full) | 0.00(0.01) | 0.39 | 0.95 |
| | Proposed (split) | 0.40(0.06) | 2.01 | 0.86 |
| | Naive | -7.55(0.01) | 7.56 | 0.00 |
| | Oracle | 0.02(0.01) | 0.33 | 0.96 |
| $\sigma_D^2 = 2$ | Proposed (full) | 0.04(0.02) | 0.60 | 0.95 |
| | Proposed (split) | 1.19(0.09) | 3.17 | 0.71 |
| | Naive | -6.64(0.03) | 6.71 | 0.00 |
| | Oracle | 0.01(0.01) | 0.33 | 0.95 |
| $\sigma_D^2 = 4$ | Proposed (full) | 0.27(0.05) | 1.66 | 0.93 |
| | Proposed (split) | 1.98(0.10) | 3.59 | 0.52 |
| | Naive | -4.39(0.08) | 5.06 | 0.06 |
| | Oracle | 0.01(0.01) | 0.33 | 0.95 |

Table 8: Average number of invalid, valid IVs and irrelevant variables in \check{S}_2 , \check{S}_3 and \check{S}_4 under simulation 3 respectively across 1000 Monte Carlo runs. Note that “Naive” is applied without including pseudo variables. The results are based on $n = 500$ and $p = 50,000$. “-” stands for “inapplicable”

| | Method | \check{S}_2 | | | \check{S}_3 | | | \check{S}_4 | | |
|------------------|------------------|---------------|-------|------------|---------------|-------|------------|---------------|-------|------------|
| | | Invalid | Valid | Irrelevant | Invalid | Valid | Irrelevant | Invalid | Valid | Irrelevant |
| $\sigma_D^2 = 0$ | Proposed (full) | 2.00 | 7.00 | 33.81 | 2.00 | 7.00 | 2.00 | 0.00 | 6.73 | 0.49 |
| | Proposed (split) | 1.99 | 6.97 | 70.16 | 1.98 | 6.72 | 1.90 | 0.19 | 6.71 | 0.05 |
| | Naive | 2.00 | 7.00 | 26.17 | - | - | - | 0.00 | 0.00 | 26.17 |
| $\sigma_D^2 = 2$ | Proposed (full) | 2.00 | 7.00 | 38.43 | 2.00 | 6.97 | 1.98 | 0.00 | 6.92 | 1.00 |
| | Proposed (split) | 1.99 | 6.96 | 76.54 | 1.99 | 6.02 | 2.25 | 0.42 | 5.92 | 0.04 |
| | Naive | 2.00 | 7.00 | 29.64 | - | - | - | 0.00 | 0.04 | 29.63 |
| $\sigma_D^2 = 4$ | Proposed (full) | 2.00 | 7.00 | 42.72 | 2.00 | 6.69 | 1.94 | 0.05 | 6.60 | 1.01 |
| | Proposed (split) | 1.99 | 6.96 | 81.84 | 1.98 | 4.32 | 2.19 | 0.82 | 4.05 | 0.11 |
| | Naive | 2.00 | 7.00 | 33.05 | - | - | - | 0.00 | 1.00 | 33.03 |

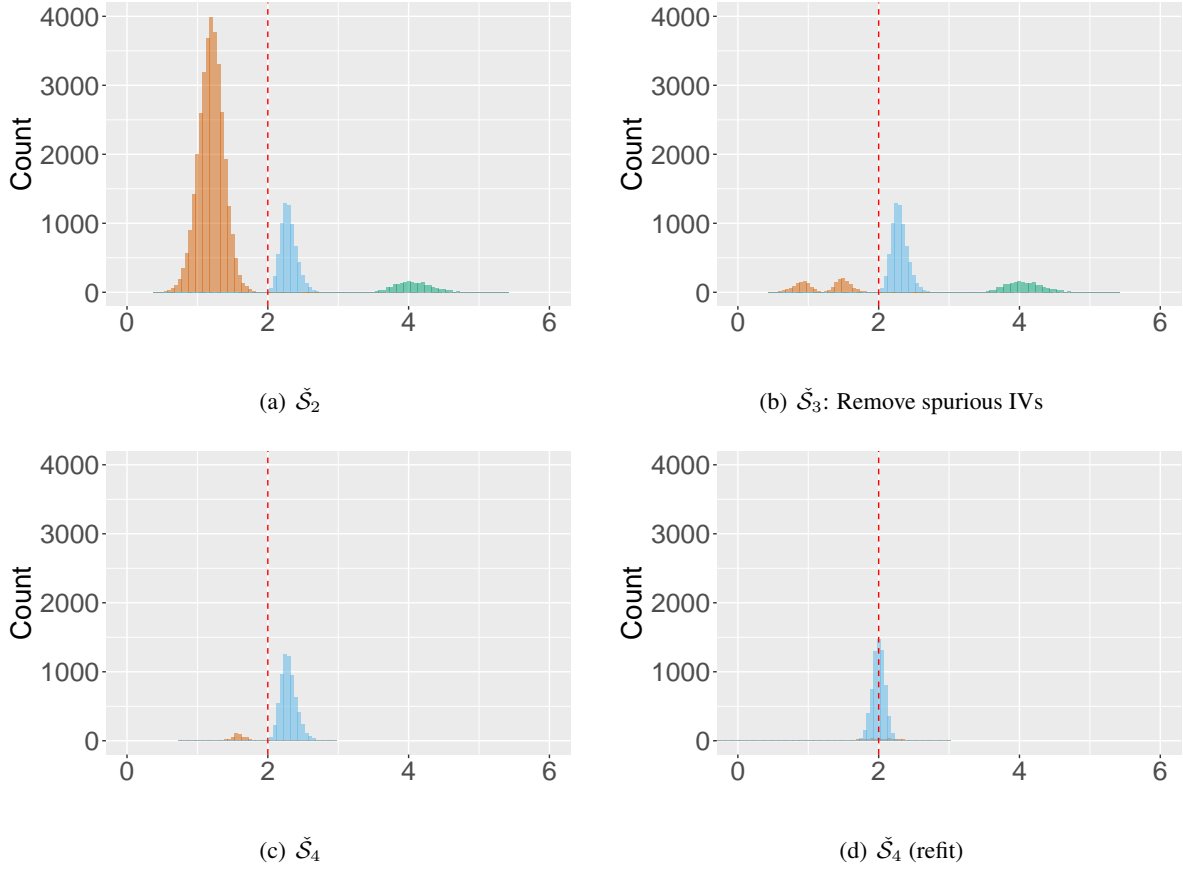


Figure 10: Plots (a)-(d) correspond to the simulation 3 where some irrelevant variables are correlated in Section F.3. Plots (a)-(c) are histograms of causal effect estimates from valid, invalid and spurious instruments in $\tilde{\mathcal{S}}_2$, $\tilde{\mathcal{S}}_3$ and $\tilde{\mathcal{S}}_4$ respectively obtained from Algorithm 2–Proposed (full) across 1000 Monte Carlo runs. The blue pile represents causal estimates from valid IVs; the green pile refers to invalid IVs; the orange pile is causal estimates from irrelevant variables, including both irrelevant variables from the initial candidate set and pseudo ones. The red dashed line is the true causal effect $\beta^* = 2$. The results are based on $(n, p, \sigma_D^2) = (500, 50, 000, 0)$. The last figure (d) gives the distribution of causal estimates from refitted model.

All the other settings remain the same as the simulation study in the main paper. Our comparison includes the proposed method using full data—Proposed (full), sample splitting—Proposed (split), the naive Algorithm 1—Naive, and the oracle method (Oracle) by assuming that we know the valid instruments a priori. We evaluate the performance in terms of bias, efficiency and validity of inference, and summarize the simulation results in Tables 9 and 10. The histogram of causal effect estimates under $\sigma_D^2 = 0$ is displayed in Figure 11.

Table 9: Performance summary for various methods and σ_D^2 under simulation 4 across 1000 Monte Carlo runs with $n = 500$ and $p = 50,000$. We make the numbers bold for the method with the best performance except the oracle estimate. Standard errors are presented in the bracket if applicable. For $SE < 0.005$, we report as $SE = 0.00$

| | Method | Bias $\times 10$ (SE $\times 10$) | RMSE $\times 10$ | Coverage (Nominal = 95%) |
|------------------|------------------|------------------------------------|------------------|--------------------------|
| $\sigma_D^2 = 0$ | Proposed (full) | -0.13(0.02) | 0.80 | 0.91 |
| | Proposed (split) | 0.07(0.07) | 2.09 | 0.79 |
| | Naive | -1.61(0.06) | 2.41 | 0.50 |
| | Oracle | -0.02(0.01) | 0.27 | 0.94 |
| $\sigma_D^2 = 2$ | Proposed (full) | -0.08(0.02) | 0.54 | 0.93 |
| | Proposed (split) | 0.08(0.06) | 1.88 | 0.81 |
| | Naive | -1.23(0.05) | 1.97 | 0.50 |
| | Oracle | -0.02(0.01) | 0.26 | 0.94 |
| $\sigma_D^2 = 4$ | Proposed (full) | -0.13(0.04) | 1.22 | 0.90 |
| | Proposed (split) | 0.35(0.11) | 3.45 | 0.78 |
| | Naive | -0.53(0.02) | 0.86 | 0.59 |
| | Oracle | -0.02(0.01) | 0.26 | 0.95 |

The simulation results in Table 9 suggest that “Proposed (full)” performs well in terms of bias, efficiency and validity of inference under multivariate unmeasured confounders. For the sample splitting—Proposed (split), although the bias is close to “Proposed (full)” when $\sigma_D^2 = 0, 2$, but the RMSE is much larger and the empirical coverage deviates from the nominal level compared to the ones obtained by the proposed method using full data. When the variance of the random error in the exposure ϵ_D increases, the performance of “Proposed (full)” remains similar, which indicates that our approach using full data works even when the variance of unobserved confounding is relatively small compared to that of the random error ϵ_D . For the sample splitting method, one can see the RMSE increases and the coverage probability decreases further below the nominal level when ϵ_D increases. The causal estimate by “Naive” is biased and the empirical coverage is far from the nominal level.

The results in Table 10 show that “Naive” misidentifies spurious instruments and some invalid instruments as valid ones, and also misses some valid instruments. The sample splitting procedure can find most valid instruments when the variance σ_D^2 is small. However, the estimated set of valid instruments will include some invalid ones since we only use part of the data and the estimates have larger variation than those obtained using the full sample. In comparison, “Proposed (full)” can locate spurious instruments with the help of pseudo variables and correctly identify most valid instruments even if σ_D^2 is large.

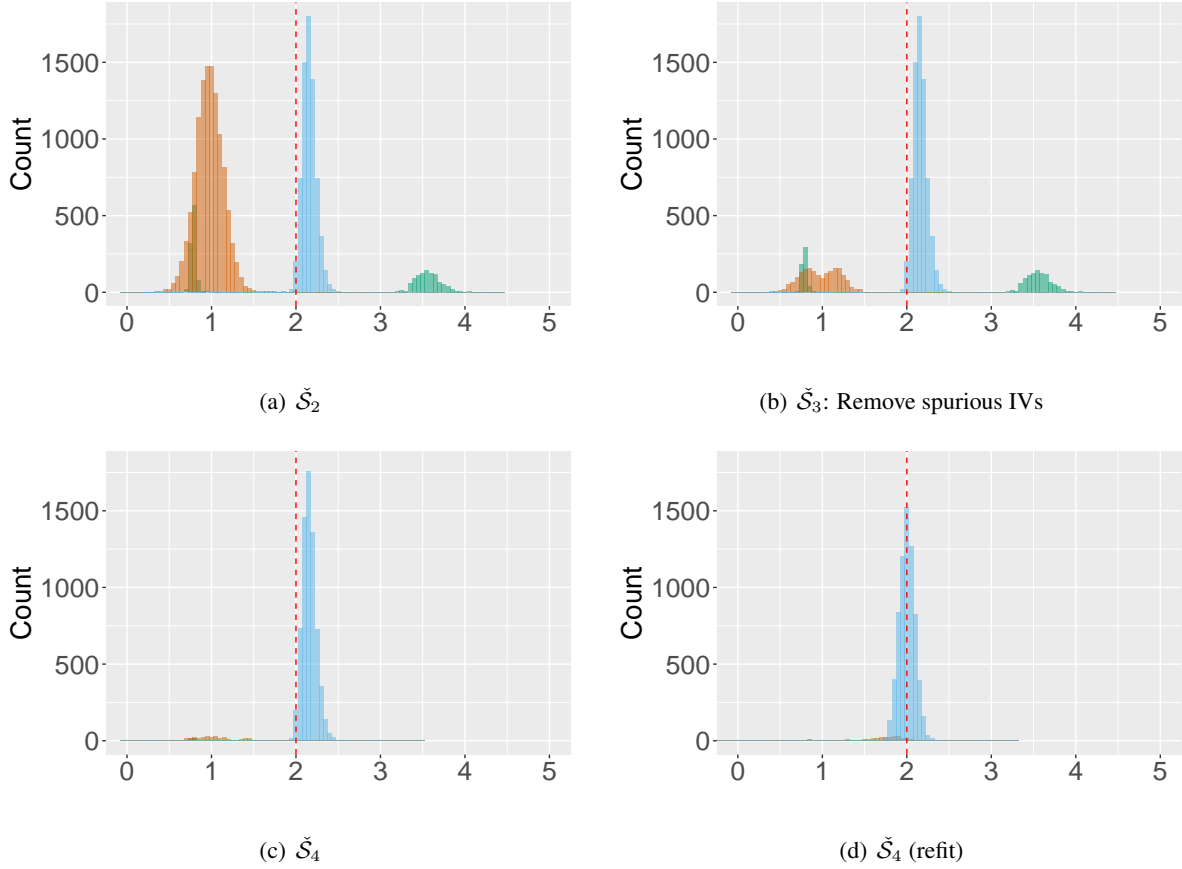


Figure 11: Plots (a)-(d) correspond to the simulation 4 where some irrelevant variables are correlated in Section F.4. Plots (a)-(c) are histograms of causal effect estimates from valid, invalid and spurious instruments in $\tilde{\mathcal{S}}_2$, $\tilde{\mathcal{S}}_3$ and $\tilde{\mathcal{S}}_4$ respectively obtained from Algorithm 2–Proposed (full) across 1000 Monte Carlo runs. The blue pile represents causal estimates from valid IVs; the green pile refers to invalid IVs; the orange pile is causal estimates from irrelevant variables, including both irrelevant variables from the initial candidate set and pseudo ones. The red dashed line is the true causal effect $\beta^* = 2$. The results are based on $(n, p, \sigma_D^2) = (500, 50, 000, 0)$. The last figure (d) gives the distribution of causal estimates from refitted model.

Table 10: Average number of invalid, valid IVs and irrelevant variables in \check{S}_2 , \check{S}_3 and \check{S}_4 under simulation 4 respectively across 1000 Monte Carlo runs. Note that “Naive” is applied without including pseudo variables. The results are based on $n = 500$ and $p = 50,000$. “–” stands for “inapplicable”

| | Method | \check{S}_2 | | | \check{S}_3 | | | \check{S}_4 | | |
|------------------|------------------|---------------|-------|------------|---------------|-------|------------|---------------|-------|------------|
| | | Invalid | Valid | Irrelevant | Invalid | Valid | Irrelevant | Invalid | Valid | Irrelevant |
| $\sigma_D^2 = 0$ | Proposed (full) | 2.00 | 7.00 | 11.95 | 1.53 | 6.99 | 1.89 | 0.03 | 6.83 | 0.31 |
| | Proposed (split) | 1.94 | 7.00 | 23.85 | 1.26 | 6.80 | 2.02 | 0.45 | 6.80 | 0.04 |
| | Naive | 2.00 | 7.00 | 4.92 | – | – | – | 0.12 | 2.85 | 4.84 |
| $\sigma_D^2 = 2$ | Proposed (full) | 2.00 | 7.00 | 16.28 | 1.73 | 6.99 | 1.88 | 0.02 | 6.89 | 0.90 |
| | Proposed (split) | 1.94 | 7.00 | 30.75 | 1.38 | 6.67 | 2.02 | 0.43 | 6.67 | 0.04 |
| | Naive | 2.00 | 7.00 | 7.29 | – | – | – | 0.34 | 4.24 | 7.25 |
| $\sigma_D^2 = 4$ | Proposed (full) | 2.00 | 7.00 | 20.82 | 1.85 | 6.61 | 2.06 | 0.06 | 6.52 | 1.26 |
| | Proposed (split) | 1.94 | 7.00 | 37.03 | 1.55 | 5.47 | 2.03 | 0.41 | 5.44 | 0.09 |
| | Naive | 2.00 | 7.00 | 9.78 | – | – | – | 0.29 | 6.32 | 9.76 |

F.5 Weak instruments – simulation 5

In this simulation, we consider a more general setting in which there are 7 strong valid instruments, 50 weak valid instruments and 2 invalid IVs. Candidate instruments Z_j , the unobserved confounding U and random error ϵ_Y are generated from independent standard normal distributions for $1 \leq j \leq p$. The random error ϵ_D follows $N(0, \sigma_D^2)$ with $\sigma_D^2 = 0, 2, 4$.

For the weak IVs Z_{10}, \dots, Z_{59} , true parameter values of the relevance strength to the exposure in absolute value are randomly generated from uniform distribution on the interval $[0.01, 0.3]$. The other parameters are given by

$$\begin{aligned}\gamma_{1:9}^* &= (3, 3, 3, 3, 3, 3, 3, 3, 3)^T \\ \pi_{1:2}^* &= (3.5, 3.5, 0, 0, \dots, 0)^T \\ \psi^* &= \phi^* = \mathbf{0} \\ \alpha_D^* &= 4; \alpha_Y^* = -3.\end{aligned}$$

Here $\gamma_{1:9}^*$ denotes the first nine elements in γ^* and analogously $\pi_{1:2}^*$ represents the first two components in π^* . The dimension of candidate instruments $p = 50,000$. Our comparison includes the proposed method using full data–Proposed (full), sample splitting–Proposed (split), the naive Algorithm 1–Naive, and the oracle method by assuming that we know the valid instruments a priori. Simulation results are presented in Tables 11 and 12. In the tables, we use “Oracle (All IVs)” and “Oracle (Strong IVs)” to distinct the oracle estimate calculated using all valid instruments (strong and weak) and the oracle estimate obtained using strong valid instruments only. Additionally, histograms of causal effect estimates under $\sigma_D^2 = 0$ are presented in Figure 12.

Performance of “Proposed (full)” is similar to the oracle estimate that only uses strong valid instruments when $\sigma_D^2 = 0, 2$. But the performance becomes undesirable as σ_D^2 further increases, this is possibly due to the fact that effect estimates have larger variances and more invalid IVs are estimated as valid ones and some valid IVs are misidentified as spurious ones as shown in Table 12. The sample splitting only uses part of the

Table 11: Performance summary for various methods and σ_D^2 under simulation 5 across 1000 Monte Carlo runs with $n = 500$ and $p = 50,000$. We make the numbers bold for the method with the best performance except the oracle estimate. Standard errors are presented in the bracket if applicable. For $SE < 0.005$, we report as $SE = 0.00$

| | Method | Bias $\times 10$ (SE $\times 10$) | RMSE $\times 10$ | Coverage (Nominal = 95%) |
|------------------|--------------------|------------------------------------|------------------|--------------------------|
| $\sigma_D^2 = 0$ | Proposed (full) | 0.02(0.01) | 0.38 | 0.94 |
| | Proposed (split) | 0.74(0.07) | 2.34 | 0.76 |
| | Naive | -7.11(0.03) | 7.19 | 0.00 |
| | Oracle(All IVs) | 0.14(0.01) | 0.35 | 0.91 |
| | Oracle(Strong IVs) | 0.01(0.01) | 0.33 | 0.95 |
| $\sigma_D^2 = 2$ | Proposed (full) | 0.11(0.03) | 0.90 | 0.94 |
| | Proposed (split) | 2.43(0.13) | 4.75 | 0.55 |
| | Naive | -4.90(0.09) | 5.65 | 0.07 |
| | Oracle(All IVs) | 0.14(0.01) | 0.34 | 0.93 |
| | Oracle(Strong IVs) | 0.01(0.01) | 0.33 | 0.95 |
| $\sigma_D^2 = 4$ | Proposed (full) | 0.71(0.08) | 2.70 | 0.88 |
| | Proposed (split) | 4.69(0.15) | 6.63 | 0.33 |
| | Naive | -2.08(0.08) | 3.31 | 0.17 |
| | Oracle(All IVs) | 0.14(0.01) | 0.34 | 0.93 |
| | Oracle(Strong IVs) | 0.01(0.01) | 0.33 | 0.96 |

samples and some invalid instruments are estimated as valid due to the loss of efficiency and its performance is getting worse as σ_D^2 increases. The “Naive” fails as it misidentifies many spurious instruments as valid instruments. The performance of “Naive” starts to improve a bit for large σ_D^2 since some valid instruments are correctly identified. This is because causal estimates have larger variation when σ_D^2 further increases and some valid instruments may have similar effect estimates to those for spurious instruments. Hence part of valid instruments are not distinguishable from the spurious ones. The difference between “Oracle(All IVs)” and “Oracle(Strong IVs)” is attributable to the bias introduced by weak instruments, which is consistent with existing literature (Nelson & Startz, 1990a; Stock & Yogo, 2005; Burgess et al., 2015).

Table 12: Average number of invalid, valid IVs and irrelevant variables in \check{S}_2 , \check{S}_3 and \check{S}_4 under simulation 5 respectively across 1000 Monte Carlo runs. Note that “Naive” is applied without including pseudo variables. The results are based on $n = 500$ and $p = 50,000$. “–” stands for “inapplicable”

| | | \check{S}_2 | | | \check{S}_3 | | | \check{S}_4 | | |
|------------------|------------------|---------------|-------|------------|---------------|-------|------------|---------------|-------|------------|
| Method | | Invalid | Valid | Irrelevant | Invalid | Valid | Irrelevant | Invalid | Valid | Irrelevant |
| $\sigma_D^2 = 0$ | Proposed (full) | 2.00 | 7.09 | 42.68 | 2.00 | 7.03 | 2.02 | 0.00 | 6.88 | 0.95 |
| | Proposed (split) | 1.99 | 7.06 | 81.10 | 1.99 | 6.45 | 2.25 | 0.34 | 6.38 | 0.03 |
| | Naive | 2.00 | 7.09 | 21.05 | – | – | – | 0.00 | 0.14 | 21.05 |
| $\sigma_D^2 = 2$ | Proposed (full) | 2.00 | 7.08 | 48.32 | 2.00 | 6.85 | 2.02 | 0.02 | 6.81 | 1.08 |
| | Proposed (split) | 1.99 | 7.03 | 87.24 | 1.98 | 4.88 | 2.21 | 0.69 | 4.63 | 0.11 |
| | Naive | 2.00 | 7.08 | 24.08 | – | – | – | 0.00 | 0.94 | 24.08 |
| $\sigma_D^2 = 4$ | Proposed (full) | 2.00 | 7.07 | 53.30 | 2.00 | 6.13 | 1.99 | 0.13 | 6.03 | 1.15 |
| | Proposed (split) | 1.99 | 7.03 | 93.18 | 1.98 | 3.17 | 2.19 | 1.03 | 2.78 | 0.22 |
| | Naive | 2.00 | 7.08 | 27.68 | – | – | – | 0.00 | 3.00 | 27.68 |

E.6 Violation of independence assumption (I3) – simulation 6

In this simulation, to examine the robustness our method, in addition to the violation of no direct effect assumption (I2), we also consider the violation of independence assumption (I3), that is, instrument can be correlated with the unobserved confounding U . Suppose we have 9 relevant instruments, among which one has direct effect on the outcome, one is correlated with U and the others are valid. Instrument Z_2 and U are bivariate normal with correlation 0.7 and variance 1. The other candidates instruments and ϵ_Y are independent standard normal. Random error ϵ_D follows $N(0, \sigma_D^2)$ with $\sigma_D^2 = 0, 2, 4$ and the true causal effect β^* is set to 2. The dimension of candidate instruments $p = 50,000$. The true parameters are given as follows.

$$\begin{aligned}\gamma^* &= (3, 3, 3, 3, 3, 3, 3, 3, 3, 0, \dots, 0)^T \\ \pi^* &= (3.5, 0, 0, 0, \dots, 0)^T \\ \alpha_D^* &= 4; \alpha_Y^* = -3.\end{aligned}$$

Our comparison includes the proposed method using full data–Proposed (full), sample splitting–Proposed (split), the naive Algorithm 1–Naive, and the oracle method (Oracle) by assuming that we know the valid instruments a priori. Empirical results are presented in Tables 13 and 14. Histograms of causal effect

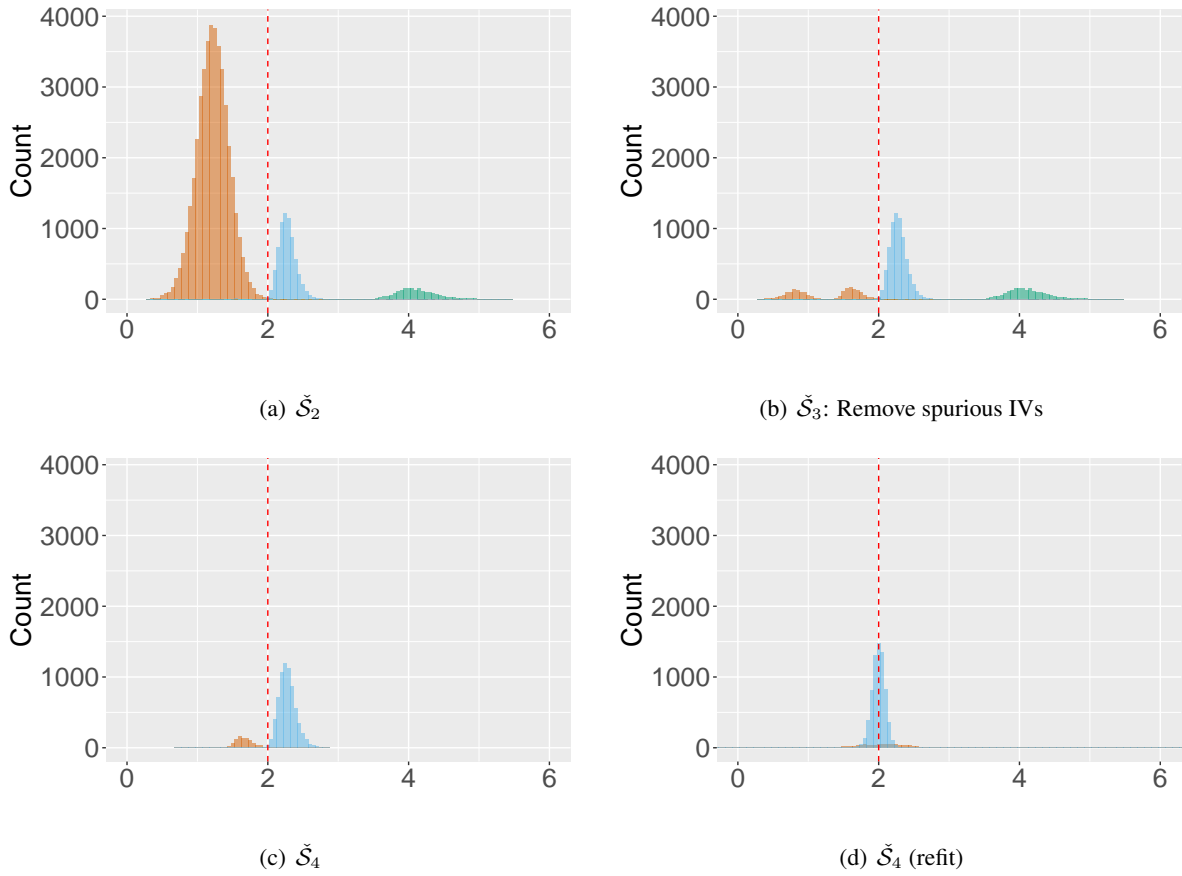


Figure 12: Plots (a)-(d) correspond to the simulation 5 when some instruments are weak in Section F.5. Plots (a)-(c) are histograms of causal effect estimates from valid, invalid and spurious instruments in $\tilde{\mathcal{S}}_2$, $\tilde{\mathcal{S}}_3$ and $\tilde{\mathcal{S}}_4$ respectively obtained from Algorithm 2–Proposed (full) across 1000 Monte Carlo runs. The blue pile represents causal estimates from valid IVs; the green pile refers to invalid IVs; the orange pile is causal estimates from irrelevant variables, including both irrelevant variables from the initial candidate set and pseudo ones. The red dashed line is the true causal effect $\beta^* = 2$. The results are based on $(n, p, \sigma_D^2) = (500, 50, 000, 0)$. The last figure (d) gives the distribution of causal estimates from refitted model.

estimates under $\sigma_D^2 = 0$ are presented in Figure 13.

Table 13: Performance summary for various methods and σ_D^2 under simulation 6 across 1000 Monte Carlo runs with $n = 500$ and $p = 50,000$. We make the numbers bold for the method with the best performance except for the oracle estimate. Standard errors are presented in the bracket if applicable

| | Method | Bias $\times 10$ (SE $\times 10$) | RMSE $\times 10$ | Coverage (Nominal = 95%) |
|------------------|------------------|------------------------------------|------------------|--------------------------|
| $\sigma_D^2 = 0$ | Proposed (full) | -0.05(0.02) | 0.54 | 0.92 |
| | Proposed (split) | 1.26(0.11) | 3.82 | 0.71 |
| | Naive | -5.38(0.10) | 6.30 | 0.03 |
| | Oracle | -0.01(0.01) | 0.26 | 0.96 |
| $\sigma_D^2 = 2$ | Proposed (full) | 0.09(0.04) | 1.20 | 0.90 |
| | Proposed (split) | 3.51(0.16) | 6.25 | 0.42 |
| | Naive | -1.51(0.03) | 1.85 | 0.01 |
| | Oracle | -0.01(0.01) | 0.26 | 0.96 |
| $\sigma_D^2 = 4$ | Proposed (full) | 0.95(0.10) | 3.34 | 0.81 |
| | Proposed (split) | 6.63(0.19) | 8.96 | 0.35 |
| | Naive | -1.40(0.01) | 1.46 | 0.00 |
| | Oracle | -0.01(0.01) | 0.26 | 0.96 |

Table 14: Average number of invalid, valid IVs and irrelevant variables in \check{S}_2 , \check{S}_3 and \check{S}_4 under simulation 6 respectively across 1000 Monte Carlo runs. Note that “Naive” is applied without including pseudo variables. The results are based on $n = 500$ and $p = 50,000$. “-” stands for “inapplicable”

| | Method | \check{S}_2 | | | \check{S}_3 | | | \check{S}_4 | | |
|------------------|------------------|---------------|-------|------------|---------------|-------|------------|---------------|-------|------------|
| | | Invalid | Valid | Irrelevant | Invalid | Valid | Irrelevant | Invalid | Valid | Irrelevant |
| $\sigma_D^2 = 0$ | Proposed (full) | 2.00 | 7.00 | 15.19 | 1.97 | 6.99 | 1.94 | 0.00 | 6.82 | 0.60 |
| | Proposed (split) | 1.98 | 6.89 | 43.37 | 1.51 | 6.24 | 2.13 | 0.36 | 5.93 | 0.18 |
| | Naive | 2.00 | 7.00 | 11.71 | - | - | - | 0.22 | 0.90 | 11.69 |
| $\sigma_D^2 = 2$ | Proposed (full) | 2.00 | 7.00 | 20.36 | 1.29 | 6.75 | 1.95 | 0.03 | 6.71 | 1.07 |
| | Proposed (split) | 1.98 | 6.88 | 51.86 | 1.03 | 4.43 | 2.13 | 0.67 | 3.61 | 0.38 |
| | Naive | 2.00 | 7.00 | 16.01 | - | - | - | 0.96 | 5.24 | 16.00 |
| $\sigma_D^2 = 4$ | Proposed (full) | 2.00 | 7.00 | 25.79 | 1.03 | 5.57 | 1.96 | 0.12 | 5.53 | 1.27 |
| | Proposed (split) | 1.98 | 6.87 | 59.66 | 0.99 | 2.09 | 2.13 | 0.79 | 1.54 | 0.91 |
| | Naive | 2.00 | 7.00 | 20.25 | - | - | - | 1.00 | 6.77 | 20.25 |

The simulation results suggest that the proposed procedure using full data achieves the best performance among the other competing methods even if the independence assumption (I3) is violated, but the results become undesirable when σ_D^2 further increases. It was shown in Table 14 that the “Proposed (full)” would miss some valid instruments and also misidentify some invalid instruments as valid ones for larger σ_D^2 . The sample splitting only uses part of the samples and some invalid instruments are estimated as valid due to the loss of efficiency and its performance is getting worse as σ_D^2 increases. The “Naive” fails since it has

misidentified some invalid instruments and many spurious instruments as valid ones.

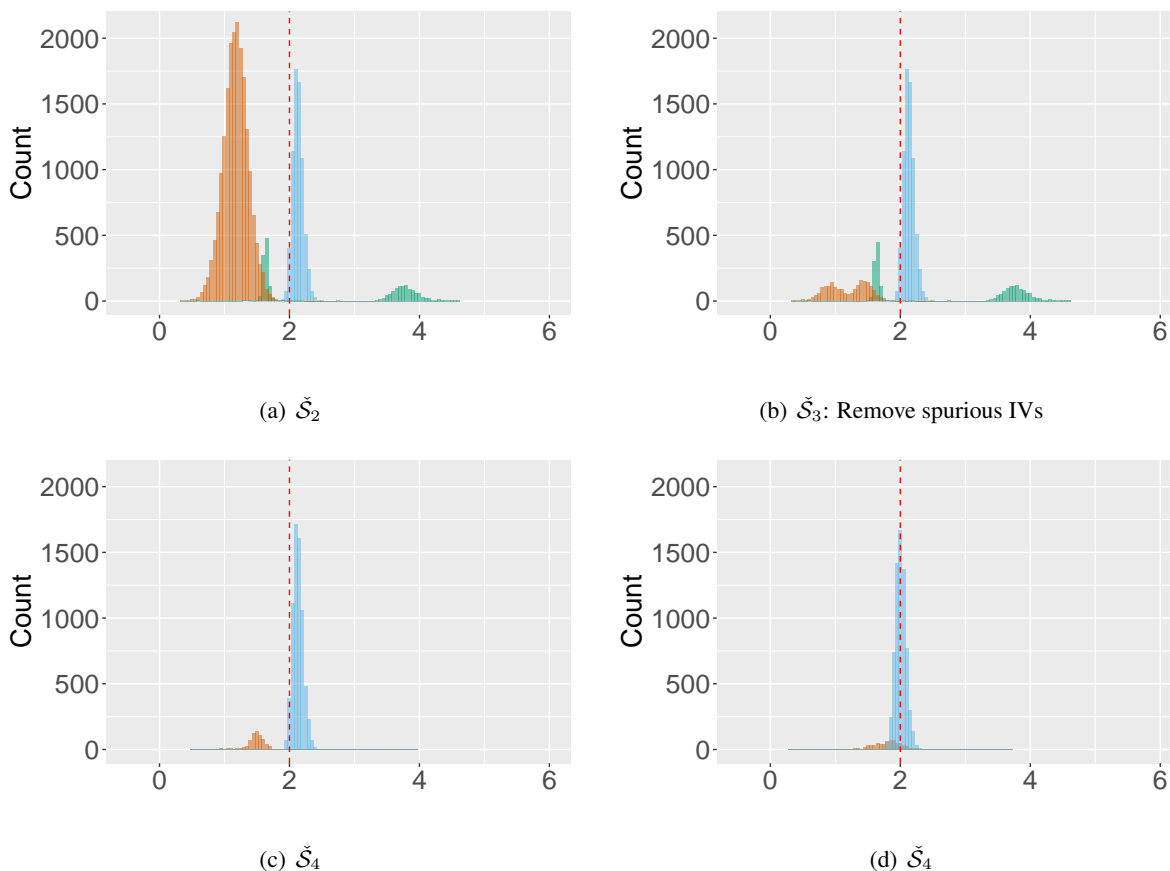


Figure 13: Plots (a)-(c) correspond to the simulation 6 where the independence assumption is violated in Section F.6. Plots (a)-(c) are histograms of causal effect estimates from valid, invalid and spurious instruments in \check{S}_2 , \check{S}_3 and \check{S}_4 respectively obtained from Algorithm 2–Proposed (full) across 1000 Monte Carlo runs. The blue pile represents causal estimates from valid IVs; the green pile refers to invalid IVs; the orange pile is causal estimates from irrelevant variables, including both irrelevant variables from the initial candidate set and pseudo ones. The red dashed line is the true causal effect $\beta^* = 2$. The results are based on $(n, p, \sigma_D^2) = (500, 50, 000, 0)$. Plot (d) gives the distribution of effect estimates from refitted model.

F.7 Competing methods in econometric literature – simulation 7

In this section, we consider some competing approaches which deal with many instruments and allow for weak IVs in the econometric literature to lend further support of our proposed method. Donald & Newey (2001) provided explicit forms for asymptotic mean squared error (MSE) of two-stage least squares (2SLS) and limited-information maximum likelihood (LIML) estimators, which is a function of the number of instruments. They found that selecting the number of instruments by minimizing MSE can improve performance in the presence weak instruments. “D2SLS” and “DLIML” refer to the refined 2SLS and LIML estimators by Donald & Newey (2001) respectively. We also include regularized 2SLS (Carrasco, 2012)

and regularized LIML (Carrasco & Tchuente, 2015) based on Tikhonov (ridge) regularization, which aim to solve the problem of many instruments efficiently when some are irrelevant. We use the same notation “T2SLS” and “TLIML” as Carrasco & Tchuente (2015) to denote these methods.

In the simulation, we assume no invalid instruments, that is, candidate instrument is either valid or irrelevant. The candidate instruments, the unobserved confounding U , the random error ϵ_Y are independently generated from independent $N(0, 1)$. The random error ϵ_D follows $N(0, \sigma_D^2)$ with $\sigma_D^2 = 0, 2, 4$. The true parameters are set as follows.

$$\begin{aligned}\gamma^* &= (2.5, 2.5, 2.5, 2.5, 2.5, 2.5, 2.5, 0, \dots, 0)^T \\ \pi_j^* &= 0, \text{ for } j = 1, \dots, p \\ \alpha_D^* &= 4; \alpha_Y^* = -3.\end{aligned}$$

Evaluation of the performance is carried out across 1000 Monte Carlo runs. Same as before, suppose there are 50,000 candidate instruments at the beginning and we first reduce the dimension of this initial set of candidate instruments to $s = 500$ via marginal screening and then apply D2SLS, DLIML, T2SLS and TLIML to the selected candidates. Then we implement Algorithm 2, the proposed method using full data. We report bias, root-mean-square error (RMSE) and empirical coverage for each method, and the oracle estimate which uses valid instruments only. We summarize the results in Table 15.

In summary, the “Proposed (full)” outperforms the other approaches for estimating the causal effect and its performance is similar to the oracle estimate when σ_D^2 is not too large.

G Estimate of precision matrix

Following van de Geer et al. (2014), to obtain the matrix $M \in \mathbb{R}^{s \times s}$ that estimates the precision matrix $\Sigma_{\hat{S}_1}^{-1}$, we first solve the node-wise lasso problems below:

$$\hat{\theta}_j^{(\hat{S}_1)} = \operatorname{argmin}_{\theta \in \mathbb{R}^s} \left(\frac{1}{n} \|Z_{\hat{S}_1, j} - Z_{\hat{S}_1, -j} \theta\|^2 + 2\lambda_j \|\theta\|_1 \right) \quad (\text{G.1})$$

for $j = 1, \dots, s$, where $Z_{\hat{S}_1, j} \in \mathbb{R}^n$ denotes the j th column of the design matrix $Z_{\hat{S}_1} \in \mathbb{R}^{n \times s}$ and $Z_{\hat{S}_1, -j} \in \mathbb{R}^{n \times (s-1)}$ is formed by columns of $Z_{\hat{S}_1}$ indexed by $\{1, \dots, s\} \setminus \{j\}$. The k th component of $\hat{\theta}_j^{(\hat{S}_1)}$ is denoted by $\{\hat{\theta}_{j,k}^{(\hat{S}_1)} : k = 1, \dots, s, k \neq j\}$. Define matrix \widehat{N} as

$$\widehat{N} = \begin{pmatrix} 1 & -\hat{\theta}_{1,2}^{(\hat{S}_1)} & \dots & -\hat{\theta}_{1,s}^{(\hat{S}_1)} \\ -\hat{\theta}_{2,1}^{(\hat{S}_1)} & 1 & \dots & -\hat{\theta}_{2,s}^{(\hat{S}_1)} \\ \vdots & \vdots & \ddots & \vdots \\ -\hat{\theta}_{s,1}^{(\hat{S}_1)} & -\hat{\theta}_{s,2}^{(\hat{S}_1)} & \dots & 1 \end{pmatrix}. \quad (\text{G.2})$$

Table 15: Performance summary for the comparison with competing methods in econometric literature-simulation 7. Results are obtained from 1000 Monte Carlo runs with $p = 50,000$. We make the numbers bold for the method with the best performance except the oracle estimate. Standard errors are presented in the bracket if applicable. For $SE < 0.005$, we report as $SE = 0.00$

| | Method | Bias $\times 10$ (SE $\times 10$) | RMSE $\times 10$ | Coverage (Nominal = 95%) |
|------------------|-----------------|------------------------------------|------------------|--------------------------|
| $\sigma_D^2 = 0$ | Proposed (full) | -0.09(0.01) | 0.39 | 0.92 |
| | T2LS | -1.89(0.01) | 1.90 | 0.00 |
| | TLIML | -1.72(0.01) | 1.73 | 0.00 |
| | D2SLS | -0.12(0.01) | 0.26 | 0.88 |
| | DLIML | -0.24(0.01) | 0.31 | 0.98 |
| | Oracle | -0.03(0.01) | 0.21 | 0.95 |
| $\sigma_D^2 = 2$ | Proposed (full) | -0.07(0.01) | 0.27 | 0.93 |
| | T2LS | -1.83(0.00) | 1.84 | 0.00 |
| | TLIML | -1.68(0.01) | 1.69 | 0.00 |
| | D2SLS | -0.19(0.01) | 0.31 | 0.79 |
| | DLIML | -0.45(0.01) | 0.50 | 0.77 |
| | Oracle | -0.03(0.01) | 0.21 | 0.95 |
| $\sigma_D^2 = 4$ | Proposed (full) | -0.09(0.02) | 0.54 | 0.91 |
| | T2LS | -1.78(0.00) | 1.79 | 0.00 |
| | TLIML | -1.64(0.01) | 1.65 | 0.00 |
| | D2SLS | -0.27(0.01) | 0.38 | 0.68 |
| | DLIML | -0.61(0.01) | 0.65 | 0.46 |
| | Oracle | -0.03(0.01) | 0.21 | 0.95 |

Let $\hat{\mathbf{T}}^2 = \text{diag}\{\hat{\tau}_{\hat{S}_{1,1}}^2, \dots, \hat{\tau}_{\hat{S}_{1,s}}^2\}$, where $\hat{\tau}_{\hat{S}_{1,j}}^2 = \|\mathbf{Z}_{\hat{S}_{1,j}} - \mathbb{Z}_{\hat{S}_{1,-j}} \hat{\boldsymbol{\theta}}_j^{(\hat{S}_1)}\|^2/n + \lambda_j \|\hat{\boldsymbol{\theta}}_j^{(\hat{S}_1)}\|_1$. Then \mathbf{M} takes the following form

$$\mathbf{M} = \hat{\mathbf{T}}^{-2} \hat{\mathbf{N}}. \quad (\text{G.3})$$

H Standard error of bias estimate

The standard error of bias estimate is given by

$$\text{SE}(\hat{b}^{(j,l)}) = \sqrt{(\hat{v}_{jj} - 2\hat{v}_{jl} + \hat{v}_{ll})/n}, \quad (\text{H.1})$$

where

$$\hat{v}_{jj} = \frac{\mathbf{M}_{jj}}{\{\hat{\gamma}_{\hat{S}_{1,j}}\}^2} \left\{ \hat{\Theta}_{11} - \frac{2\hat{\Gamma}_{\hat{S}_{1,j}}}{\hat{\gamma}_{\hat{S}_{1,j}}} \hat{\Theta}_{12} + \left(\frac{\hat{\Gamma}_{\hat{S}_{1,j}}}{\hat{\gamma}_{\hat{S}_{1,j}}} \right)^2 \hat{\Theta}_{22} \right\} \quad (\text{H.2})$$

$$\hat{v}_{ll} = \frac{\mathbf{M}_{ll}}{\{\hat{\gamma}_{\hat{S}_{1,l}}\}^2} \left\{ \hat{\Theta}_{11} - \frac{2\hat{\Gamma}_{\hat{S}_{1,l}}}{\hat{\gamma}_{\hat{S}_{1,l}}} \hat{\Theta}_{12} + \left(\frac{\hat{\Gamma}_{\hat{S}_{1,l}}}{\hat{\gamma}_{\hat{S}_{1,l}}} \right)^2 \hat{\Theta}_{22} \right\} \quad (\text{H.3})$$

$$\hat{v}_{jl} = \frac{\mathbf{M}_{jl}}{\{\hat{\gamma}_{\hat{S}_{1,j}}\}\{\hat{\gamma}_{\hat{S}_{1,l}}\}} \left\{ \hat{\Theta}_{11} - \left(\frac{\hat{\Gamma}_{\hat{S}_{1,j}}}{\hat{\gamma}_{\hat{S}_{1,j}}} + \frac{\hat{\Gamma}_{\hat{S}_{1,l}}}{\hat{\gamma}_{\hat{S}_{1,l}}} \right) \hat{\Theta}_{12} + \left(\frac{\hat{\Gamma}_{\hat{S}_{1,j}}}{\hat{\gamma}_{\hat{S}_{1,j}}} \right) \left(\frac{\hat{\Gamma}_{\hat{S}_{1,l}}}{\hat{\gamma}_{\hat{S}_{1,l}}} \right) \hat{\Theta}_{22} \right\} \quad (\text{H.4})$$

and $\hat{\Theta}_{11}, \hat{\Theta}_{12}, \hat{\Theta}_{22}$ take the following form

$$\hat{\Theta}_{11} = \frac{1}{n} \|\mathbf{Y} - \tilde{\mathbf{Z}}_{\hat{S}_1} \tilde{\boldsymbol{\Gamma}}_{\hat{S}_1}\|_2^2, \quad \hat{\Theta}_{22} = \frac{1}{n} \|\mathbf{D} - \tilde{\mathbf{Z}}_{\hat{S}_1} \tilde{\boldsymbol{\gamma}}_{\hat{S}_1}\|_2^2, \quad \hat{\Theta}_{12} = \frac{1}{n} (\mathbf{Y} - \tilde{\mathbf{Z}}_{\hat{S}_1} \tilde{\boldsymbol{\Gamma}}_{\hat{S}_1})^\text{T} (\mathbf{D} - \tilde{\mathbf{Z}}_{\hat{S}_1} \tilde{\boldsymbol{\gamma}}_{\hat{S}_1}).$$